UNIVERSITÀ DEGLI STUDI DI BRESCIA

Dipartimento di Medicina Molecolare e Traslazionale

UNIVERSITÀ
DEGLI STUDI
DI BRESCIA

DOTTORATO DI RICERCA IN

Genetica Molecolare, Biotecnologie e Medicina Sperimentale

settore scientifico disciplinare

BIO/13

CICLO

XXXIII

TITOLO TESI

miR-9-5p in neuronal dendritic remodeling: the role of stress

DOTTORANDO: Jessica Mingardi

Jessica Mingardi

RELATORE: Prof. Alessandro Barbon

Alessandro Barbon

Anno Accademico 2019/2020

RIASSUNTO

Lo stress è considerato un fattore di rischio per lo sviluppo di malattie neuropsichiatriche come la depressione. Gli individui possono rispondere agli eventi stressanti attivando risposte adattative che consentono loro di adeguarsi e reagire agli stimoli. In alcuni casi, l'esposizione prolungata o il carico eccessivo dello stress insieme ad una predisposizione genetica, possono determinare l'instaurarsi di risposte maladattative che possono favorire l'insorgere di patologie neuropsichiatriche. I meccanismi alla base della diversa risposta non sono ancora del tutto chiari. L'uso di modelli animali di depressione basati sullo stress ha messo in luce alterazioni morfologiche a carico dei dendriti dei neuroni dell'ippocampo, suggerendo che i cambiamenti maladattativi indotti dallo stress abbiano un ruolo chiave nell'eziopatogenesi della depressione. È stato dimostrato che il trattamento con il farmaco antidepressivo ad azione rapida ketamina (KET) è in grado di recuperare rapidamente la riduzione dendritica indotta dallo stress. Utilizzando il Chronic Mild Stress (CMS) come modello animale di depressione, abbiamo precedentemente mostrato una riduzione della lunghezza e della complessità dei dendriti apicali dei neuroni piramidali della regione CA3 dell'ippocampo selettivamente negli animali vulnerabili. Queste alterazioni erano completamente recuperate dalla somministrazione acuta di KET.

Nel mio progetto di dottorato mi sono occupata di studiare i meccanismi molecolari alla base delle alterazioni morfologiche indotte dallo stress e da KET. In particolare, ci siamo focalizzati sul ruolo svolto dai microRNA, una classe di molecole di RNA non codificanti che agiscono a livello post-trascrizionale controllando l'espressione genica. Abbiamo riscontrato una riduzione dei livelli di miR-9-5p selettivamente nell'ippocampo degli animali vulnerabili che è completamente recuperata da KET. Un risultato simile è stato trovato anche utilizzando un modello di stress cronico *in vitro* in cui il trattamento ripetuto con corticosterone di colture primarie ippocampali ha ridotto significativamente la lunghezza dei dendriti insieme ad una diminuzione dei livelli di espressione di miR-9-5p; KET ha recuperato entrambi i cambiamenti. Per indagare se miR-9-5p fosse in grado di indurre direttamente un rimodellamento dell'albero dendritico, abbiamo utilizzato dei vettori per modulare l'espressione di miR-9-5p in colture primarie ippocampali dimostrando che la sua down-regolazione influisce in modo negativo sul rimodellamento dendritico e sulla densità delle spine mentre la sua over-espressione ha l'effetto opposto. L'analisi bioinformatica ha permesso di identificare e selezionare alcuni target di miR-9-5p che sono stati poi validati mediante il saggio della Luciferasi. Successivamente, l'espressione dei due target, SIRT1 e REST, è stata valutata nell'ippocampo dei ratti sottoposti a CMS e KET. I nostri risultati suggeriscono che l'alterazione dei

livelli di miR-9-5p possa essere coinvolta sia nei meccanismi di vulnerabilità/resilienza allo stress che nell'effetto antidepressivo rapido di KET.

TABLE OF CONTENTS

LIST OF FIGURES

LIST OF TABLES

ABSTRACT

Stress is considered a risk factor for the pathogenesis of neuropsychiatric disorders, including depression. Individuals can respond to stressful stimuli activating coping strategies that allow them to adapt and react to the stressors. Sometimes, prolonged exposure or excessive load of the stress combined with a genetic predisposition may lead to the development of maladaptive responses that can favor the onset of neuropsychiatric conditions. The mechanisms underneath the different response are not fully known. The use of animal models of depression showed morphological alterations of the dendrites of hippocampal neurons suggesting that stress-induced maladaptive changes may have a role in the etiopathogenesis of depression. It was shown that the treatment with the fast-acting antidepressant ketamine (KET) rapidly rescued the dendritic simplification induced by stress. Using the Chronic Mild Stress (CMS) animal model of depression, we demonstrated a reduction of the length and complexity of the apical dendrites of the CA3 hippocampal neurons selectively in the CMS-V animals. The alterations were completely reverted by acute KET.

My doctoral project was focused on the study of the molecular mechanisms underneath the morphological changes induced by stress and KET. In particular, we focused our attention on the role of miRNAs, a class of non-coding molecules of RNA that act regulating post-transcriptional gene expression. Using the CMS, we found a reduction of miR-9-5p levels selectively in the hippocampus of vulnerable animals that was completely rescued by KET. A similar result was found also using an *in vitro* model of chronic stress in which the repeated treatment with corticosterone of primary hippocampal neurons significantly reduced both dendritic length and miR-9-5p expression; KET successfully rescued both changes. To assess whether miR-9-5p was able to directly induce the dendritic remodeling, we used vectors designed to modulate miR-9-5p expression in primary hippocampal cultures. We demonstrated that miR-9-5p down-regulation negatively affects the dendritic remodeling and the density of spines while its over-expression exerted the opposite effect. The bioinformatic analysis allowed to identify and select a list of miR-9-5p targets that were further validated using the Luciferase assay. Then, the expression of those genes that were confirmed as targets, SIRT1 and REST, has been evaluated in the hippocampus of rats subjected to CMS and KET and in primary neurons treated with corticosterone and KET. Our results suggest that the changes in miR-9-5p expression may be involved both in the mechanisms of vulnerability/resilience to stress and in the fast antidepressant effect of KET.

1. INTRODUCTION

1.1 The concept of stress

1.1.1 The stress response

The word "stress" is often used in our everyday speaking to refer to different kind of experiences thus becoming sometimes ambiguous. The term was first biologically defined in 1956 by the physician Hans Selye who defined stress as a "non-specific response of the body to any demand placed upon it" (Selye, 1956). Based on this definition, stress has been used to identify biological and psychological processes activated in response to challenges that are able to alter the physiological homeostasis of the organism (Popoli et al., 2011). When a stimulus is perceived as threatening ("stressor"), our body starts a series of biochemical, hormonal, functional and behavioral adjustments (Selye, 1936) aimed at restoring the disrupted homeostasis, a process named "allostasis" (McEwen, 1993). Under physiological conditions, the cease of the stressor leads to a rapid return to baseline levels. However, when the stress is prolonged or overwhelming, progressive and sustained changes may accumulate ("allostatic load or overload") leading to a pathogenic condition of the brain (McEwen, 2007) (Fig. 1).

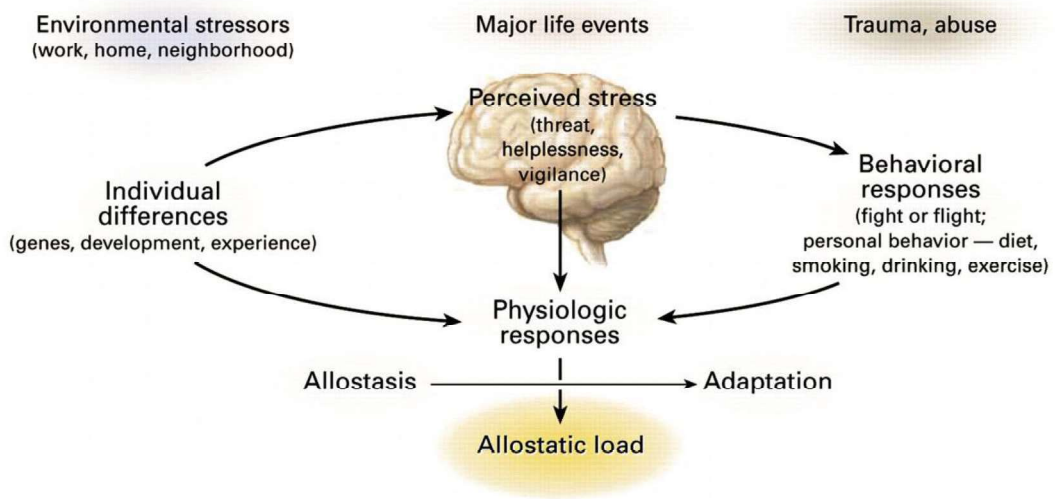

Figure 1. Allostasis and allostatic load in stress response
Harmful stimuli induce physiologic and behavioral responses that lead to allostasis and adaptation. Over time, however, allostatic load can accumulate, increasing the risk of disease. From McEwen, 1998.

The brain has a central role in these processes since it is the organ that determines what is novel and possibly threatening or stressful thus determining the trajectories of our body's response. The brain itself undergoes architectural and molecular rearrangements to adapt to environmental changes in order to produce behavioral responses adequate to the individual's experiences (McEwen, 2007). The first mechanism activated in response to stress by the brain is the rapid activation of the autonomic nervous system, resulting in the secretion of adrenaline and noradrenaline (Joëls et al., 2012). These catecholamines regulate body functions involved in the "fight-or-flight" response, including increased heart and respiratory rates, pupillary response and release of metabolic energy sources. The second mechanism by which the brain reacts to stress is the activation of the hypothalamic–pituitary–adrenal (HPA) axis, a neuroendocrine circuit that integrates emotional, cognitive, and autonomic inputs to coordinate behavioral and hormonal responses to stress (Lucassen et al., 2014) (Fig. 2). Briefly, the corticotropin-releasing factor (CRF) is released from the paraventricular nucleus of the hypothalamus and stimulates the anterior pituitary to produce the adrenocorticotropic hormone (ACTH), leading to the synthesis and release of glucocorticoids from the adrenal cortex. These hormones have a wide range of actions throughout the body including energy balance and glucose utilization. The impact of glucocorticoids on the brain is mediated by two main receptors, the glucocorticoid receptor (GR) and the mineralcorticoid receptor (MR) (McEwen & Akil, 2020). They are widely distributed in brain regions that control emotions and behaviors such as the hippocampus (HPC), the amygdala and the prefrontal cortex (PFC) (Joëls & Baram, 2009). In particular, brain MR is constitutively activated at basal cortisol concentrations (having high affinity for glucocorticoids), is involved in learning and memory processes, in the regulation of normal neuronal functioning and acts as a quick sensor for shifts in glucocorticoid levels (Joëls et al., 2012). GR shows instead less affinity for cortisol than for other glucocorticoids, thus being activated by cortisol only at high stress concentrations (Gomez-Sanchez, 2014). Once activated, brain GR assists the brain's reaction to stressful conditions, by suppressing HPA axis and modulating MR activity (Joëls et al., 2012). Both GRs and MRs may produce effects via genomic or non-genomic mechanisms (McEwen et al., 2015). Indeed, they are ligand-activated transcription factors that upon binding of glucocorticoids (corticosterone in rodents, cortisol in humans) lead to either positive or negative regulation of the expression of their target genes. Further, they can also directly stimulate the release of excitatory amino acids via membrane-associated receptors and indirectly regulate the release of GABA and glutamate (McEwen & Akil, 2020). These effects are biphasic thus the timing and the levels of glucocorticoids expression are critical.

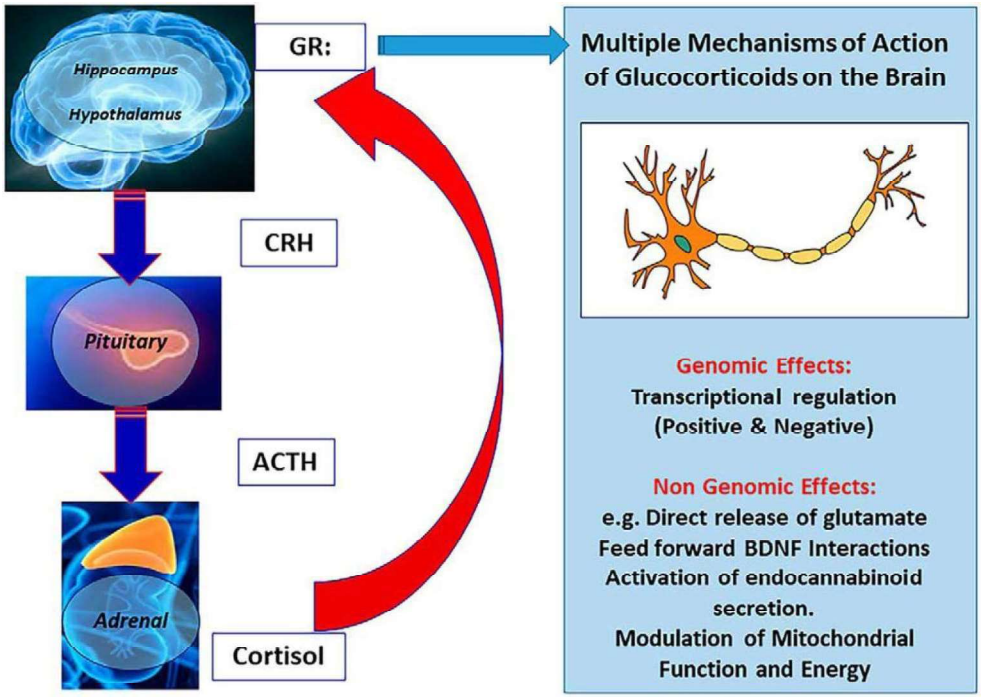

Figure 2. Key elements of the limbic HPA axis

Glucocorticoids feed back to the brain to restrain the stress response activating their receptor GRs and MRs, that are expressed in multiple brain regions especially the hippocampus. Glucocorticoids effects in the brain involve direct and indirect genomic actions but also direct stimulation of glutamate release, stimulation of endocannabinoid production and actions in mitochondria to affect $Ca2^{+}$ buffering and free radicals formation. From McEwen, 2020

1.1.2 Vulnerability versus resilience

Individuals may respond in different ways to identical stressful stimuli. The ability to cope with stress and develop adaptive responses is a phenomenon called “resilience” (Russo et al., 2012). Those who are resilient are able to react to internal or external stressors activating coping mechanisms that protect the organism from the detrimental effects of stress (McEwen, 2017). This ability can be positively influenced by different skills such as optimism, cognitive-flexibility, self-esteem and parental relationships (Southwick et al., 2005). Genetic findings and preclinical research on animal models are only now providing consistent evidence on the biological processes underlying resilience (Russo et al., 2012). On the other hand, the excessive duration and/or load of stress, together with a genetic predisposition and environmental factors, could lead in some other individuals, defined “vulnerable”, to the activation of maladaptive responses that often translate in a higher risk of developing stress-related disorders, such as depression (McEwen, 2017). Luckily, despite the strong impact of stress on health and mood, only less than 20% of the individuals exposed to prolonged stress develops a stress-related disorder, whereas most of the people maintain normal psychological and physical functioning (Han & Nestler, 2017). The individual traits that allow the adaptive or maladaptive outcomes depend

upon the unique neurological capacity of each individual, which is built upon life experiences (McEwen, 2017). Understanding the molecular mechanism underneath stress vulnerability and resilience may represent an important step towards developing useful strategies to prevent or treat stress-related disorders.

1.1.3 Stress effect on brain plasticity and connectivity

The discovery of the presence of GRs and MRs in the hippocampus (HPC) pioneered the study about the effects of stress on brain architecture demonstrating their involvement in modulating structural plasticity. The HPC is a sensitive and plastic region of the brain with an established role in memory formation and emotional behavior. It also plays a role in shutting off the HPA stress response, explaining why damage or atrophy of the HPC lead to a more prolonged HPA response to psychological stressors (Jacobson & Sapolsky, 1991). The HPC undergoes adaptive changes in response to acute or chronic stress, whatever they serve to protect against permanent damage or enhance vulnerability to damage (McEwen, 2007). One type of change involves the replacement of neurons in the dentate gyrus (neurogenesis) still taking place in adult life. Certain types of acute stress and many chronic stressors suppress neurogenesis or cell survival in the dentate gyrus, and the mediators of these inhibitory effects include excitatory amino acids acting via N-methyl-D-aspartate (NMDA) receptors and endogenous opioids (Gould et al., 1997). Another form of plasticity is the remodeling of dendrites of hippocampal neurons. Chronic stress induces shrinkage of dendrites of hippocampal CA3 and dentate gyrus neurons as well as loss of spines in CA1 neurons (McEwen et al., 2016). Further, not only CA3 region of the HPC shows dendritic reorganization with chronic stress. Apical dendrites of rat CA1 neurons were reported to be shorter in adulthood after chronic neonatal bedding stress (Brunson, 2005), and a comparison of stressors revealed differences within the HPC and its functional connectivity to other brain regions (Maras et al., 2014). Indeed, other brain regions are subjected to the effect of glucocorticoids on structural plasticity although sometimes different from those regarding the HPC. In the basolateral amygdala (BLA), a form of severe chronic stress produced an expansion of the dendrites whereas the same stress induced a shortening of dendrites in the CA3 region of the hippocampus of rats (Vyas et al., 2002). At the same time, spine density was downregulated in the medial amygdala depending on the action of tissue plasminogen activator (tPA), the same mediator that is involved in the chronic stress-dependent reduction of spine density on hippocampal CA1 neurons (Pawlak et al., 2005). Another brain region in which stress induces structural changes is the prefrontal cortex (PFC), where glucocorticoids have a biphasic effect. Acute stress induces a potentiation of NMDAR- and AMPAR-mediated synaptic currents in

PFC pyramidal neurons and enhances working memory via a GR-dependent mechanism (Yuen et al., 2009). On the other hand, chronic stress significantly reduced AMPA and NMDA receptor-dependent synaptic transmission and cell surface expression (Yuen et al., 2012). As in the HPC, the structural remodeling of the PFC neurons is reversible when the stressful stimulus is ended in young animals (Liston et al., 2006) but not as rapidly or absent in middle aged and aged animals (Bloss et al., 2010).

1.1.4 The role of stress as an environmental risk factor for neuropsychiatric disorders

Beyond the genetic predisposition, environmental factors play a key role in the pathogenesis of neuropsychiatric disorders such as depression. Stress has been recognized as the major predisposing and triggering factor for depression that is itself considered the most common stress-related disorder (Nestler et al., 2002). Emotional trauma (including grief, social rejection, physical or sexual abuse), major life changes (such as health condition, childbirth, financial difficulties, natural disasters, war) and adversities in childhood or adolescence (including maltreatment, neglect or bullying) are widely recognized as important risks for mental health (American Psychiatric Association, 2013; Heim et al., 2008; Lindert et al., 2014). Exposure to acute or chronic stressors produces a sequence of hormonal, biochemical and neuronal outcomes, that may precipitate in the onset of pathological changes typical of depression. Accordingly, the majority of animal models to study depression is nowadays based on the repeated exposure to stress paradigms (Gururajan et al., 2019). Importantly, considering the heterogeneity of depression these models are not able to reproduce the human condition in its entirety, but they successfully induce depression-like traits in rodents.

1.1.5 Animal models to study stress-dependent remodeling of brain morphology

Morphological defects in specific brain areas have been associated both with a depressive-like phenotype in preclinical studies and with depression in patients (Krishnan & Nestler, 2008). Stress emerged as an important player in determining these changes and therefore has been used in most of the animal paradigms where it has been demonstrated to reproduce the phenotypic and behavioral changes and the structural alterations typical of depressed individuals (McEwen et al., 2016). Social defeat stress is one of the most used paradigms and is based on the exposure of rodents to an emotional and psychological stress represented by a dominant and aggressive rodent of the same species (Krishnan & Nestler, 2011). Defeated animals show several depressive-like behaviors including social avoidance and cognitive impairments. Maternal separation has been used to study the impact of adverse early life experiences as predisposing factors in the onset of mental disorders in the adulthood (Krishnan & Nestler, 2011). The repeated separation of the rodent pups from the mother

in the early postnatal days leads to a sustained activation of the HPA axis that results in behavioral, cognitive and brain-structural abnormalities that persist in the adulthood. Recently, the Chronic Mild Stress (CMS) animal model has been widely used in the study of the pathological and therapeutic mechanisms underlying depression. It is based on the repeated exposure of rodents to a variable sequence of mild and unpredictable stressors that end producing a chronic depressive-like phenotype (Krishnan & Nestler, 2011). The primary behavioral outcome of the model is the hedonic response of rodents to rewarding stimuli, measured as preference for a palatable sucrose solution or its consumption. Several studies reported that CMS induced changes of neuronal and brain structure (Willner, 2017). In particular, CMS has been associated with atrophy of dendrites, reduced number of dendritic spines and reduced neurogenesis in the same brain areas showing volumetric reduction in depression (Banasr et al., 2007; Li et al., 2011; Toth et al., 2008). As a consequence of stress exposure, an aberrant HPA axis activation can lead to a failure of the negative feedback systems that regulate the stress-induced release of cortisol (corticosterone in rodents) in the systemic circulation (Anacker et al., 2011). This condition is a common clinical feature of depression and thus preclinical studies have recapitulated the HPA hyperactivity by supplementation of corticosterone, for example, via injections or by adding it to the water (Gururajan et al., 2019). There are also examples of the use of corticosterone in neuronal cell cultures allowing to reproduce *in vitro* the biological condition during a stressful event (Yuen et al., 2011). Most of the studies analyze the effect of a single exposure to corticosterone or dexamethasone, a synthetic glucocorticoid, using variable doses of the hormones and for a different time course (Groc et al., 2008; Horowitz et al., 2020; Mazzelli et al., 2020; Qi et al., 2005).

1.2 Major depressive disorder

1.2.1 Epidemiology, symptoms and diagnosis

Depression, referred also as clinical depression or unipolar depression, is a common mental disorder defined as “a mood disorder that causes distressing symptoms that affect how you feel, think, and handle daily activities, such as sleeping, eating, or working” (National Institute of Mental Health, 2018). The Global Burden of Disease (GBD) epidemiological study, made by the World Health Organization in 2015, estimated that depression affect the 4.4 % of global population (World Health Organization, 2017) (Fig. 3). The prevalence of this disorder varies depending on country, age and sex reaching a peak in older adulthood with a rate of 7.5 % among females aged between 55-74 and 5.5 % among males. Of the approximately 300 million people suffering from depression, half of them

live in the Western Pacific and South-East Asia regions. Among others mental disorders, depression causes considerable losses both in health and from a socio-economic point of view being one of the largest contributors to disability. Moreover, severe forms often lead to an increased risk of suicide which represents a major issue especially in the age range of 15-29 years old.

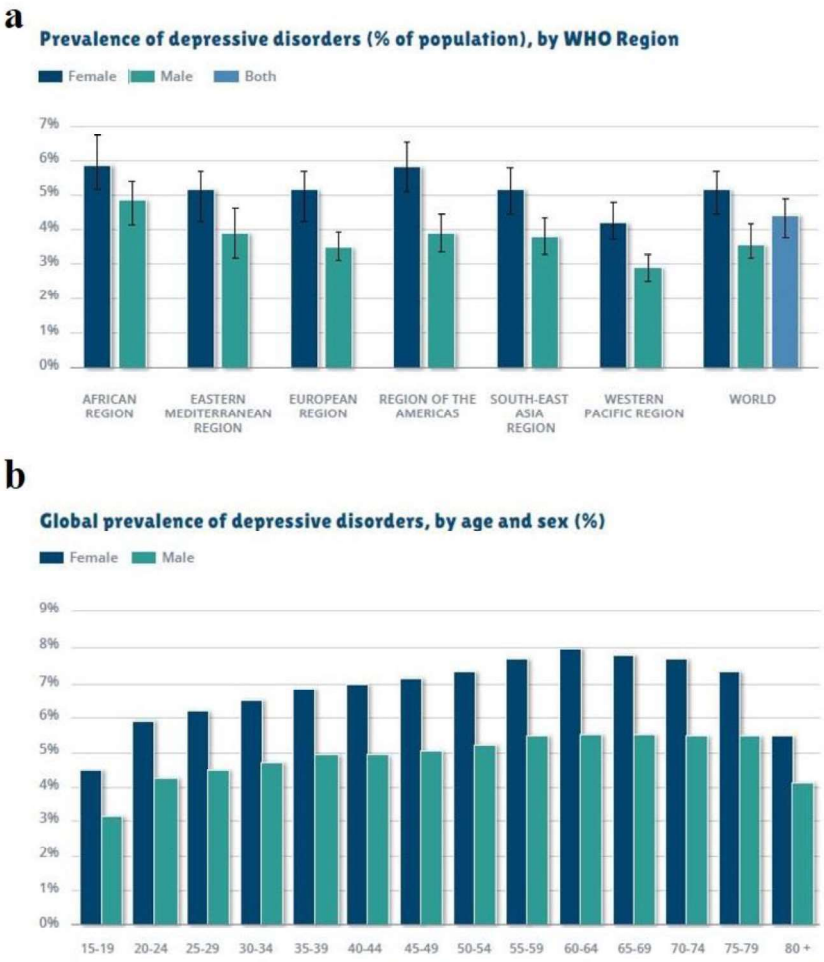

Figure 3. Prevalence of major depressive disorder in the world population
Global prevalence (% of the world population) of depression (a) by sex and world region, and (b) by sex and age. Data from the 2015 Global Burden of Disease study, promoted by the World Health Organization.

Depression is a complex and heterogeneous disorder characterized by the presence of both mental and physical alterations. Two of these alterations are considered core symptoms of depression: a persistent low mood and loss of interest or pleasure ("anhedonia"). This last phenomenon is supposedly linked to a dysfunction of the brain reward system (Nestler et al., 2002). The lack of reactivity to pleasurable stimuli results in extremely impaired behavior, including loss of motivation, withdrawal from social situations and reduced sex drive (American Psychiatric Association, 2013).

According to the criteria included in the DSM-V, depression is defined by the persistent presence for at least two weeks of one or both the core symptoms, together with four (or more) of the following symptoms:

- Alteration in appetite and weight loss or gain
- Insomnia or hypersomnia
- Psychomotor agitation or retardation
- Fatigue or loss of energy
- Feelings of worthlessness or excessive or inappropriate guilt
- Diminished ability to think or concentrate
- Recurrent thoughts of death and suicidal ideation

Usually the diagnosis of depression is conducted by a psychiatrist who records the patient's symptoms and biographical history, in order to identify relevant biological, psychological and social factors that may be impacting on its mood (Otte et al., 2016). The examination includes the use of clinical interviews, such as the Structured Clinical Interview for DSM (SCID), or rating scales, such as the Hamilton Rating Scale for Depression (HAM-D) and the Montgomery-Asberg Depression Rating Scale (MADRS) (Kennedy, 2008; Pettersson et al., 2015). However, it is estimated that only 50 % of depression cases are correctly diagnosed (Bech, 2006). Although novel tools to make the diagnosis more accurate have been developed, to date, no clinically relevant biomarkers have yet been found (Gadad et al., 2018).

1.2.2 Etiopathogenesis

The research on the pathophysiology of depression and the relative development of therapeutic drugs has been based for over fifty years on the so-called monoamine hypothesis of depression (Sanacora et al., 2012). This hypothesis claims that deficits in monoamines (in particular, serotonin, noradrenaline and dopamine) underlie the pathophysiology of depression. It was postulated after the observation that drugs able to increase the synaptic availability of monoamines produce an antidepressant effect (Frazer, 1997). Later, the dysregulation of the monoaminergic system was confirmed by neuroimaging analysis and analysis of monoamine metabolites in depressed patients (Meyer et al., 2006). However, this theory is characterized by some inconsistencies such as the discrepancy between the immediate increase of monoamines levels induced by drugs and the late

onset of the antidepressant effect (usually after 2-3 weeks of chronic treatment) (Sanacora et al., 2012). Moreover, not all patients respond to the pharmacological treatments which also induce important side effects. More recently, the glutamate system has been considered to have a primary role in the etiology of depression (Musazzi et al., 2013; Sanacora et al., 2012). Although it was not initially considered a neurotransmitter, glutamate is nowadays recognized as the most abundant excitatory neurotransmitter in the brain, with glutamatergic neurons representing the 80 % of total neurons and forming 85 % of all synapses in the neocortex (Douglas & Martin, 2007). Disruptions of glutamate neurotransmission regulation has been linked to the pathophysiology of stress-related disorders, including depression (Popoli et al., 2011) (Fig. 4a). The first suggestion of the glutamate's involvement was the preclinical discovery that the antagonism of the NMDA receptor exerts an antidepressant effect (Trullas & Skolnick, 1990). Subsequently, analysis on depressed patients showed alterations in the levels of glutamate and its metabolites in the plasma, cerebrospinal fluid and limbic/cortical brain areas. Importantly, neuroimaging studies on depressed patients found volume and connectivity alterations in the same cortical and limbic brain regions where abnormalities of the glutamate system have been reported (Drevets, 2001; Price & Drevets, 2010) (Fig. 4b). These regions, namely HPC, PFC/FC and amygdala, are involved in fundamental brain functions such as cognition, stress response, emotional behavior and memory thus suggesting a possible link between structural changes and impaired mood and behavior (Drevets, 2001).

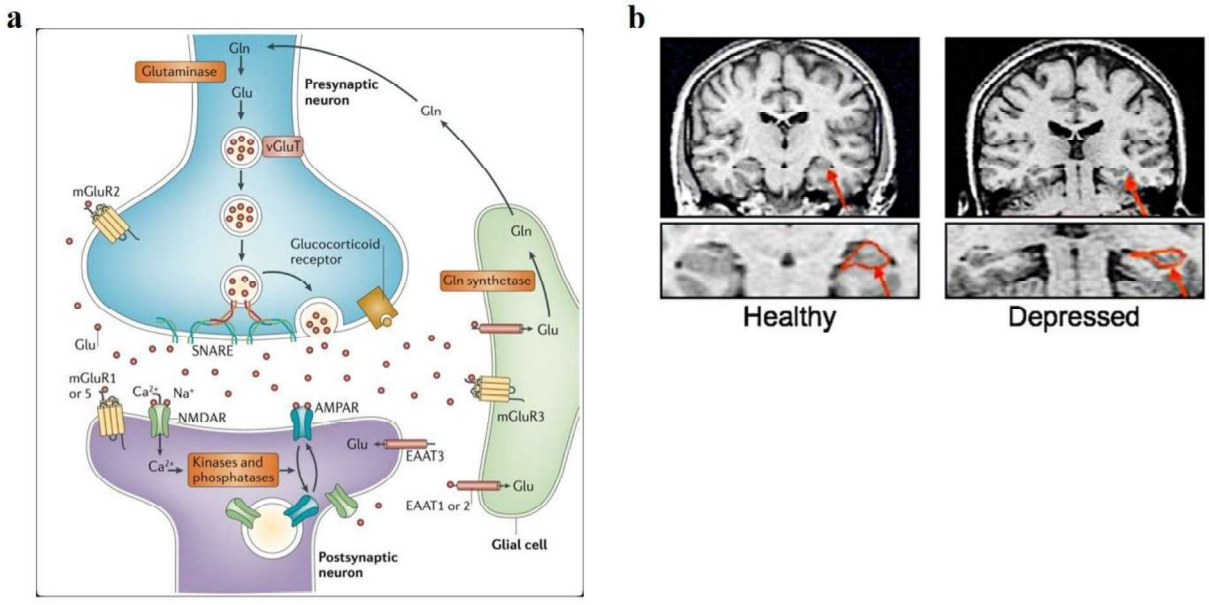

Figure 4. Dysfunctions in the glutamatergic system are involved in the pathophysiology of depression in the same brain areas were morphological changes are present in depressed patients

(a) Tripartite glutamate synapse. Neuronal glutamate (Glu) is synthesized from glutamine (Gln) supplied by glial cells, and then packaged into synaptic vesicles. Fusion of vesicles with the presynaptic membrane allows glutamate release into the extracellular space.

Here, glutamate binds its ionotropic and metabotropic receptors (both at pre- or post-synaptic level). Glutamate is then cleared from the synapse through excitatory amino acid transporters (EAATs) of glial cells, and converted to glutamine by glutamine synthetase. Glutamine is subsequently released by glial cells and taken up by neurons, completing the glutamate–glutamine cycle. From Popoli et al., 2012. (b) Hippocampal volume reduction in depression. Comparison of the volume of the hippocampus between a healthy control and a depressed patient. Modified from Bremner et al., 2000.

Considering the volumetric changes, the involvement of neurotrophic factors was suggested and, in particular, a decrease in brain derived neurotrophic factor (BDNF) was thought to have a primary role in the pathophysiology (Autry & Monteggia, 2012; Castrén & Rantamäki, 2010; Krishnan & Nestler, 2008). This neurotrophic hypothesis came from preclinical evidences that BDNF-mediated signaling is reduced in cortical and limbic brain areas of stress-based animal models of depression (Duman & Monteggia, 2006). BDNF is the main neurotrophin in the adult brain, where is involved in the regulation of neuronal development and survival, synapse formation, synaptic plasticity and synaptic function (Huang & Reichardt, 2001; Waterhouse & Xu, 2009). Recent studies reported that BDNF protein synthesis at synapses plays a critical role in the regulation of local spines and dendritic morphology (Baj et al., 2011; Verpelli et al., 2010). Importantly, BDNF is interconnected with the glutamate system: it promotes the release of both spontaneous and stimulated glutamate release (Autry & Monteggia, 2012) and regulate AMPA and NMDA receptors (Rose et al., 2004), in turns glutamate stimulates the synthesis of BDNF (Mattson, 2008). Accordingly, brain and plasma levels of BDNF were found reduced in depressed patients (Karege et al., 2005; Sen et al., 2008), whereas a concomitant rescue of BDNF levels and structural changes was reported in HPC and PFC/FC, following antidepressant treatments (Castrén & Rantamäki, 2010). Given this interconnection between the glutamate hypothesis and the neurotrophic hypothesis, a new theory called neuroplasticity hypothesis, has recently emerged. In agreement with it, the functional and morphological changes observed in the brain of depressed patients depend on the disruption of the synaptic plasticity (Duman et al., 2017). This property allows the brain to receive and store complex information and to develop adaptive responses to different stimuli. The changes in synaptic functions, neurotrophins levels and remodeling of neuronal circuitry associated with depression suggest that synaptic plasticity may be involved in both the pathophysiology of depression and in the action of antidepressant therapies (Duman et al., 2017; Sanacora et al., 2012).

1.2.3 Therapeutic approaches for major depressive disorders

The standard treatment for depression consists in a combination of psychotherapy and medication with antidepressant drugs. The currently used pharmacological treatments rely mostly on drugs acting

on monoaminergic targets based on the discovery made in 1960s that molecules able to increase the synaptic availability of monoamines exerts an antidepressant effect (Nestler et al., 2002). In particular, two classes of drugs were discovered: the monoamine oxidase inhibitors (MAOI) and the tricyclic antidepressant (TCA), that respectively increase synaptic availability of monoamines by reducing their catabolism (MAOI) or by blocking their presynaptic reuptake (TCA) (Frazer, 1997). Since then, the discovery of their molecular mechanism allowed the development between the 1980s and 1990s of other drugs with a better tolerability (second generation medications, as for example the selective serotonin-reuptake inhibitors (SSRI)) (Frazer, 1997). Although effective in releasing depressive behaviors, monoaminergic drugs have important limitations. First, they need several weeks (sometimes months) of chronic treatment to exert the antidepressant effect representing a problem for forms of depression with risk of suicide (Racagni & Popoli, 2008). Further, they showed adverse effects such as tachycardia, headache, sexual dysfunction, insomnia, fatigue, anxiety, dizziness, constipation, weight gain, reduced appetite, or nausea (Gelenberg et al., 2010). The side effects together with the retarded appearing of therapeutic outcomes often dissuade patients from correctly following the therapy. Moreover, it has been estimated that more than one-third of patients adequately treated for depression do not respond to first-line antidepressant treatments (Souery et al., 2007); among them, 15–33% also fail to respond to two or more different antidepressants, and is identified as treatment resistant (Gaynes, 2009). These data highlight the importance in finding new pharmacological targets that may allow a faster and more tolerable treatment of depression.

1.3 Ketamine

Ketamine (KET) is a racemic mixture of two optical enantiomers, (S)- and (R)-ketamine, that belongs to the class of arylcyclohexylamines (Fig.5). It was serendipitously synthetized in the attempt to lessen the side effects and the abuse potential of phencyclidine (PCP) (Mion & Villevieille, 2013). Ketamine is mostly used as a chlorohydrate racemic mixture for its anesthetic, analgesic and antidepressant effects.

Figure 5. Ketamine chemical structure
Adapted from Pubchem database of chemical molecules

It was approved for clinical use firstly in 1970 (Dundee et al., 1970) after it was demonstrated that the intravenous infusion of 1-5 mg/kg of KET was able to induce anesthesia, without affecting cardiovascular and respiratory functions (Domino et al., 1965). KET induces a specific type of anesthesia named "dissociative anesthesia" that is characterized by catatonia, amnesia, and catalepsy but lack complete unconsciousness. It is accompanied during the recovering from the anesthesia by an experience similar to a detachment from the body and environment with a distorted perception of reality and time (Zanos et al., 2018). The psychotomimetic effects limited its use as anesthetic and made KET a popular recreational drug with severe consequences on abusers ranging from cognitive impairments to cortical structural and functional deficits (Tyler et al., 2017). Intravenous KET is nowadays used also as an analgesic to reduce chronic and acute postoperative pain. The analgesic effect is achieved at lower doses of KET (0.1-0.5 mg/kg) allowing a reduced psychotomimetic risk (Kurdi et al., 2014).

1.3.1 Pharmacology

KET is a non-competitive antagonist of the NMDA receptor (NMDAR) that binds to the allosteric phencyclidine site located within the channel pore of the NMDAR resulting in decreased channel opening time and frequency. NMDAR is historically the first target of KET discovered but many works shown other mechanisms through which ketamine may exert its effect, for example interacting with AMPA, opioid, cholinergic, nicotinic, muscarinic and monoaminergic receptors (Kohrs & Durieux, 1998; Mion & Villevieille, 2013; Tyler et al., 2017). KET can be administered via multiple routes (i.e. i.v., i.m., intranasal, epidural and intrarectal), being the i.v. infusion the most typical since it rapidly produces maximum plasma concentrations. However, intranasal route is an attractive alternative since it is less invasive, results in rapid systemic absorption and is not subject to first-pass hepatic metabolism (Zanos et al., 2018). To note, the Food and Drug Administration (FDA) recently approved intranasal spray of (S)-ketamine (Spravato) as rapid-acting antidepressant for treatment-resistant patients (U.S. Food and Drug Administration, 2019). KET displays low binding to plasma proteins and high liposolubility, and is rapidly distributed in highly perfused tissues, including the brain. KET is extensively metabolized in the liver but also in kidneys, intestine and lungs, to the active metabolite norketamine that is later mainly hydroxylized in 6-hydroxy-norketamine (Tyler et al., 2017).

1.3.2 Preclinical and clinical evidences of the antidepressant effect of ketamine

The first suggestion that modulation of NMDA receptor function could lead to antidepressant response dated back in the 1980s at the evidence that chronic exposure to uncontrollable and inescapable stressors disrupts long-term potentiation (LTP) (Shors et al., 1989), a molecular mechanism of neural plasticity that is dependent on NMDA receptor (Harris et al., 1984). The reduction of NMDA receptor functionality was identified as a common outcome of classical antidepressants (Skolnick et al., 1996). Moreover, different antagonists of the NMDA receptor were shown to be able to mimic the effects of clinically effective antidepressants in animal models (Trullas & Skolnick, 1990). By the mid-1990s, several other preclinical studies suggested that NMDA receptor antagonists had antidepressant properties (Skolnick et al., 2009). These preclinical data together with the increasing discoveries of glutamate system involvement in depression, prompted clinical studies on ketamine's antidepressant activity. It was 2000 when KET was reported for the first time to have an antidepressant effect in humans (Berman et al., 2000). In a placebo-controlled, double-blinded trial, Berman and collaborators administered a sub-anesthetic dose of KET (0.5 mg/kg, 40 minutes infusion) to depressed patients and found a robust antidepressant effect within 4 hours post-infusion. Subsequently, Zarate and colleagues performed a series of randomized controlled studies in treatment-resistant major depressed patients (TRD), who failed at least two conventional antidepressant treatments (Zarate et al., 2006). They demonstrated that a subanesthetic-dose of KET (0.5 mg/kg, i.v.) administered over 40 minutes led to rapid, robust and relatively sustained antidepressant effect in TRD patients.

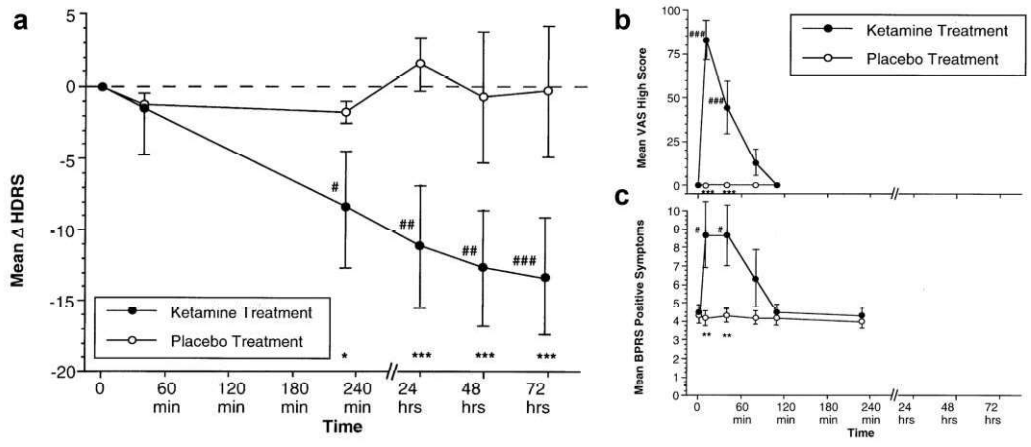

Figure 6. Ketamine fast antidepressant effect in depressed patients

The fast antidepressant effects of ketamine (a), measured as variation in the Hamilton Depression Rating Scale (ΔHDRS), emerges as soon as (b) euphoric (VAS = visual analog scale) and (c) psychotigenic (BPRS = Brief Psychiatric Rating Scale) effects decrease. Comparison to baseline (#) and between groups (*). Modified from Berman et al., 2000

Since then, other clinical trials reported the rapid (within 2 to 4 hours after treatment) and sustained (from few days to more than 2 weeks) antidepressant effect of a single sub-anesthetic dose of KET (Machado-Vieira et al., 2017). Interestingly, it has been shown that KET is also effective to induce a rapid amelioration of suicidal ideation in depressed patients (Ballard et al., 2014) and to reduce anhedonia (Lally et al., 2014). Importantly, Murrough and collaborators (Murrough et al., 2013) demonstrated that the antidepressant effect of KET was not due to its dissociative effects as showed by a higher response rate for the patients administered with KET compared to those who received a psychoactive placebo, namely midazolam. Although robust, the response to KET is transient and the remission period relatively short. Repeated infusions of KET have been tested to overcome this issue and preliminary data suggest that multiple infusions are well tolerated and effective (Diamond et al., 2014) and may be a potential way for extending ketamine's action up to several months (Murrough et al., 2013). However, repeated daily administration of KET in animals has been shown to produce major side effects, including deficits in glutamate and gamma-aminobutyric acid (GABA) synapses, depletion of dopamine levels, and cognitive impairment (Braun et al., 2007; Neill et al., 2010). This highlights the need of more studies on the safety of chronic ketamine treatment. The prospective follow-up data have suggested that, used at subanesthetic doses, KET do not have a long-term psychotogenic risk in healthy human subjects (Perry et al., 2007) and depressed patients (Lahti et al., 2001). However, even at low sub-anesthetic doses, KET treatment induces transient euphoric and psychotomimetic effects in the first hours following its administration (Berman et al., 2000), thus restricting its use to clinical settings and clinical trials (Perry et al., 2007). Despite KET limitations, the discovery of its fast antidepressant effect has led to a sudden increase of research on fast-acting antidepressants, raising hope for more efficient treatments (Machado-Vieira et al., 2009).

1.3.3 Molecular mechanisms of ketamine: its role in plasticity

KET acts at the synaptic level targeting different signaling pathways implicated in synaptic plasticity (Thomas & Duman, 2017). Administration of KET in rodents was shown to rapidly induce (within 30-60 minutes) a transient burst of glutamate in many regions of the brain, including medial prefrontal cortex, that was necessary for its antidepressant effect (Moghaddam et al., 1997). Indeed, the blockade of AMPA receptors prevented KET antidepressant effect highlighting the important role of the AMPA-glutamate interplay in ketamine's antidepressant effect (Maeng et al., 2008). Paradoxically the inhibition of NMDAR induced by KET led to an augmented glutamate signaling. This was explained by the fact that low doses of KET may preferentially bind to NMDARs in an open conformation like those present on the GABAergic interneurons that have a higher tonic firing

compared to pyramidal neurons and so are more likely to be open at any time. The blockade of NMDARs on GABAergic interneurons translate in a reduced inhibitory activity on glutamatergic pyramidal neurons ("the disinhibition hypothesis") (Thomas & Duman, 2017). The disinhibition of pyramidal neurons induces a burst of glutamate that starts a signaling cascade whose primary targets are postsynaptic AMPA receptors. Their activation induces the ion channels to open and depolarize the postsynaptic cell leading to the opening of L-type voltage-gated calcium channels that end up with the release of BDNF (Lepack et al., 2015). Once released, BDNF binds to its receptor tropomyosin receptor kinase B (TrkB) which mediates the activation of the mTORC1 signaling pathway. Each of these steps is necessary for the antidepressant effect of KET and promotes the synaptic changes that parallel its activity. mTOR is a serine/threonine kinase that regulates neurogenesis and dendritic spine growth (Lipton & Sahin, 2014). Li and collaborators showed that KET rapidly and transiently activates mTOR, leading to a long-lasting increase in synaptic proteins and number of spines in PFC/FC (Li et al., 2010). Conversely, blockade of mTOR signaling completely prevented KET induction of synaptogenesis (Li et al., 2010). KET administration also results in similar rapid and transient increase in the phosphorylation of the translation initiation factor 4E-binding protein (4E-BP) and of the p70 ribosomal protein S6 kinases (p70S6K), respectively resulting in de-repression and activation of protein translation (Li et al., 2010). KET also interacts with the pathway of the serine/threonine kinase glycogen synthase kinase-3 (GSK-3) by rapidly promoting its phosphorylation that leads to a deactivation of the enzyme that is necessary for the antidepressant effect (Beurel et al., 2011). Indeed, the administration of subthreshold doses of ketamine together with the GSK-3 inhibitor lithium induced an activation of mTORC1, phosphorylation of GSK-3, synaptoneurogenesis and antidepressant action (Liu et al., 2013). The mechanism of this effect is not clear, but it may be a downstream consequence of BDNF release, which activates Akt, a protein that phosphorylates GSK-3; or it may result directly from mTORC1 activity, which activates p70S6 kinase, which also phosphorylates GSK-3 (Thomas & Duman, 2017). The activation of mTORC1 eventually drives protein translation, including of BDNF. Although classical antidepressants were already able to change the levels of this neurotrophin following several weeks of administration, ketamine administration rapidly increases total BDNF protein levels within 30 minutes.

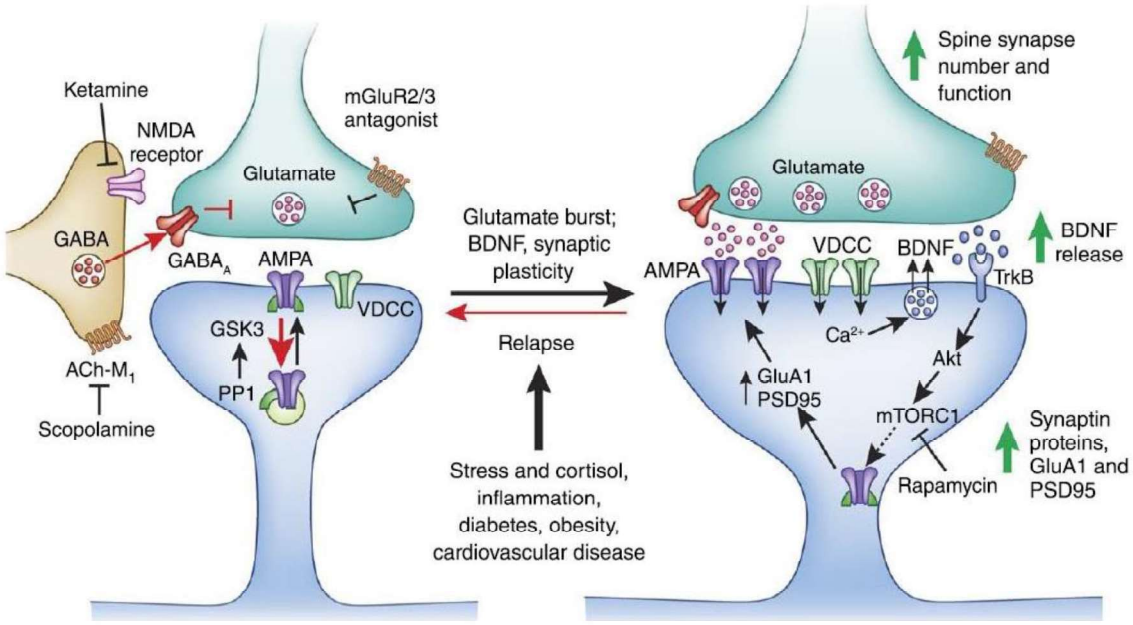

Figure 7. Mechansisms of action of the fast acting antidepressant ketamine in the medial prefrontal cortex

Ketamine causes a burst of glutamate that is thought to occur via disinhibition of GABA interneurons; the tonic firing of these GABA interneurons is driven by NMDA receptors. The glutamate burst stimulates AMPA receptors causing depolarization and activation of voltage dependent Ca2+ channels, leading to release of BDNF and stimulation of TrkB-Akt that activates mTORC1 signaling leading to increased synthesis of proteins required for synapse maturation and formation (i.e., GluA1 and PSD95). Under conditions where BDNF release is blocked (BDNF Met knockin mice) or neutralized (BDNF neutralizing antibody) or when mTORC1 signaling is blocked (rapamycin infusion into the mPFC) the synaptic and behavioral actions of ketamine are blocked. From Duman et al., 2017

Further, it has been shown by Autry and colleagues that KET promotes the synthesis of BDNF in the hippocampus also by preventing the activation of eEF2 kinase (eEF2K) (Autry et al., 2011). Normally, in response to spontaneous synaptic glutamate release, NMDAR triggers the activation of eEF2K that phosphorylates its target protein, eEF2, that inhibits BDNF synthesis; ketamine's NMDA antagonism removes this inhibition. BDNF was proved to be necessary for the antidepressant action of KET as demonstrated by the lack of antidepressant effect of KET in mice with *Bdnf* gene knockdown in the forebrain (Autry et al., 2011) and intra-mPFC infusion of a BDNF-neutralizing antibody (Lepack et al., 2015). Moreover, mice carrying the human *BDNF*^{Val66Met} (rs6265) single nucleotide polymorphism, do not present KET-induced antidepressant effects (Liu et al., 2012). Interestingly, patients carrying the Met rs6265 allele do not respond to KET treatment (Laje et al., 2012). KET is also able to inhibit NMDAR that are located extra-synaptically (Kadriu et al., 2019). Those receptors mainly contain GluN2B subunits which are tonically activated by low levels of glutamate. The activation of GluN2B-containing NMDARs under basal conditions inhibits mTOR-dependent signaling suppressing protein synthesis and thus maintaining synaptic homeostasis. The genetic deletion from cortical neurons of the GluN2B in knockout mice mimicked KET

antidepressant effect and increased the frequency of individual excitatory synaptic events onto pyramidal neurons in layers II/III of the PFC (Miller et al., 2014). Further, optogenetic depletion of GluN2B from pyramidal neurons in the mPFC induced a strong antidepressant-like behavior in mice (Miller et al., 2017). To note, a more recent body of works demonstrated that ketamine's metabolite, (2R,6R)-hydroxynorketamine (HNK), is sufficient to produce an antidepressant response even though it was shown to have a very low binding affinity for the NMDAR suggesting new possible mechanisms beyond NMDAR antagonism (Zanos et al., 2016). HNK in fact induces an increase in glutamate signaling together with the insertion of AMPA receptors in cell membranes. Importantly, Zanos and collaborators (Zanos et al., 2016) showed that the antidepressant effect of HNK was not accompanied in mice by the side effects due to NMDAR inhibition.

1.4 microRNAs

1.4.1. Biogenesis and function

miRNAs are short (~22 nt) single strand non-coding molecules of RNA with a primary role in controlling gene expression (Bartel et al., 2004). They were first discovered by the group of Victor Ambros in the nineties while studying the larval development of *C. elegans* (Lee et al., 1993). Rosalind Lee and Rhonda Feinbaum found that *lin-4*, a gene involved in the timing of larval development, produced a pair of small RNAs instead of a protein that had antisense complementarity to multiple sites in the 3'UTR of the lin-14 gene. They demonstrated that this interaction reduced the amount of LIN-14 protein without changing the levels of lin-14 mRNA therefore suggesting the translational repression as the mechanism that triggers the passage to the second stage of cells division. Almost a decade later, another gene in *C. elegans*, *let-7*, was found to encode a ~22 nt regulatory RNA which acted to promote the transition to adult cell fates (Reinhart et al., 2000). *Let-7* homologs were identified also in fly and human genomes together with let-7 RNA itself (Pasquinelli et al., 2000). Both let-7 and lin-4 were named small temporal RNA (stRNA) given their role in controlling the timing of larval development but in the following years many other ~22 nt RNAs were discovered in Drosophila, human and worms whose expression was not dependent on the stage of development but mainly on the cell types. Because of this reason, the term microRNA (or miRNA) started to be used to refer to small regulatory RNAs that displayed similar features but different functions. Since then this class has grown exceedingly (Lagos-quintana et al., 2002) and, to date, approximately 4800 mature miRNAs sequences and 8480 precursor sequences are deposited in

miRbase database (updated to October 2018) comprising those expressed in animals and plants (Griffiths-Jones, 2004).

miRNAs are mostly transcribed from genes located in regions of the genome that are distant from previously annotated genes suggesting their independency in transcription (Bartel et al., 2004). A number of miRNA genes however is found in the introns of pre-mRNA in the same orientation as the mRNAs indicating that they are processed from the introns and not from their own promoters. Further, some miRNA genes are clustered in the genome and are transcribed as a multi-cistronic primary transcript; these miRNAs are often related to each other (Lagos-Quintana, 2001). miRNA genes represent in human, Drosophila and in C. elegans approximately the 1% of the predicted genes in the genome. The majority of miRNAs are conserved among related animals, for example human and mouse, but often also between distant lineages. miRNAs present in the plants mostly come from regions of the genome distinct from previously annotated genes and like those in animals are evolutionarily conserved (Reinhart et al., 2002). Their initial classification was difficult because of the presence of many other short RNAs in plants. The discovery of miRNAs in both animals and plants suggested a common origin from a shared ancestor but animal and plant miRNAs also display individual characteristics that together with the fact that there are no reports of conserved miRNAs between the two reigns does not exclude the possibility that they developed independently from their last common ancestor (Bartel et al., 2004).

Transcription of primary miRNA transcripts (pri-miRNA) from miRNA genes depends on the genomic locations of the host genes. Usually, when the gene resides in the intron of a protein-coding host gene, the pri-miRNA is transcribed by the RNA polymerase Pol II; however, characteristics of the pri-miRNA deriving from different-located genes, suggest that also in these case the most involved RNA polymerase remains Pol II and not Pol III. For instance, the pri-miRNAs are polyA tailed, often long more than 1 kb (longer than the typical Pol III transcripts) and contain runs of uridine residues (that would terminate Pol III transcription). Once the pri-miRNA is transcribed in the nucleus, it is cleaved by the Drosha RNase III endonuclease, in a complex with DGCR8 protein (DiGeorge Syndrome Critical Region 8), which releases a 60-70 nt miRNA precursor (pre-miRNA) that is characterized by a stem loop with 5' phosphate and ~2 nt 3' overhang (Lee et al., 2002) (Fig. 8). The pre-miRNA is actively transported to the cytoplasm by Ran-GTP and the export receptor Exportin-5 (Yi et al., 2003). In the cytoplasm, Dicer, another RNase III endonuclease, cuts the pre-miRNA after recognizing the double-stranded portion and in particularly the 5' phosphate and the 3' overhang (Lee et al., 2003). Usually Dicer acts in concert with TRBP (or TARBP2). The product of Dicer activity is an imperfect duplex consisting of the mature miRNA and of a fragment similar in

size derived from the opposing arm of the pre-miRNA, typically referred as miRNA*. In plants, the miRNA:miRNA* duplex is produced by the activity of a Dicer-like protein (DCL1) which is a nuclear protein that makes a first cut to the pri-miRNA in the nucleus, then a second cut is made probably again by DCL1 before the duplex exit the nucleus exported by HASTY, an ortholog of Exportin-5 (Reinhart et al., 2002). From this moment on, the pathway of animal and plant miRNAs are overlapping. The miRNA:miRNA* duplex is incorporated as a single-stranded RNA in the RNA-induced silencing complex (RISC), a ribonucleoprotein complex that recognizes the target transcript based on perfect or almost perfect complementarity between the mature miRNA and the target mRNA (Bartel et al., 2004). It is composed by endonucleases, such as members of the Argonaute protein family, which mediate the cut in the middle of the complementary site. Argonaute and its homologs possess a PAZ and a PIWI domains that are able to bind to RNAs long at least 5 nt or double-stranded RNAs. Other proteins that take part in the RISC-complex are Fragile-X-related protein, nuclease Tudor-SN and the suspected RNA-binding protein VIG (Caudy et al., 2002). miRNAs themselves take part in miRNA ribonucleoprotein complex (miRNP) together with other proteins such as, in humans, eIF2C2 (human homolog of Argonaute) to direct cleavage of specific target sites (Mourelatos et al., 2002). After the mature miRNA is loaded onto the RISC, the miRNA* is released and later degraded. The choice of which strand of the duplex is loaded and which one is degraded depend mostly on the stability of their ends (Bartel et al., 2004).

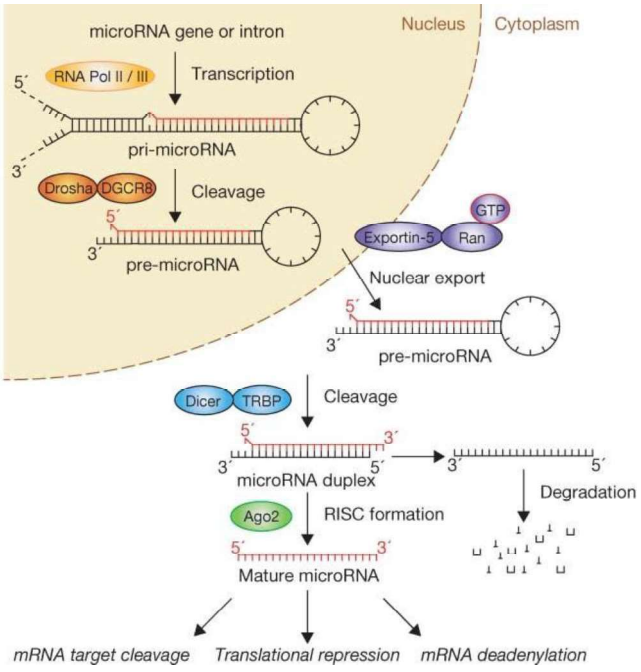

Figure 8. Canonical pathway of miRNA processing

The primary miRNA transcript (pri-miRNA) is transcribed by RNA polymerase II or III and cleaved by the microprocessor complex Drosha–DGCR8 (Pasha) in the nucleus. The resulting precursor hairpin, the pre-miRNA, is exported from the nucleus by Exportin-5–Ran-GTP. In the cytoplasm, the RNase Dicer in complex with the double-stranded RNA-binding protein TRBP cleaves the pre-miRNA

hairpin to its mature length. The functional strand of the mature miRNA is loaded together with Argonaute (Ago2) proteins into the RNA-induced silencing complex (RISC), where it guides RISC to silence target mRNAs through mRNA cleavage, translational repression or deadenylation, whereas the passenger strand (black) is degraded. From (Winter et al., 2009)

The miRNA can thus direct the RISC to downregulate gene expression by two different mechanisms: the mRNA cleavage or the translational repression (Zeng et al., 2003; Zeng et al., 2002). The choice is determined by the target mRNA: if there is perfect complementarity to the miRNA, the target will be cleaved, while if there is insufficient or imperfect complementarity, the RISC will inhibit the translation of the mRNA. Several evidences show that the translational repression is the most common mechanism in animals as suggested by the lower degree of complementarity between metazoan miRNAs and their targets (Bartel et al., 2004). On the other end, the cleavage is more often found in plants (Rhoades et al., 2002). The most efficient translational repression is obtained when multiple RISC cooperate, thus explaining the presence of multiple miRNA complementary sites in many targets of metazoan miRNAs. The recognition of the target is mediated mainly by residues 2-8 in the 5' of the miRNA, often called "seed sequence", which are also the most conserved among homologous miRNAs (Bartel et al., 2004; Lai, 2002; Lewis et al., 2003). This sequence pairs to the complementary sequence present in the 3' untranslated region (3'UTR) of the target directing the RISC activity. The identification of miRNA targets was broadly helped by the development of computational methods that look for multiple conserved regions of miRNAs complementarity within 3'UTRs (Lewis et al., 2003). The evolutional conservation of the sites is used as one of the criterions in the computational analysis, so that the many 3'UTR segments that base-pair equally and stably are excluded. In this way, the perfect base pairing of the 7 nt segment of the miRNA with the target mRNA is not sufficient although most relevant determinant of target prediction (Bartel et al., 2004). For instance, proteins or the structure of the mRNA could influence the accessibility to the binding site. Through their actions, miRNAs control gene expression at different levels and in different ways. Some targets belong to a group of genes that must be evolutionarily switched off in specific cell type and so the miRNAs prevent the expression of their encoded proteins; while some others act fine tuning the expression of their target allowing for a customized protein expression in each cell type.

1.4.2 Role of microRNAs in the CNS

Since the discovery of miRNAs, it was suggested that they could regulate the phases of development and have tissue-specific functions. Indeed, miRNAs showed embryonic- or adult- specific expression pattern together with the ability to be expressed in specific cells or organs (Rajman & Schratt, 2017). In the CNS, these features are extremely important and, as demonstrated by several works, miRNAs

can regulate gene expression in specific neuronal cell types, regions of the brain and at different stages of development (Rajman & Schratt, 2017). They also can be involved in promoting neuronal diseases or exert a protective role. In mammals, a tight spatiotemporal regulation of gene expression is essential for the passage from embryogenesis to postnatal stages. miRNAs are involved in determining the fate of both the major cell types of the brain: neurons and glia (Paridaen & Huttner, 2014). Indeed, it was reported that many miRNAs are differentially expressed within primary cultures enriched for neurons, astrocytes, oligodendrocytes and microglia (Jovicic et al., 2013). Neurogenesis mainly took place during embryonic development, continuing in postnatal stage only in specific areas of the brain i.e. the sub-ventricular zone of the hippocampus (Paridaen & Huttner, 2014). miR-9 is a highly expressed miRNA in the brain and is widely involved in neurogenesis; for instance, its over-expression in mice induces neuronal differentiation through the targeting of the nuclear receptor TLX that regulate neural stem cell renewal (Zhao et al., 2009). By a feedback mechanism, TLX is then able to negatively regulate miR-9 expression highlighting the fine-tuning mechanism with whom this miRNA controls the balance between stem cell renewal and differentiation. Other miRNAs, like let-7b or miR-20a/20b and miR-23, control neurogenesis targeting yet the expression of TLX or the downstream effector of Wnt signaling, cyclin D1 (Ghosh et al., 2014; Zhao et al., 2010). Sometimes, miRNAs function depends on the context; for instance, miR-9 activity increases the number of progenitor cells in *Xenopus* hindbrain while it induces cell apoptosis in the forebrain (Bonev et al., 2011). In the central nervous system (CNS), the presence of specific types of neurons is essential to guarantee the multitude of functions that the brain accomplishes. For example, it was demonstrated that miR-133b promotes dopaminergic neurons differentiation in mice midbrain cultures by targeting the transcription factor Pitx3 (Kim et al., 2007). Interestingly, the levels of this miRNA are decreased in the brains of patients suffering from Parkinson's disease (Kim et al., 2007). Further, motor-neurons differentiation was shown to be controlled by miR-218 by negatively regulating interneuron-specific genes (Thiebes et al., 2015). The neuronal migration is another process in which miRNAs play a role. For example, elevated levels of miR-134 diminish neuronal migration directly regulating the levels of Doublecortin (Dcx), a gene encoding for a microtubule-associated protein involved in migration (Gaughwin et al., 2011). Interestingly, miR-134 belongs to the miR-379~410 cluster that produces other miRNAs with an opposite activity being able to promote migration through the reduction of N-cadherin expression (Rago et al., 2014). Once they reach their correct localization, neurons begin to grow axons and dendrites to establish functional connections. Several findings showed that miRNAs are present in axons and some of them are enriched in this compartment suggesting their role in axonal branching and guidance by the regulation of local protein synthesis (Natera-Naranjo et al., 2010). For example, miR-124 and miR-29a induce axonal branching in hippocampal and cortical neurons,

respectively (Franke et al., 2012; Li et al., 2014). Further, axonal growth is impaired in rat cortical neurons by miR-338 and miR-181c through the modulation of the expression of targets involved in the axon guidance machinery (Kos et al., 2016, 2017). miRNAs are reported to be involved not only in the pre-synaptic site but also in the post-synapses where they participate in dendritogenesis (Sambandan et al., 2017; Siegel et al., 2009). For instance, miR-132 regulates both dendritic growth and branching of hippocampal neurons by targeting p250GAP (Magill et al., 2010). miR-134 instead, controls dendritic growth of rat hippocampal neurons only in an activity-dependent way by targeting Pum2 (Fiore et al., 2009); its overexpression was shown to control dendritogenesis also *in vivo* in the mouse cortex. Importantly, expression alteration of miRNAs that have a role in dendritic dynamics has been linked to different diseases. For example, Lippi and collaborators (Lippi et al., 2016) found that the inhibition in young mice of miR-101, that controls dendritic growth in the CA3 and CA1 of the hippocampus by its target sodium transporter NKCC1, causes cognitive impairment in adulthood. Interestingly, miR-101 targets also Ank2 and Kif1a which are involved in synaptic spines plasticity conferring a key role to this miRNA in regulating the neuronal balancing (Lippi et al., 2016). Dendritic spines are dynamic structures that allow communication between neurons; their morphological and functional rearrangements depend on external stimuli to which they respond undergoing the well-known process of synaptic plasticity. Decades ago, a pivotal work by Schratt and collaborators (Schratt et al., 2006), showed for the first time that miRNAs are involved in this process. In particularly, they found that miR-134 negatively regulated the size of dendritic spines by inhibiting the synthesis of Limk1, a kinase involved in actin polymerization. In the following years many other papers described miRNAs involved in synaptic plasticity (Edbauer et al., 2010; Jasińska et al., 2016; Olde Loohuis et al., 2015).

1.4.3 Role of microRNAs in the response to stress

The response to stress activated by the brain has been shown to be mediated by epigenetic mechanisms such as the activity of miRNAs. The regulation of this response requires a concerted effort by numerous miRNAs, including miRNA clusters and families, and although initially a protective mechanism, stress-induced alterations in miRNA expression are linked to neurodegeneration and to the pathogenesis of neurodegenerative diseases (Hollins & Cairns, 2016). miRNAs are ideal molecules to coordinate the stress response given their ability to fine-tune the expression of numerous genes in a rapid and reversible way. Evidences are present that the exposure to environmental stressors can modulate the expression of miRNAs and of their synthesis machinery (Hollins & Cairns, 2016; Lopizzo et al., 2019). Recent findings showed that lower levels of Dicer1,

as a consequence of stress exposure, are associated with an enhanced vulnerability to stress (Dias et al., 2014). Moreover, genome analysis in a cohort of depressed patients vs healthy controls, reported that polymorphisms within genes such as DGCR8 and AGO1 are associated with an increased risk for depression (He et al., 2012). Stress-induced changes in miRNAs expression can also depend on the brain region (Rinaldi et al., 2010). For example, after acute restraint stress the expression of let-7a, miR-9 and miR-26a/b is increased in the PFC of mice but not in the HPC (Rinaldi et al., 2010). The chronic administration of corticosterone, used to induce a depressive-like phenotype in rats, was shown to change the expression of 26 miRNAs in the PFC of the animals (20 miRNAs upregulated and 7 downregulated) (Dwivedi et al., 2015). Many of the targets of those miRNAs are genes associated with inflammation, synaptic plasticity, cell differentiation, cell survival and adhesion. For example, a negative correlation was reported between genes such as BDNF, AKT1, CREB1 and CAMKIIa with miR-101, miR-218, miR-29a, miR-181c, miR-124, miR-30e and miR-365 (Dwivedi et al., 2015). Another animal model of depression, the repeated inescapable shock, induced an alteration in the expression of miRNAs (miR-96, miR-141, miR-182, miR-183, miR-183*, miR-198, miR-200a, miR-200a*, miR-200b, miR-200b*, miR-200c and miR-429) in the PFC of rats that did not exhibited learned helplessness (Smalheiser et al., 2011). Interestingly, those changes were absent in the animals that showed resilience to the protocol (Smalheiser et al., 2011). Changes in the expression of miRNAs were associated with alteration of neuronal morphology and neural circuitry using acute and chronic immobilization stress (Meerson et al., 2010). Different authors found that miR-134, miR-17-5p and miR-124, which are involved in the regulation of dendritic spines and control of neuronal development and differentiation, are differentially expressed after stress in the CA1 of the hippocampus and in the central nucleus of the amygdala (Beveridge et al., 2009; Schratt et al., 2006; Yu et al., 2008). miRNAs play an important role during brain development, a period in which brain is plastic and more sensitive to external stimuli, by a precise spatial and temporal regulation of gene expression. Recent works suggest that miRNAs can be susceptible to stress insults taking place in this phase (Hollins & Cairns, 2016). For example, it is known that maternal stress can induce permanent alterations in fetal neurodevelopment and subsequent offspring behavior (Huizink et al., 2004). Zucchi and collaborators exposed pregnant rats daily to restraint of the body and forced swimming from gestational day 12 to 18 and then measured miRNAs expression in the brain of newborn offspring (Zucchi et al., 2013). They found 336 miRNAs differentially expressed in response to gestational stress, including miR-103, miR-323, miR-98 and miR-219 (up-regulated) together with a downregulation of genes involved in development and axon guidance. Importantly, the alterations seen in the offspring could be passed on to future generations as elegantly demonstrated in a work of (Yao et al., 2014). The application of stress daily from gestational day 12 to 18 induced a delayed

development in F1, with a stronger impact on F2 and F3. Importantly, the F2 generation showed also alteration in the expression of miRNAs with neuronal function and associated with neuropsychiatric disorders such as miR-23b, miR-96, miR-141, miR-182, miR-183, miR-200a, miR-200b, miR-200c, miR-429 and miR-451 (Yao et al., 2014). It was demonstrated that exposure of male mice to chronic variable stress before breeding induced in the offspring alteration in the HPA axis and in global gene expression (Rodgers et al., 2013). Those changes were attributed to the transgenerational transmission of a series of upregulated miRNAs in the paternal sperm that are able to modify the epigenetic profile and behavior of the offspring (Rodgers et al., 2015). After the exposure to stress, the activation of the HPA axis and the action of glucocorticoids are essential to promote a healthy behavioral response. Several studies showed stress-induced alteration of miRNAs that could affect the regulation of the HPA axis. For example, the upregulation of miR-34c found in the amygdala of adult mice after both acute and chronic stress was shown to modulate anxiety-like behavior by targeting the corticotropin releasing hormone receptor 1 (CRHR1) (Heinrichs & Koob, 2004). Further, it was demonstrated that miR-124 and miR-18 regulate the expression levels of GR proteins in the brain (Uchida et al., 2008; Vreugdenhil et al., 2009) and are both altered following stress exposure (Mannironi et al., 2013; Meerson et al., 2010). The many evidences in support of miRNAs role in stress response constitute a promising key in the study of stress-related disorders, like depression. Indeed, several works in literature showed alterations of miRNAs expression in post-mortem brain samples of depressed patients (Lopez et al., 2014; Smalheiser et al., 2012; Torres-Berrío et al., 2017) as well as in the peripheral blood, cerebrospinal fluid and sperm samples (for a complete review on this topic see (Lopizzo et al., 2019)).

1.4.4 Role of microRNAs in the action of psychotropic drugs

Considering the role that miRNAs might exert in the pathogenesis of depression, it is conceivable that they could be involved as well in the response to antidepressant treatments and represent a putative tool to monitor the efficacy of those drugs. For example, miR-1202 was found reduced by post-mortem analysis in the PFC of depressed patients selectively in those without a history of antidepressant treatment as compared to depressed patients in treatment with antidepressant drugs (Lopez et al., 2014). The *in vitro* treatment of neuronal precursor cells (NPC) with acute or chronic imipramine or citalopram further demonstrated that only the chronic treatment was able to increase miR-1202 levels and subsequently reduced the expression of its target glutamate metabotropic receptor 4 (GRM4) (Lopez et al., 2014). The authors also suggested that plasma levels of miR-1202 may be used as a biomarker of antidepressant response, as supported by other findings (Fiori et al.,

2017). Another miRNA already strongly associated with the pathophysiology of depression is miR-16. Song and collaborators (Song et al., 2015) found decreased levels of this miRNA in the cerebrospinal fluid of drug-free depressed patients compared to control together with a reduction of serotonin levels explained by the reduced ability of miR-16 to target the serotonin transporter (SERT) and thus leading to an increased serotonin reuptake. Conversely, a study in mice showed that the injection of the Selective-Serotonin-Reuptake-Inhibitor (SSRI) fluoxetine in the raphe nuclei caused a downregulation of miR-16 in the HPC of mice and a concomitant increase in SERT expression, suggesting that the fluoxetine-induced downregulation of the miRNA in the HPC has an antidepressant activity (Launay et al., 2011). SERT, which is a well-known vulnerability gene for depression, is targeted also by miR-135. Indeed, increased blood levels of miR-135a were found in depressed patient undergoing cognitive behavioral therapy (CBT) but not in those treated with escitalopram for 12 weeks assuming a role for blood miR-135a as a biomarker of drug effect (Issler et al., 2014). In a work of Grieco and collaborators, a single injection of ketamine induced in 24 h an increase of a cluster of five intronic miRNAs (miR-764-5p, miR-1912-3p, miR-1264-3p, miR-1298-5p and miR-448-3p) within the 5HTR2C gene in the hippocampus of mice (Grieco et al., 2017). Interestingly, the effect was specific for ketamine since the treatment with fluoxetine did not upregulate the expression of the cluster and it was restricted to the HPC as no changes were found in the PFC. Using GSK3 knockin mice to administer the learned helplessness paradigm the authors showed that resilient animals, but not vulnerable, to the paradigm displayed increased hippocampal levels of miR-448-3p and miR-1264-3p and that the administration of an antagonist to miR-448-3p diminished the antidepressant effect of ketamine (Grieco et al., 2017). Another group found that chronic unpredictable mild stress (CUMS) decreased miR-29b-3p levels in the PFC of depressive-like rats while its target GRM4 (metabotropic glutamate receptor 4) was upregulated (Wan et al., 2018). Ketamine treatment instead significantly increased miR-29b-3p (and decreased GRM4) both in depressive-like rats and primary neurons mediating cell survival, cytodendrite growth, increase in extracellular glutamate concentration, together with relief of depressive behaviors (Wan et al., 2018). Together these examples suggest that miRNAs may have an important role in mediating the effect of antidepressant drugs, including novel fast-acting agents such as ketamine.

2. AIMS

Stress is considered a major risk factor for the pathophysiology of neuropsychiatric disorders, including mood disorders such as depression. Although the response of the body to stressful stimuli is evolutionarily an active phenomenon aimed at reestablishing the disrupted homeostasis, our body and especially our brain, could follow different trajectories in response to stress (Popoli et al., 2011). The genetic predisposition combined with the experiences of each individual can differently determine the outcome of the stressful event. Those who manage to activate adaptive responses to stress are able to copy with struggling situations returning to normality at the cease of the stress. Instead, those people who fail in copying with stress activate a series of maladaptive changes that can favor the onset of stress-related pathological conditions (McEwen, 2007). The mechanisms underneath these trajectories are not yet fully understood making the research in this field essential to understand the pathophysiology of disorders in which stress play a key role. Indeed, there are several evidences in literature, both from preclinical experiments and clinical observations, that show an important role of stress in determining the morphological and functional alterations in the brain typical of depression (Kang et al., 2012). Understanding the molecular determinants of these changes could offer insights in the discovery of new targets that can be used also in the development of pharmacological treatments. Above all, the fast-acting antidepressant ketamine provides an example of new promising molecules that are able to induce a rapid and sustained antidepressant effect together with the modulation of the synaptic plasticity (Duman et al., 2017). Recently, a class of non-coding RNAs, microRNAs, has gained attention for their ability to control gene expression thus regulating the production of proteins in a spatial- and temporal-specific manner (Bartel et al., 2004). Interestingly, it was demonstrated that they are involved in the response to stress and in the action of antipsychotic drugs (Hollins & Cairns, 2016; Rajman & Schratt, 2017).

In my thesis project, I aimed at studying the role of microRNAs in the morphological and functional changes induced by chronic stress and the fast-acting antidepressant ketamine in the hippocampus of rats subjected to the Chronic Mild Stress animal model of depression and in primary hippocampal cultures. The first part of the project was focused on analyzing in the hippocampus of rats the differential expression of a series of microRNAs using different techniques. After selecting two miRNAs of particular interest because of their expression pattern and their prior validated involvement in neuronal functioning and in the response to stress, miR-9-5p and miR-135a-5p, we studied their role in directly regulating the morphological changes that we previously observed in the CMS animals (Tornese et al., 2019) using primary neuronal cultures. In parallel, we also set up an *in vitro* model to test whether the changes found in the *in vivo* model directly depend on the stress

hormone corticosterone and to see whether the expression of the selected miRNAs were modulated as well. Since microRNAs exert their function mainly by negatively controlling the expression of target genes, we performed prediction analysis of their targets and validated a list of selected genes involved in synaptic plasticity and neuronal function in order to understand the pathways controlled by miR-9-5p and miR-135a-5p to produce their effect on neuronal morphology. In the last part, we focused on analyzing whether alteration in the expression of the target genes was present in the hippocampus of CMS rats to thus demonstrate a possible mechanism by which the microRNAs modulation influences the stress response. Considering the increasing interest of the new rapid antidepressant ketamine in the treatment of depression and the lack of a completely explained mechanism of action, we also examined the effect of this drug on the expression of the microRNAs both in the CMS rats and in primary hippocampal cultures to elucidate a putative new mechanism of action of this drug.

3. MATERIALS & METHODS

3.1 Animals

Experiments were performed in accordance with the European Community Council Directive 2010/63/UE and approved by the Italian legislation on animal experimentation (Decreto Legislativo 26/2014, authorization N 308/2015-PR). Sprague-Dawley male rats weighing 150 to 175 g (Charles River, Calco, Italy) were housed two per cage at 20–22 °C, 12 h light/dark cycle (light on 7:00 a.m. off 7:00 p.m.), water and food ad libitum, except when required for Chronic Mild Stress.

3.2 Chronic Mild Stress (CMS) paradigm

The rats belonging to CMS group were exposed once or twice daily to random, mild and unpredictable stressors for five weeks (Strekalova et al., 2011; Tornese et al., 2019). Stressors were performed at different time of the day and with a different length of time, in order to minimize prediction. The following stressors were included in the CMS paradigm:

- food deprivation: rats were food deprived for 8-12 h;
- water deprivation: rats were water deprived for 8-12 h;
- over-crowding: rats were randomly housed five per cage for 6-12 h;
- social isolation: each rat was individually housed in a cage for 6-12 h;
- soiled cage: rats were housed in cage soiled with 500 ml of water in the sawdust, for 6-12 h;
- cage tilting: cages were tilted 45° left or right for 6-12 h;
- light-on overnight: rats were housed in a room light turned on from 7:00 p.m. to 7 a.m.;
- light/dark cycle reversal: rats were housed in a room with inverted 12h light/dark cycle (light off from 7:00 a.m. to 7 p.m.; light on from 7:00 p.m. to 7 a.m.);
- forced swim: rats were forced to swim in an upright Plexiglas cylinder (40 cm tall, 30 cm in diameter) filled with cold water (20° C), under conditions in which escape was not possible, for 5 minutes once a week.

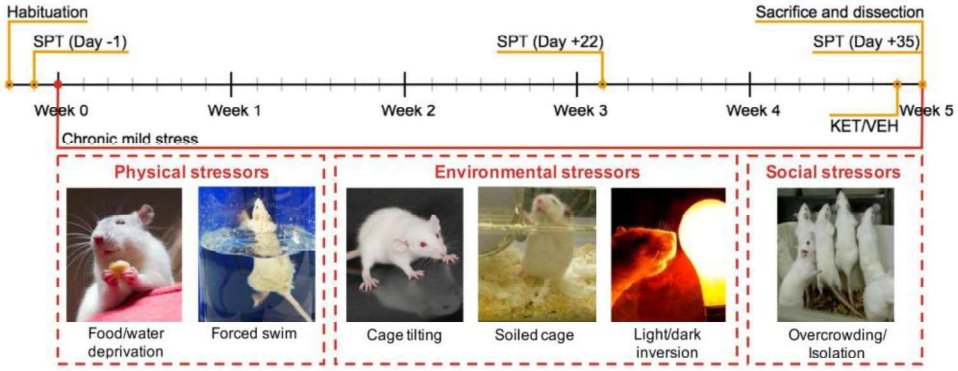

Figure 9. Experimental plan of CMS

Rats were subjected once or twice daily to unprepictable and mild stressors for five weeks. Sucrose preference (SP) test was performed to assess the anhedonic phenotype. Ketamine or vehicle were acutely administered 24 h before sacrifice. From Tornese et al., 2019

3.3 Sucrose preference test

Sucrose preference test was performed as previously reported (Strekalova et al., 2011; Tornese et al., 2019). Two days before the start of CMS, sucrose habituation was performed exposing animals to two bottles containing both 1% w/v sucrose in tap water, for 2h. Animals were subjected to sucrose preference test one day before the start of CMS (to assess baseline preference), after 3 and 5 weeks (1h before sacrifice). Sucrose preference test consisted in presenting rats with two bottles, one containing 0.5% w/v sucrose solution and one containing tap water, for 1h. The position of the bottles was inverted after 30 min. Sucrose preference was calculated as: [sucrose solution intake (ml)/total fluid intake (ml)]x100]. After 3 weeks of CMS, sucrose preference test was used to divide stressed animals in CMS resilient (CMS-R) and vulnerable (CMS-V), applying a cut-off of preference at 55% (Tornese et al., 2019).

3.4 Drug treatment

After 5 weeks of CMS, half of the CMS-V rats were intraperitoneally injected with a single sub-anesthetic dose (10 mg/kg) of racemic ketamine (MSD Animal Health, Milan, Italy), while the remaining animals received physiological solution (0.9% w/v NaCl) (Tornese et al., 2019).

3.5 Cell cultures

3.5.1 Primary hippocampal neurons

Primary hippocampal neurons were prepared as described in (Goslin & Banker, 1991). Briefly, hippocampi from mice embryos at embryonic day 16.5 were dissociated mechanically and neurons were resuspended in Neurobasal™ medium supplemented with B27 (Gibco™, Thermo Fisher

Scientific) containing 30 U/ml Penicillin, 30 mg/mL Streptomycin (Sigma-Aldrich), 0.75 mM Glutamax (Gibco™, Thermo Fisher Scientific) and 0.75 mM L-Glutammine (Gibco™, Thermo Fisher Scientific). Depending on following experiments, neurons were seeded 100.000 cells/ 1.9 cm^2 on 0.1 mg/mL Poly-D-Lysine-coated glass coverslip or 250.000 cells/ 10 cm^2 in 0.02 mg/ml Poly-D-Lysine-coated 6-multiwell plates and maintained at 37°C under a 5% CO_2 humid atmosphere. Three days after seeding, half of the medium was replaced with 24 hours-astrocyte-conditioned medium. After, half of the medium was changed every seven days up to maximum four weeks.

3.5.2 HEK293T cells

HEK293T cells were cultured at 37°C and 5% CO_2 in DMEM medium (Invitrogen) supplemented with 10% of heat-inactivated fetal bovine serum (FBS), 30 U/mL Penicillin, 30 mg/mL Streptomycin (Sigma-Aldrich), 1% minimum Eagle's medium nonessential amino acids (Gibco™, Thermo Fisher Scientific), 1 mM sodium pyruvate (Gibco™, Thermo Fisher Scientific). Cells were split at approximately 80% confluency.

3.6 In situ hybridization

3.6.1 Brain and slices preparation

After sacrifice, freshly right or left hemispheres were rinsed in 1X phosphate buffer saline (PBS) and fixed in 4% paraformaldehyde (PFA) (Sigma-Aldrich) in PBS at 4° C. After 24 h, hemispheres were moved on fresh 4% PFA in PBS and kept at 4° C. After 3 days, hemispheres were moved on PBS containing 30% sucrose, and kept at 4° C until slices preparation. Hemisphere sections of 40 µm were coronally sliced on a cryostat and stored in cryo-protectant sectioning buffer (30% ethylene glycol, 30% glycerol and 0.05M phosphate buffer) at −20 °C.

3.6.2 In situ hybridization

In situ hybridization was developed using the Vectastain® Elite ABC Peroxidase Staining Kit (Vector Laboratories, Segrate, Italy) (La Via et al., 2013). Free-floating sections were post-fixed overnight (ON) in 4% PFA at room temperature (RT) and washed three times in 0.1X Tween 20 in PBS (PBS-T). The slices were then permeabilized with 2.3% w/v sodium metaperiodate in H_2O for 5', and quickly washed in H_2O. The sections were incubated in 1% w/v sodium borohydride in 0.1M Tris-HCl buffer (pH 7.5) for 10', and washed in PBS-T at RT. The slices were digested with 8 µg/ml of proteinase K (Sigma-Aldrich) in PBS-T for 5' and washed in PBS-T. After digestion, the tissue slices

were fixed in 4% PFA for 5' and washed in PBS-T at RT. According to (Pena et al., 2009), slices were incubated twice for 10' in a freshly prepared solution containing 0.13 M 1–methylimidazole (Sigma-Aldrich), 300 mM NaCl, pH 8.0 adjusted with HCl. Subsequently, slices were incubated for 1 h in a solution of 0.16 M 1–ethyl–3– (3–dimethylaminopropyl) carbodiimide (EDC) (Sigma-Aldrich, Milan, Italy) at RT in a humified chamber and then washed twice in PBS. Slices were then incubated ON at 40° C (miR-9-5p) or 50° C (miR-135a-5p) in hybridization solution (20 mM Tris-HCl pH 7.5, 10% dextran sulfate, 1 mM EDTA, 1x Denhardt's solution, 300 mM NaCl, 100 mM DTT, 0.5 mg/mL salmon sperm DNA, 0.5 mg/mL polyadenylic acid, and 25% formamide) containing 100 nM 5'-3'-DIG-labeled probe (mmu-miR-9-5p: 5'-ATACAGCTAGATAACCAAAGA-3'; mmu-miR-135a-5p: 5'-TCACATAGGAATAAAAAGCC-3'; Scramble-miR: 5'-GTGTAACACGTCTATACGCCCA-3'; miRCURY LNA miRNA Detection Probe, Exiqon).
The following day, the slices were washed in 2X SSC-T (saline sodium citrate containing 0.1% v/v Tween 20), formamide-free at 40°C for 10'. Subsequently, the slices were detected using the peroxidase method with biotinylated donkey anti-mouse IgG antibodies and diaminobenzidine as chromogen (Vector Laboratories, Segrate, MI, Italy). The images of in situ hybridization experiments were acquired using an LSM 510 Meta microscope (Carl Zeiss Microscopy, Jena, Germany) with an Achroplan 10x objective at a 2048 (x/y) pixel resolution. The hybridization signal in the soma and in the dendrites was determined measuring the optical density with Adobe Photoshop (version CC 2017). The signal of pyramidal neurons in CA1, CA3 and DG hippocampal regions have been analyzed; 3–4 rats/group, 2–3 slices/rat. All the experiments were coded and analyzed in a blinded manner.

3.7 RNA Isolation, reverse transcription and Real-Time PCR

3.7.1 RNA Isolation

Rat hippocampus

Dissected hippocampi (HPC) were immediately frozen in ethanol/dry ice bath and kept at -80° C until RNA extraction. 100 mg of frozen HPC were added with 1 ml of Tri-Reagent (Sigma-Aldrich, Milan, Italy), and homogenized with steel beads in a TissueLyser LT (Qiagen, Milan, Italy) at 50 Hz for 3'. Homogenized tissue was centrifuged in a 5415R Micro-Centrifuge at 12,000 g for 10' at 4° C, 200 µL chloroform were added to the RNA-containing supernatant and total RNA was extracted using Directzol RNA MiniPrep (Zymo Research, Freiburg, Germany), according to manufacturer's instructions (Bonini et al., 2016). The concentration of the eluted RNA was measured on a NanoVue Plus Spectrophotometer (GE Healthcare Europe GmbH, Milano, Italy).

Neuronal cultures

Neuronal cultures were washed with RNAse-Free PBS and mechanically harvested in 1 mL of TRIzol™ (Thermo Fisher Scientific). An equal amount of 100% ethanol was added to each sample lysed in TRIzol™ and mixed thoroughly. The mix was transferred into a *Zymo-Spin™ IICR Column* and centrifuged at 12.000 g for 30'' to ensure RNA binding to the column. The column was then incubated with 80 µL of DNase I 15' at RT, for digesting Dnases. After two washes with *Direc-zol™ RNA PreWash* (12,000 g for 30'') and one wash with *RNA Wash Buffer* (12,000 g for 30''), the RNA bound to the column was eluted with 40 µL of Dnase/Rnase-Free water. The concentration of the eluted RNA was measured on a Nanodrop™ ND-1000 Spectrophotometer (Thermo Fisher Scientific).

3.7.2 Reverse transcription

For miRNAs, reverse transcription was carried out using miRCURY® LNA® RT kit (Exiqon) following manufactory instructions. Briefly, 2 µL of each template RNA (previously adjusted to 5 ng/µL) were added on ice to 5X miRCURY RT Reaction Buffer, 10X miRCURY RT Enzyme Mix and RNase-free water to a final reaction volume of 10 µL. The complete reaction mix was incubated on an Eppendorf Mastercycler® gradient thermal cycler as follows: 60' at 42° C; 5' at 95° C; hold at 4° C.

For mRNAs, total RNA was reverse transcribed using Moloney Murine Leukemia Virus Reverse Transcriptase (M-MLV RT) (ThermoFisher Scientific). 1 µg of each template RNA was incubated with 0,3 µg/mL Random Primers (ThermoFisher Scientific), 10 mM dNTPs (ThermoFisher Scientific), 5X First Strand Buffer (250 mM Tris-HCl (pH 8.3), 375 mM KCl, 15 mM Magnesium Chloride; ThermoFisher Scientific), 0,1 M DTT (ThermoFisher Scientific), 200U M-MLV RT (ThermoFisher Scientific), and water to a final volume of 20 µL at 37°C for 2 h followed by 10 minutes at 75°C to inactivate the enzyme.

3.7.3 Quantitative Real-Time polymerase chain reaction

Quantitative Real-Time PCR (qPCR) was performed using iTaq Universal SYBR Green supermix (Bio-Rad Laboratories).

miRNAs

For each well of the 96-multiwell (FRAMEstar®, 4titude® from Brooks Life Sciences) the following reaction mix was prepared on ice: 5 µl of SYBR Green; 1 µl of forward + reverse primers 10 µM

(miRCURY® LNA® miRNA PCR assay, Exiqon) (list of probes is reported in Table 1); 4 µl of cDNA, diluted 1:80 in nuclease-free water. The reaction was performed on a 7900HT Fast PCR Systems (Applied Biosystems, Monza, Italy) (RNA from rats HPC) or 7500 PCR System (Applied Biosystems, Monza, Italy) (RNA from neuronal cultures). PCR cycling conditions were: 10' at 95° C; 40 cycles of: 10'' at 95° C, 1' at 60° C. The relative expression of miRNAs was calculated using the comparative C_t ($\Delta\Delta C_t$) method and was expressed ad fold change. The mean of SNORD68 and RNU1A1 was used as a control reference.

mRNAs

2 µL of cDNA (20 ng) was mixed on ice with 10 µl of SYBR Green, 2 µl of forward + reverse primers mix (10 pmol/µL) (list of primers is reported in Table 2), and water to a final volume of 20 µL. The reaction mix was run on a 7500 PCR System (Applied Biosystems, Monza, Italy). PCR cycling conditions were: 2' at 50°C, 10' at 95° C; 40 cycles of: 15'' at 95° C, 1' at 60° C. The relative expression of mRNAs was calculated using the comparative C_t ($\Delta\Delta C_t$) method and was expressed ad fold change. The geometric mean of Gapdh, Actin-β and Hprt was used as a control reference.

Table 1. Probes used for Real Time PCR to measure miRNAs expression in the HPC of rats and in neuronal cultures

Gene	Probe ID	NCBI / miRBase reference
miR-9-5p	YP00204513	MIMAT0000441: 5'UCUUUGGUUAUCUAGCUGUAUGA
miR-135a-5p	YP00204762	MIMAT0000428: 5'UAUGGCUUUUUAUUCCUAUGUGA
miR-15a-5p	YP00204066	MIMAT0000068: 5'UAGCAGCACAUAAUGGUUUGUG
miR-16-5p	YP00205702	MIMAT0000069: 5'UAGCAGCACGUAAAUAUUGGCG
miR-26a-5p	YP00206023	MIMAT0000082: 5'UUCAAGUAAUCCAGGAUAGGCU
miR-26b-5p	YP00204172	MIMAT0000083: 5'UUCAAGUAAUUCAGGAUAGGU
miR-29a-5p	YP00204430	MIMAT0004503: 5'ACUGAUUUCUUUUGGUGUUCAG
miR-29b-3p	YP00204679	MIMAT0000100: 5'UAGCACCAUUUGAAAUCAGUGUU
miR-30a-5p	YP00205695	MIMAT0000087: 5'UGUAAACAUCCUCGACUGGAAG
miR-34a-5p	YP00204486	MIMAT0000255: 5'UGGCAGUGUCUUAGCUGGUUGU
miR-34c-5p	YP00205659	MIMAT0000686: 5'AGGCAGUGUAGUUAGCUGAUUGC
miR-124-5p	YP00204266	MIMAT0004591: 5'CGUGUUCACAGCGGACCUUGAU
miR-125a-5p	YP00204339	MIMAT0000443: 5'UCCCUGAGACCCUUUAACCUGUGA
miR-132-5p	YP00204552	MIMAT0004594: 5'ACCGUGGCUUUCGAUUGUUACU
miR-134-5p	YP00205989	MIMAT0000447: 5'UGUGACUGGUUGACCAGAGGGG
miR-137	YP00206062	MIMAT0000429: 5'UUAUUGCUUAAGAAUACGCGUAG
miR-195	YP00205869	MIMAT0000461: 5'UAGCAGCACAGAAAUAUUGGC
miR-210-3p	YP00204333	MIMAT0000267: 5'CUGUGCGUGUGACAGCGGCUGA
miR-let-7d-5p	YP00204124	MIMAT0000065: 5'AGAGGUAGUAGGUUGCAUAGUU
SNORD68	YP00203911	NR_028128
RNU1A1	YP00203909	NR_004411

Table 2. Primers used for Real Time PCR to measure mRNAs expression in the HPC of rats and in neuronal cultures

Gene	Primer Sequence
Rest	Forward 5'-TCGACACATGCGTACTCACT-3'
	Reverse 5'-TTGTGAACCTGTCTTGCGTG-3'
Gsk-3β	Forward 5'-GGCCACAGGAAGTCAGTTAC-3'
	Reverse 5'-AGTAGAAGAAATACCGCAATCGGA-3'
Sirt1	Forward 5'-CAGGTTGCAGGAATCCAAAGG-3'
	Reverse 5'-TCTCCACGAACAGCTTCACA-3'
Shank2	Forward 5'-ATTGCTGTAATGACGCCCAC-3'
	Reverse 5'-TGCCGCTCTTCCTCTGTTAT-3'
SynI	Forward 5'-CTCAGCAGCACAACATACCC-3'
	Reverse 5'-CAATCTTCTGGACACGCACA-3'
Bdnf	Forward 5'-TCCCTGGCTGACACTTTTGA-3'
	Reverse 5'-TTCCTCCAGCAGAAAGAGCA-3'
Arc	Forward 5'-GCCGCCAAACCCAATGTGA-3'
	Reverse 5'-GTCGCCGGTGGGCACGTA-3'
Akt1	Forward 5'-AGACTGTGGCTGATGGACTC-3'
	Reverse 5'-TTGCCCAGTAGCTTCAGGTA-3'
Extl3	Forward 5'-GTGATCGCATTGTGGGGTTC-3'
	Reverse 5'-TGGCGATATCCTCACAGTTGA-3'
Ctnnd2	Forward 5'-AGCACTGGTGAGACTCCTTC-3'
	Reverse 5'-GCTGTATTTTCCGGTCGTCC-3'
Nptx2	Forward 5'-ACCGGCAGAAGACAGAGAAC-3'
	Reverse 5'-ACGTCTTCTTGATCTTGCCG-3'
L1cam	Forward 5'-ACAAGGACCAGAAGTACCGG-3'
	Reverse 5'-CTGCCCTCTACTGCCATGTA-3'
Actin-β	Forward 5'-CCTCTATGCCAACACAGTGC-3'
	Reverse 5'-CCTGCTTGCTGATCCACATC-3'
Gapdh	Forward 5'-GTTGTGGATCTGACATGCCG-3'
	Reverse 5'-GGTGGAAGAATGGGAGTTGC-3'
Hprt	Forward 5'-GGTGAAAAGGACCTCTCGAAG-3'
	Reverse 5'-GCTTTTCCACTTTCGCTGATG-3'

3.8 DNA constructs

Vectors to overexpress and downregulate miR-9-5p and miR-135a-5p were designed starting from TWEEN-Lenti vector (7970bp) (Fig. 10), that contains the Green Fluorescent Protein (GFP) coding sequence under the control of a hPGK promoter. TWEEN-Lenti vector was kindly given by Prof. Leonardo Elia (University of Brescia).

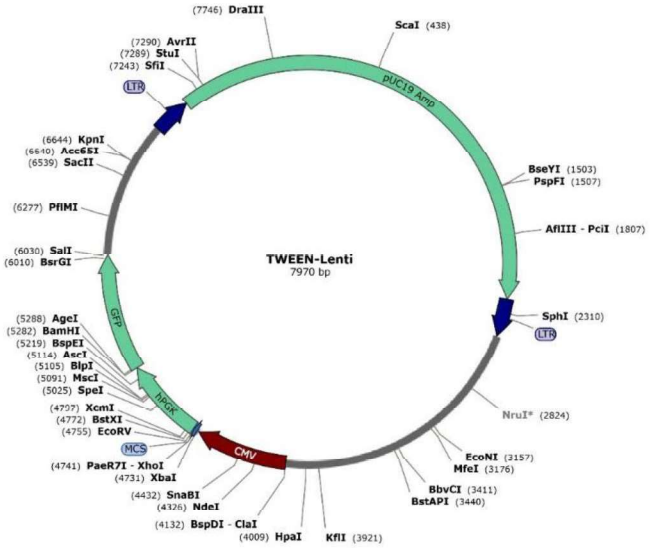

Figure 10. Map of TWEEN-Lenti vector

To obtain the overexpression of miR-9-5p and miR-135a-5p, oligonucleotides were designed specific to the sequence of mmu-miR-9-5p and mmu-miR-135a-5p and annealed *in vitro* to produce dsRNA. Briefly, 1000 pmol of both primer Top and primer Bottom (Eurofins Genomics) were added to 10X Annealing buffer (400 mM Tris-HCl, 500 mM NaCl, 100 mM $MgCl_2$) to a final volume of 100 µL. The reaction mix was denatured 10' at 95°C and then annealed for 45' at 25°C. 40 pmol of annealed oligonucleotides were phosphorylated with T4 Polynucleotide Kinase (Thermo Fisher Scientific) for 20' at 37°C, followed by inactivation with EDTA 0,5 M. The CMV promoter present in the original vector was substituted with the Polymerase III specific promoter H1 using ClaI and XbaI (Fermentas, Thermo Fisher Scientific) to obtain Twl-PGKgfp-H1 (7595 bp, from now on called Twl-H1). After digestion of the vector with XhoI and XbaI, ds-miR9-5p and ds-miR-135a-5p oligonucleotides were cloned in Twl-PGKgfp-H1 using T4 DNA Ligase (Thermo Fisher Scientific) for 1 hour at 22°C. The vectors obtained are Twl-PGKgfp-H1-miR-9-5p (7650 bp, from now on called Twl-H1-miR-9) (as an example, Fig. 11) and Twl-PGKgfp-H1-miR-135a-5p (7650 bp, from now on called Twl-H1-miR-135).

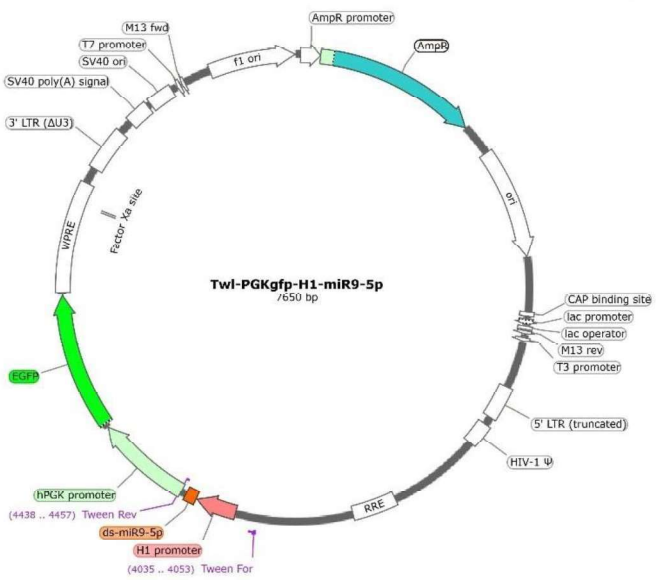

Figure 11. Map of Twl-H1-miR-9 vector

The downregulation vectors were generated by designing a sponge that consists in 3 repeats of a complementary sequence to miR-9-5p or miR-135a-5p interspersed with spacer nucleotides (Giusti et al., 2014). The site for the enzymatic cut of PstI (Fermentas) was inserted within the sequences to allow following screening. Specific oligonucleotides (Eurofins Genomics) were prepared following the same protocol as reported before for over-expression vectors. The Red Fluorescent Protein (RFP) was cloned under the control of the CMV promoter using XhoI and XbaI to obtain Twl-PGKgfp-CMVrfp (from now on called Twl-GFP/RFP). The oligonucleotides were then inserted in the 3'UTR of the GFP digesting Twl-PGKgfp-CMVrfp with SalI. Briefly, Sponge-miR-9-5p or Sponge-miR-135a-5p oligonucleotides were cloned in Twl-PGKgfp-CMVrfp with T4 DNA Ligase (Thermo Fisher Scientific) for 1 hour at 22°C. The vectors obtained are Twl-PGKgfp-CMVrfp-sponge-miR-9-5p (8761bp, from now on called Twl-sponge-miR-9) (as an example, Fig. 12) or Twl-PGKgfp-CMVrfp-sponge-miR-135a-5p (8761bp, from now on called Twl-sponge-miR-135). The presence of the RFP served as a control for the transfection, while the expression of GFP was controlled by the presence of endogenous miR-9-5p or miR-135a-5p binding to the sponge. The empty vectors Twl-H1 and Twl-GFP/RFP were used as controls. The list of the oligonucleotide sequences is reported in Table 3.

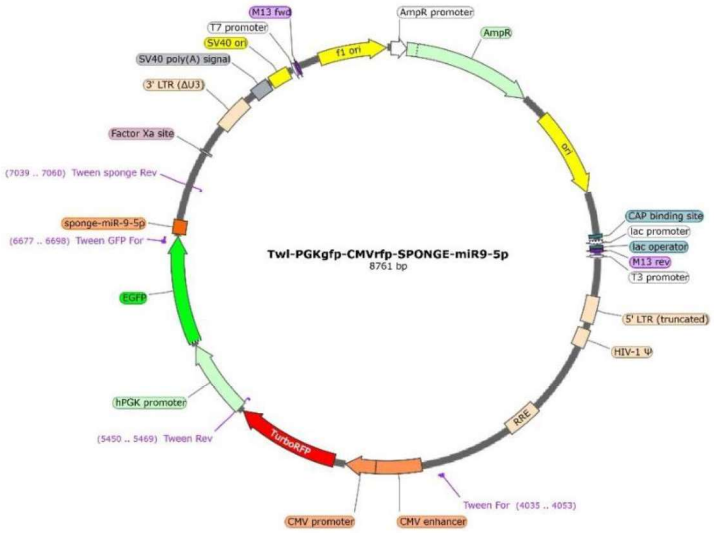

Figure 12. Map of Twl-sponge-miR-9

Table 3. List of primers used to obtain sequences to over-express or down-regulate miR-9-5p and miR-135a-5p

Name	Sequence
ds-miR-9-5p	*Top* : 5'-CTAGAGTCTTTGTTATCTAGCTGTATGACTGCAGTCATACAGCTAGATAACCAAAGATTTTTTC-3'
	Bottom : 5'-TCGAGAAAAAATCTTTGGTTATCTAGCTGTATGACTGCAGTCATACAGCTAGATAACCAAAGACT-3'
Sponge-miR-9-5p	*Top* : 5'-TCGACTCATACAGCTAGATAACCAAAGATGACTGCAGCGTTCATACAGCTAGATAACCAAAGATGAGTCAGTCATTCATACAGCTAGATAACCAAAGAG-3'
	Bottom : 5'-TCGACTCTTTGGTTATCTAGCTGTATGAATGACTGACTCATCTTTGGTTATCTAGCTGTATGAAC*GCTGCAGTCATCTTTGGTTATCTAGCTGTATGAG-3'*
ds-miR-135a-5p	*Top* : 5'-CTAGAGTATGGCTTTTTATTCCTATGTGACTGCAGTCACATAGGAATAAAAAGCCATATTTTTTC-3'
	Bottom : 5'-TCGAGAAAAAATATGGCTTTTTATTCCTATGTGACTGCAGTCACATAGGAATAAAAAGCCATACT- 3'
Sponge-miR-135a-5p	*Top* : 5'-TCGACTCACATAGGAATAAAAAGCCATATGACTGCAGCGTTCACATAGGAATAAAAAGCCATATGA GTCAGTCATTCACATAGGAATAAAAAGCCATAG-3'
	Bottom: 5'- TCGACTATGGCTTTTTATTCCTATGTGAATGACTGACTCATATGGCTTTTTATTCCTATGTGAACGCT GCAGTCATATGGCTTTTTATTCCTATGTGAG-3'

5 to 10 ng of each vector were used to transform competent *E.Coli* bacteria (XL-1 Blue). Briefly, XL-1 Blue were incubated with the plasmid DNA for 30 min on ice, shock heated at 42°C for 30'' and placed again on ice for 5'. 800 µL of Luria Broth (LB, Sigma-Aldrich) were added to the cells and incubated at 37°C for 1h with shaking at 250 rpm. 50 to 150 µL of bacterial resuspension were plated on 10 cm^2 agar-plates containing 50 µg/mL Ampicillin (Sigma-Aldrich) and incubated overnight at 37°C. The colonies present on the plates were let growing in LB medium ON at 37°C under shaking conditions. Plasmid DNA was purified using PureYeld™ Plasmid Miniprep System (Promega, Italy) according to manufacturer's instructions and checked for insertions presence with PCR (PCR cycle conditions: 95°C for 3'; 36 cycles of 95°C for 30'', 56°C for 15'', 72°C for 30''; hold at 4°C) (List of primers is reported in Table 4).

Table 4. List of primers used for PCR and Sanger sequencing

Name	Primer Sequence
Tween For	5'-GGGGGGTACAGTGCAGGGG-3'
PGK For	5'-CGTTGACCGAATCACCGACCTCTC-3'
Tween-CMV For	5'-TAGGCGTGTACGGTGGGAGGTC-3'
Tween-GFP For	5'-GGGATCACTCTCGGCATGGACG-3'
Tween-sponge For	5'-CGGCCGCGTCGACTCACATAG-3'
pmirGLO For	5'-GCAAGATCCGCGAGATTCTCAT-3'
Tween-sponge Rev	5'-GGTTGCGTCAGCAAACACAGTG-3'
Tween Rev	5'-CCCAACCCCGTGGGAATTCG-3'
pmirGLO Rev	5'-ATCTTATCATGTCTGCTCGAAGC-3'

The Sanger DNA sequencing was performed using an ABI3100 sequencer (Applied Biosystem, Perkin-Elmer). The reaction mix is composed of : 1 µL of BigDye™ Terminator v3.1 (ThermoFisher Scientific); 2 µL of 5X Sequencing Buffer, 1 µL of 4 pmol/µL primer (list of primers reported in Table 4), 500 ng of plasmid DNA and water until the final volume of 10 µL is reached. The extension program is as follows: 1' at 96°C, followed by 25 cycles of repeated three steps made of 10'' at 96°C, 5'' at 50°C, 4' at 60°C. After this process, another purification step is made with Dye Terminator removal (DTR) columns to eliminate all the excess of fluorescent terminator dye. Then, the samples are dried at 95°C, resuspended in formamide and denatured at 95°C for 3 min before being processed in the sequencer to obtain the electropherogram.

In order to assess the functioning of the down-regulation vectors Twl-sponge-miR-9 and Twl-sponge-miR-135, HEK293T cells seeded at 50,000 cells/ 1,9 cm^2 in a 24-wells plate were transduced with lentiviruses prepared as reported in paragraph 3.9. The amount of lentivirus was chosen according to previous experiments of titration performed using progressive dilutions of the lentivirus in order to obtain the condition of 100% of cells/slide infected with the lentivirus. Six hours later the same cells were transfected using calcium phosphate with mimics of miR-9-5p or miR-135a-5p (miRCURY LNA miRNA mimic, Exiqon). 24 h later cells were fixed with 4% PFA in PBS, the slides were mounted on glass coverslips and images were captured using an LSM 510 confocal microscope (Carl Zeiss, Jena, Germany).

For morphological analysis, we used GFP expressing vector (pRRLSIN.cPPT.PGK-GFP.WPRE; plasmid #12252) (Fig. 13) purchased from Addgene. This plasmid allows the expression of the

enhanced green fluorescent protein (EGFP) under the control of the human phosphoglycerate kinase 1 promoter (hPGK).

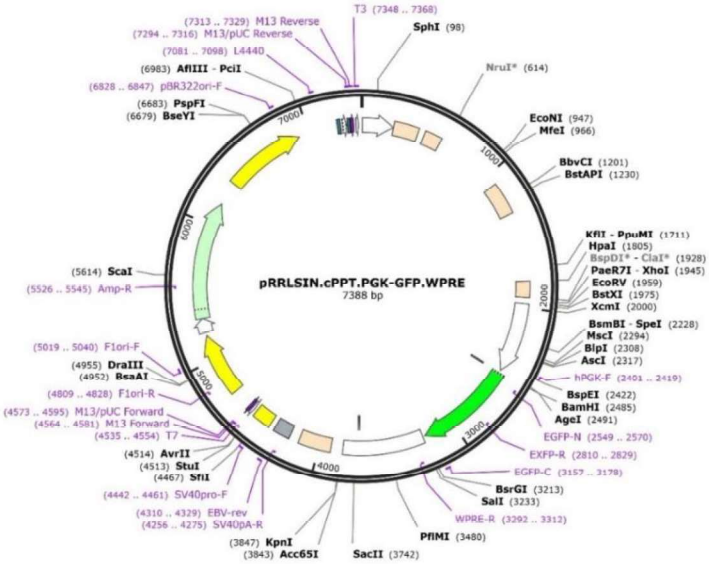

Figure 13. Map of pRRLSIN.cPPT.PGK-GFP.WPRE purchased from Addgene

3.9 Lentivirus production

Lentivirus were produced according to (Filippini et al., 2017). The HEK293T cells were plated at low passages (no more than P7) 24 h before transfection at a density of 9.5×10^6 in 150 mm dish; the medium was changed 2h before transfection. The plasmids mix for one dish is prepared by adding: VSV-G envelope gene in pMD2.G backbone vector 7µg, PACKAGING plasmids pCMV ΔR8.74 II Gen.Pack 16.25µg, pRSV-rev plasmid 6.25µg, TRANSFER Vector containing the transgene (Twl-H1 or Twl-GFP/RFP or Twl-H1-miR-135 or Twl-H1-miR-9 or Twl-sponge-miR-9 or Twl-sponge-miR-135) 32µg. The plasmid solution is made up with a final volume of 1125 µL with 0.1X TrisEDTA (TE 0.1X)/dH_2O (2:1); 125 µL of 2.5 M $CaCl_2$ are added to the suspension; the mixture is maintained 5 min at RT. The precipitate is formed by adding dropwise 1250 µl of 2X HBS (HEPES-buffered saline: 50 mM HEPES, 280 mM NaCl, 1.42 mM $Na_2HPO_4\cdot7H2O$) solution to the mixture. The suspension should be added immediately to the cells following the addition of 2X HBS. The calcium phosphate-plasmid DNA mixture is maintained on the cells for 14-16 h, after which the medium is replaced with fresh medium. After 24 h and 48 h from medium replacement, the cells supernatant is collected. Then, after the ultracentrifugation of the supernatant at 26,500 rpm for 2 h at 4°C, the viral pellet is resuspended in PBS and kept at -80° C.

3.10 Transfection of neuronal cultures for morphological analysis

Neuronal cultures were transfected at DIV7 (GFP expressing vector) or DIV11 (miRNAs expression vectors) using Magnetofection™ Technology (Oz Biosciences, Marseille, France) according to the manufacturer's protocol. Each plasmid was incubated with NeuroMag magnetic beads in the ratio of 1 µg (DNA):3.5 µL (NeuroMag) in 100 µL of Neurobasal™ for 20 minutes and added drop-by-drop to the cells. The cells were than incubated on a magnetic plate for 15 min at 37°C. After 1 h medium was completely changed, and neurons were maintained at 37°C under a 5% CO_2 humid atmosphere.

Seventy-two hours post-transfection, neuronal cells transfected with miRNAs expression vectors were washed in 1X HBSS and fixed in 4% PFA for 20' at RT. Then cells were washed 3 times for 5' in PBS and mounted on coverslip using SlowFade™ Diamond Antifade Mountant (ThermoFisher, USA).

Neuronal cultures transfected with GFP expressing vector were kept undisturbed except for the weekly change of medium until DIV17 when they were used for live imaging acquisition and drug treatments.

3.11 Confocal microscopy and imaging analysis

<u>miRNAs expression vectors</u>

Fluorescently labeled cells were acquired using a confocal microscope LSM880 Upright (Carl Zeiss, Jena, Germany) with a 20x objective at a resolution of 1980 (x/y) pixel. Pictures represent maximum intensity projections of 5 consecutive optical sections taken at an 8 µm interval (Fig. 14a). Total dendritic length and number of branches were manually traced using Simple Neurite Tracer from Fiji (Schindelin et al., 2012) (Fig. 14b). For each condition a minimum of 15 cells was analyzed. The number of spines was measured manually using ImageJ (NIH, Bathesda, USA) and spine density was calculated by quantifying the number of spines in a 10 µm dendritic segment (Fig. 14c). For each condition, spines of three secondary dendrites from a minimum of 15 cells were analyzed.

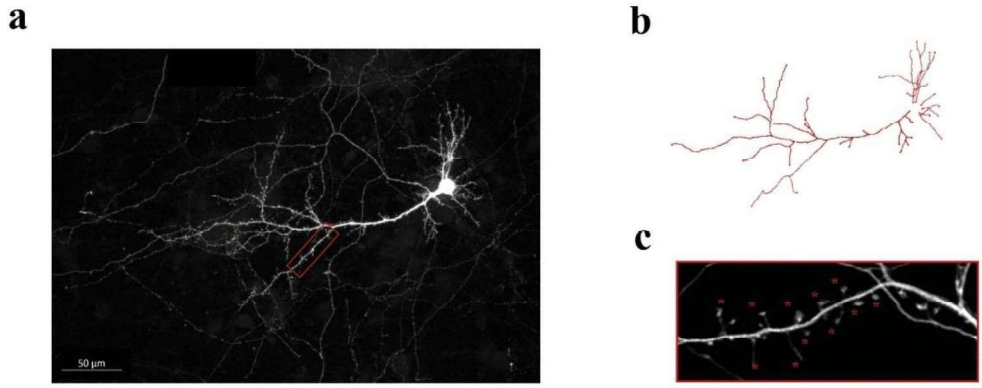

Figure 14. Analysis of dendritic morphology and spine density of primary hippocampal neurons transfected with miRNA expression vectors

(a) Maximum Intensity Projection of the picture of a fluorescently-labeled neuron captured with a Zeiss LSM880 confocal microscope. Images of neurons with a pyramidal-like shape were taken 72 h after the transfection with the miRNA expression vectors. (b) Reconstruction of neuronal dendrites was made with Fiji using the function "Simple Neurite Tracer". (c) The density of dendritic spines was measured manually counting the number of spines along a 10 µm segment of the secondary dendrites.

GFP expression vector

Fluorescently labeled cells were acquired using a confocal microscope LSM880 Inverted (Carl Zeiss, Jena, Germany) with a 20x objective at a resolution of 3964 (x/y) pixel. Pictures represent maximum intensity projections of 8 consecutive optical sections taken at an 0.96 µm interval. Images were taken at living cells kept in a humid chamber at 37°C and 5% CO_2 (T0) and after being fixed with 4% PFA (T1). A minimum of 10 cells were acquired for each condition. Total, apical and basal dendritic length of each cell at T0 and T1 was measured using Simple Neurite Tracer from Fiji (Schindelin et al., 2012). Difference between T0 and T1 measurements within the same cell is expressed as ΔT1-T0 (µm) (Fig.15).

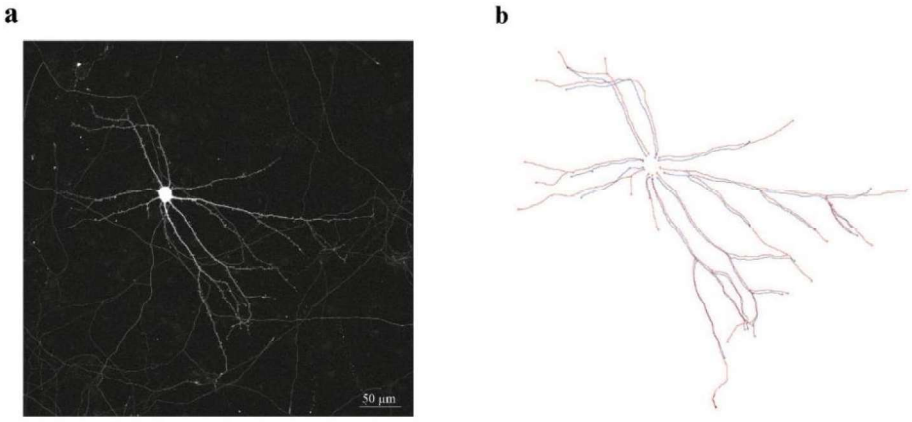

Figure 15. Analysis of dendritic morphology of primary hippocampal neurons transfected with the GFP expression vector

(a) Maximum Intensity Projection of the picture of a fluorescently-labeled neuron captured with a Zeiss LSM880 confocal microscope. Images were taken at DIV17 (T0) maintaining the cells alive at 37°C and 5% CO_2 and at DIV21 (T1) after the cells were

fixed in 4% PFA. (b) Recontruction of neuronal dendrites at T0 (red line) and T1 (blue line) was made with Fiji using the function "Simple Neurite Tracer".

3.12 In vitro corticosterone and ketamine treatment

RNA and protein extraction

DIV17 hippocampal neurons were treated with corticosterone 200 nM (or dimethyl sulfoxide, DMSO) (Sigma-Aldrich) twice daily (9.00 am and 17.00 pm) for three days. Half of the medium was replaced during every morning treatment with astrocyte-conditioned medium. At the end of the protocol, ketamine 1μM (MSD Animal Health, Milan, Italy) was added to the cells (KET treatment group) for 4 h. Cells were then washed with 1X HBSS and harvested for RNA or protein extraction in 1mL of TRIzol™ (Thermo Fisher Scientific) and 100μL of RIPA, respectively.

Morphological analysis

DIV7 hippocampal neurons seeded in 2-wells Lab-Tek® II (Nunc®, Sigma-Aldrich) at 210,500 cells/ 4 cm^2 density were transfected with GFP expression vector using Magnetofection™ Technology (Oz Biosciences, Marseille, France) according to the manufacturer's protocol. Fluorescently labeled cells were firstly acquired at DIV17 (T0) using an LSM880 inverted confocal microscope (Zeiss, Jena, Germany) with a 20X objective. T0 acquisition was performed maintaining the cells in a 5% CO_2 atmosphere at 37°C to keep the cells alive. Cells were then treated with corticosterone and ketamine as previously described and, at the end of the protocol, fixed with 4% PFA. A second registration of the same cells was performed at DIV20 (T1) using the same acquisition settings.

3.13 Analysis of miR-9-5p targets and *in vitro* validation

3.13.1 Bioinformatic target prediction

To perform target predictions for miR-9-5p we used TargetScan (Lewis et al., 2005), mirDB (Chen & Wang, 2020) and microT-CDS (Reczko et al., 2012). Given the elevated number of predicted targets, the following criteria were used to select the targets for reporter gene assays: (i) presence of at least one conserved 8mer, 7mer-m8, or 7mer-A1 site, (ii) reported validation of the interaction present in literature, (iii) reported importance for brain function and plasticity. The list of selected targets is the following: SIRT1, GSK-3β, REST, SORT1, DRD2, NTRK3, ELAVL1.

3.13.2 Preparation of plasmids for the Luciferase-based assay

Short and long constructs of the 3' untranslated region (3' UTR) containing the binding site for the microRNA were cloned into a pmirGLO Dual-Luciferase expression vector (Promega) (Fig. 16).

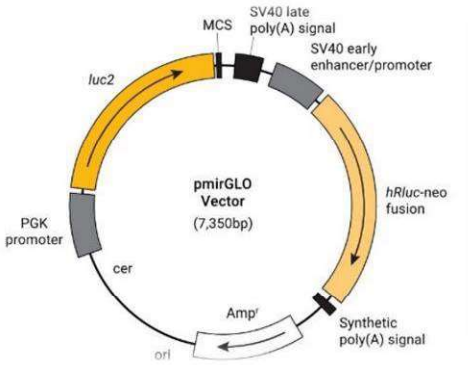

Figure 16. Map of pmirGLO vector purchased from Promega

As shown in the map, pmirGLO vector is a dual-reporter vector that allows the concomitant expression of both *Firefly* and *Renilla* luciferase

A sequence spanning 30 bp on either side of the binding site of miR-9-5p on GSK-3β, DRD2, SIRT1, SORT, NTRK3, ELAVL1 and REST 3' UTRs was obtained annealing specific oligonucleotides (see Table 5 for the complete list of oligonucletides) and later cloned into the pmirGLO vector by digestion with XbaI/SacI or XhoI/XbaI (NEB). Following the cut, the inserts and the vector were ligated using T4 DNA Ligase (NEB) in 20 µL of reaction mixture composed of 1 µL of T4 DNA Ligase, 2 µL of 10X T4 DNA Ligase Buffer, 50 ng of cut vector, 37.5 ng of cut insert, and water. The mixture was incubated 10' at RT and then the enzyme was heat inactivated at 65°C for 10'. XL-1 Blue bacteria were transformed with the ligated plasmids following the same protocol as described in paragraph 3.8 and correct insertions were validated by sequencing of the plasmidic DNA with pmirGLO For and pmirGLO Rev (sequences of primers are reported in Table 4).

Table 5. List of oligonucleotides used for cloning vectors for Luciferase assay (short constructs)

Gene		Primer sequence (5'-3')
Drd2	Top	CGCTCCAACTCTGTAACATCACCATACATGCACCAAACCAATAAAACCTTGACAAGAGTCATTCCCAT
	Bottom	CTAGATGGGAATGACTCTTGTCAAGGTTTTATTGGTTTGGTGCATGTATGGTGATGTTACAGAGTTGGAGCGAGCT
Sort1	Top	CAACCTGAACTTTAATGTCTTTTGGAACAAAACCAAAGTTTAAGATTTGCCATATGACGACGTGGTGAT
	Bottom	CTAGATCACCACGTCGTCATATGGCAAATCTTAAACTTTGGTTTTGTTCCAAAAGACATTAAAGTTCAGGTTGAGCT
Ntrk3	Top	CCTGGGTTCTTAAGGCAAGTGCCCTGTAAACACCAAAGTCTTGTATTTTCTACTCTCAGCCAGCATTGT
	Bottom	CTAGACAATGCTGGCTGAGAGTAGAAAATACAAGACTTTGGTGTTTACAGGGCACTTGCCTTAAGAACCCAGGAGCT
Elavl1	Top	CTTTTGTAAGCCCAGGCACCAATGAGAACGGACCAAAGAGTTTCAGGGCAGCTCCAGTATATTCCAGAT
	Bottom	CTAGATCTGGAATATACTGGAGCTGCCCTGAAACTCTTTGGTCCGTTCTCATTGGTGCCTGGGCTTACAAAAGAGCT
Sirt1	Top	CATGTTAATGTAAAGGGAACAGCTTATCTAGACCAAAGAATGGTATTTCACACTTTTTTGTTTGTAACT
	Bottom	CTAGAGTTACAAACAAAAAAGTGTGAAATACCATTCTTTGGTCTAGATAAGCTGTTCCCTTTACATTAACATGAGCT
Rest	Top	TCGAGAGTTGGTTGAACTTGGAATTGACTGGGAGGCCAAAGATTTAAAAAGCAGATTTTCTCAAGACACAGTT
	Bottom	CTAGAACTGTGTCTTGAGAAAATCTGCTTTTTAAATCTTTGGCCTCCCAGTCAATTCCAAGTTCAACCAACTC
Gsk-3β	Top	CTGGGCCCTGAGGTAGATCTTGGTTCACCTGACCAAAGGCCGCCTGCTTCTCCCGGTATTGTTTTGAGT
	Bottom	CTAGACTCAAAACAATACCGGGAGAAGCAGGCGGCCTTTGGTCAGGTGAACCAAGATCTACCTCAGGGCCCAGAGCT

Rat GSK-3β 3'UTR (839 bp), SIRT1 3'UTR (403 bp) and REST 3'UTR (1825 bp) were amplified from wild-type rat cDNA (primer sequences listed in Table 6). The inserts were cloned into pmirGLO vector (Promega) by digestion with XbaI/SacI or XhoI/SalI (Thermo Fisher Scientific) in O Buffer for 2 h at 37°C. Cut vector and inserts were run on a 1% agarose gel, purified by gel purification kit (Fisher Molecular Biology) and ligated at 22 °C for 1 h with T4 DNA Ligase (Thermo Fisher Scientific). XL-1 Blue bacteria were transformed with the ligated plasmids following the same protocol as described in paragraph 3.8 and correct insertions were validated by sequencing of the plasmidic DNA with pmirGLO For and pmirGLO Rev (sequences of primers are reported in Table 4).

Table 6. List of primers used for cloning vectors for the Luciferase assay (long constructs)

Name	Primer Sequence
Gsk3β-UTR	Forward: 5'-TGTTCAGGGCAGTGATTCTGTT-3'
	Reverse: 5'-TTCTCCTGCCGTGCGCAATGA-3'
Sirt1-UTR	Forward: 5'-TTTTCTCGAGGTTCCATCATTTCTG-3'
	Reverse: 5'-ATCCGTCGACCAAACTCTGAG-3'
REST-UTR	Forward: 5'-GCTAGCCTCGAGGTGACATTTTGCTGGAATAACCTCTG-3'
	Reverse: 5'-TGCAGGGTCGACATCACGTTCAACTTATCCTATACAGTCTT-3'

3.13.3 Luciferase-based assay

The Dual Luciferase® Reporter assay (E1910, Promega) was used according to the manufacturer's protocol. HEK293T cells were plated at 1 x 10^4 cells/well on 96-well plates in 1X DMEM without Pen/Strep and the day after co-transfected with 100 ng of pmirGLO-GSK-3β-UTR or pmirGLO-SIRT1-UTR or pmirGLO-REST-UTR construct vector and 2 µM of miR-9-5p or miR-135a-5p mimics (Dharmacon) or negative siRNA (Dharmacon) using DharmaFECT Duo (0.12 µL/well; Dharmacon) according to the manufacturer's instruction. Forty-eight hours post-transfection, cells were washed with PBS and lysed by gently rocking for 20 min at RT in 20 µL of 1X PLB (Passive Lysis buffer*).* 100 µL of LARII (Luciferase Assay Reagent) were dispensed in each wells and *Firefly* luciferase activity was measured by reading luminescence (0.1 sec) with an EnSight™ Multimode Plate Reader (PerkinElmer). Further, a second reading of the *Renilla* luciferase activity was performed after adding 100 µL of Stop & Glo® Reagent. *Firefly* luciferase signal was normalized to

Renilla signal and expressed as Relative Luciferase Activity. All transfections were performed in triplicate and the experiment was repeated at least three times.

3.14 miR-9-5p expression modulation in neuronal cultures for RNA and protein extraction

DIV11 hippocampal neurons were transfected with miR-9-5p miRCURY LNA miRNA Inhibitor, miR-9-5p LNA miRNA mimic or negative control (Exiqon) using Magnetofection™ Technology (Oz Biosciences, Marseille, France) according to the manufacturer's protocol. Briefly, inhibitor and negative control were incubated with NeuroMag magnetic beads in the ratio of 25 pmol (miRNA):3.5 µl (NeuroMag) or 5pmol (miRNA):3.5 µl (NeuroMag) for mimic in 200 µl of Neurobasal™ for 20 minutes and added drop-by-drop to the cells. The cells were than incubated on a magnetic plate for 15 min at 37°C. After 1 h medium was completely changed and neurons were maintained at 37°C under a 5% CO2 humid atmosphere. After 72h, cells were washed with 1X HBSS and mechanically harvested in 1mL of TRIzol™ (Thermo Fisher Scientific) for RNA extraction or in 100 µL of RIPA for protein purification.

3.15 Western-blotting

3.15.1 Protein preparation and quantification

Cells harvested from primary hippocampal cultures (approximately 300,000 cells) were solubilized with RIPA (50 mM Tris-HCl, pH 7.4, 150 mM NaCl, 1 mM EDTA, 0.1% SDS, 1% NP-40, 0.25% sodium deoxycholate and Roche protease inhibitor tablets). The suspension was then sonicated and immediately frozen.

HPC (approximately 200 mg) were homogenized in 2 ml of ice-cold Homogenization Buffer (HB: 10 mM Tris, 0.32 M sucrose, EGTA 0.1 mM, pH 7.4). Protease inhibitors (Sigma-Aldrich) and phosphatase inhibitors (PhI) (Thermo Fisher Scientific) were added to HB in order to protect samples from degradation. 200µL of homogenate were aliquoted and immediately frozen.

Proteins concentration was quantified with the bicinchoninic acid (BCA) protein concentration assay (Sigma–Aldrich, St. Louis, MO, USA) using known concentration of bovine serum albumin (BSA) as reference.

3.15.2 SDS-PAGE

Equal amounts of proteins (10 or 30 µg) were diluted in 1X NuPAGE™ LDS Sample Buffer (Thermo Fisher Scientific) and 1X DTT (1,4-Dithiothreitol, Fluka BioChemika) and denatured at 75° C for

10’. Samples were loaded in handmade 7,5% or 10% polyacrylamide gels (for the composition, see Table 7). Proteins were electrophoresed in a Mini-PROTEAN Electrophoresis cell (Bio-Rad) containing running buffer (25 mM Tris-HCl, 250 mM Glycine, 0.1% SDS), by applying 70 V for 10’ and then 130 V with a Power PAC basic power supply (Bio-Rad). Electrophoresis was controlled with the use of Precision Plus Protein Dual Color standards (Bio-Rad).

Table 7. SDS-PAGE gel composition

Running gel (10%)	Running gel (7,5%)	Stacking gel (4%)
10% v/v Acrylamide/Bis-acrylamide (29:1)	7,5% v/v Acrylamide/Bis-acrylamide (29:1)	4% v/v Acrylamide/Bis- acrylamide (29:1)
375 mM Tris-HCl pH 8.8	375 mM Tris-HCl pH 8.8	125 mM Tris-HCl pH 6.8
0.1% v/v SDS	0.1% v/v SDS	0.1% v/v SDS
0.1% v/v Ammonium persulfate	0.1% v/v Ammonium persulfate	0.1% v/v Ammonium persulfate
0.04% v/v Tetramethylethylenediamine	0.04% v/v Tetramethylethylenediamine	0.1% v/v Tetramethylethylenediamine
H_20 to final volume	H_20 to final volume	H_20 to final volume

3.15.3 Immunoblotting

Following electrophoresis, proteins were transferred on nitrocellulose membranes (GE Healthcare Europe GmbH) in a Mini-PROTEAN Electrophoresis cell (Bio-Rad) containing transfer buffer (NuPAGE™ Transfer Buffer 1X, 20% v/v methanol), by applying 200 mA for 2 or 3 h at 4° C with a Power PAC basic power supply (Bio-Rad). The membranes were blocked for 1 h with 5% w/v non-fat dry milk in Tris-buffered saline containing Tween 20 (TBS-T: 20 mM Tris, 137 mM NaCl, 0.1% v/v Tween 20, Sigma-Aldrich) to avoid non-specific binding. Membranes were then incubated ON at 4° C with specific antibodies diluted in TBS-T containing 3% w/v non-fat dry milk (a list of the antibodies and their experimental conditions are reported in Table 8). After 3 washes of 10’ with TBS-T, membranes were incubated for 1 h at RT with IRDye fluorescent-labeled secondary antibodies (LI-COR Biosciences). Membranes were then washed 10’ in TBS-T for three times, protecting membranes from light. Protein bands were detected on an Odyssey Fc Imaging System (LI-COR Biosciences) at 700 or 800 nm, depending on the fluorophore used. Protein bands were quantified on Image Studio software (version 5.2, LI-COR Biosciences). Data are presented as optical density ratios of the investigated protein band normalized on GAPDH or α-TUBULIN in the same line and are expressed as percentage of controls.

Table 8. List of primary and secondary antibodies used for Western-blotting

Protein	Primary antibody	Secondary antibody
Gsk-3β	Mouse monoclonal (Abcam # 05-412) 1:1000 ON at 4° C	Goat anti-mouse IgG (H+L) (IRDye 926-32210, LI-COR) 1:2000 in TBS-T for 1 h at RT
Sirt1	Rabbit monoclonal (Abcam ab189494) 1:500 ON at 4° C	Goat anti-rabbit IgG (H+L) (IRDye 926-32211, LI-COR) 1:2000 in TBS-T for 1 h at RT
Rest	Rabbit polyclonal (Abcam ab202962) 1:500 ON at 4° C	Goat anti-rabbit IgG (H+L) (IRDye 926-32211, LI-COR) 1:2000 in TBS-T for 1 h at RT
Gapdh	Mouse monoclonal (Millipore cod. Mab374) 1:8000 ON at 4° C	Goat anti-mouse IgG (H+L) (IRDye 926-68020, LI-COR) 1:2000 in TBS-T for 1 h at RT
α-Tubulin	Mouse monoclonal (Abcam ab7291) 1:20000 ON at 4°C	Goat anti-mouse IgG (H+L) (IRDye 926-68020, LI-COR) 1:2000 in TBS-T for 1 h at RT

3.16 Statistical Analysis

Data were shown as mean ± standard error of mean (SEM). Statistical analysis of the data was performed using GraphPad Prism 8 (GraphPad Software Inc., USA). Student's t test followed by Welch's correction was applied in Luciferase assay experiments and in the analysis of morphological changes after miR-9-5p and miR-135a-5p modulation. For all the other experiments, One-way ANOVA followed by Tuckey's post-hoc test or Newman-Keuls Multiple Comparison was used. Statistical significance was assumed at $p<0.05$.

4. RESULTS

4.1 Chronic Mild Stress impairs apical dendritic arborization of hippocampal neurons in the CA3 of CMS-V rats. Ketamine has a rapid restorative effect

In Tornese et al. (Tornese et al., 2019), we used the Chronic Mild Stress (CMS) protocol to induce a depressive-like phenotype in rats. Applying the Sucrose Preference Test to measure anhedonia, we were able to distinguish between resilient (CMS-R) and vulnerable animals (CMS-V) depending if the rats showed a preference that was higher than the threshold (55 %) (Strekalova et al., 2011) or lower, respectively. Importantly, the injection of a single sub-anesthetic dose of ketamine (10 mg/Kg) to CMS-V rats was able to completely revert the anhedonic phenotype in 24 h, as shown by the rescue of the Sucrose Preference in CMS-V+KET (Fig. 17).

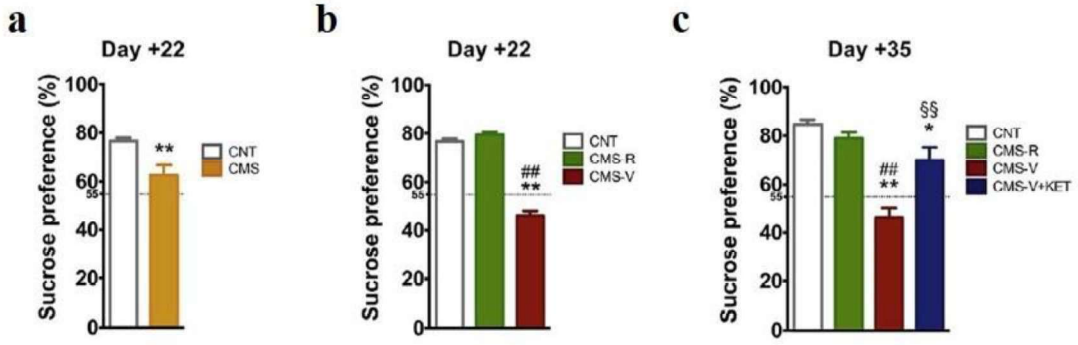

Figure 17. Sucrose Preference Test (SPT)

(a) SPT of CNT and CMS rats at Day +22 of CMS. (b) Separation of resilient and vulnerable animals applying a cut-off at 55% of sucrose preference at Day +22 of CMS. (c) SPT of CNT and CMS rats at Day +35 of CMS, 24 h after KET/VEH treatment. Data are shown as means + SEM. n = 25-30. *p<0.05 vs CNT; **p<0.001 vs CNT; ##p<0.001 vs CMS-R; §§p<0.001 vs CMS-V. Modified from Tornese et al., 2019

Morphological analysis of hippocampal pyramidal neurons revealed peculiar changes induced by chronic stress and ketamine. In particularly, there was a significant reduction of the total length of apical dendrites (but not basal) in the CA3 of CMS-V rats together with a dendritic simplification (Fig.18). These alterations were not present in the CMS-R and were completely reversed by KET.

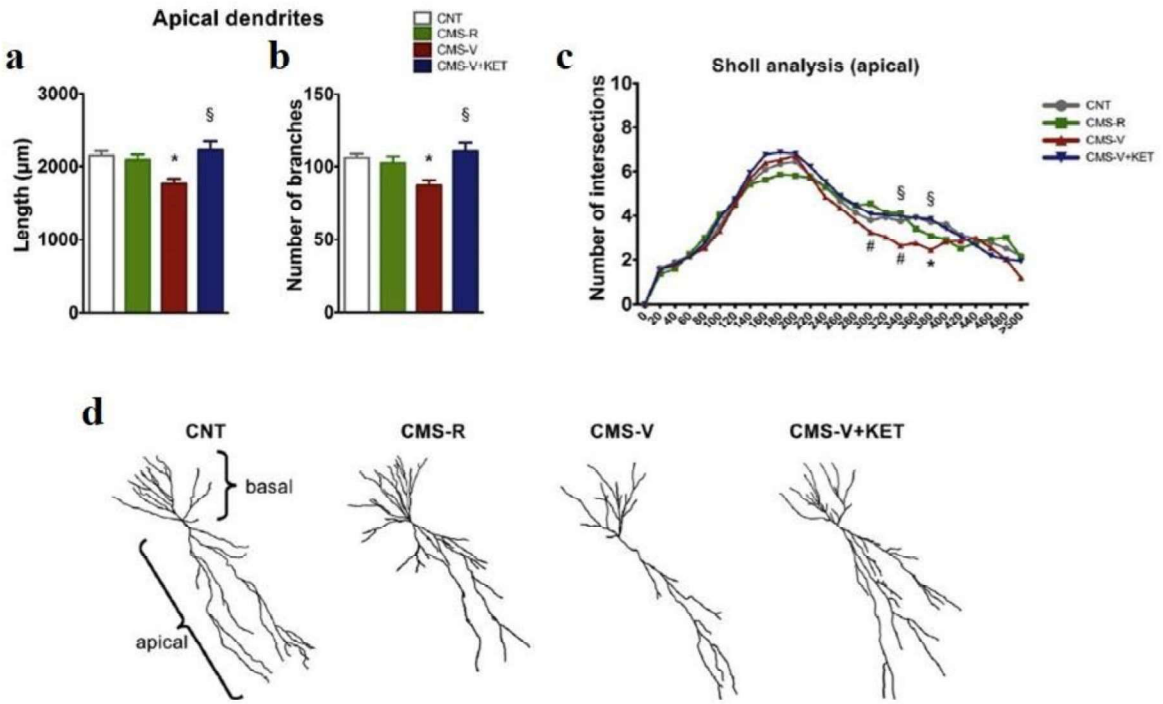

Figure 18. Dendritic morphology and Scholl analysis of CA3 pyramidal neurons

(a) Total length and (b) number of branches of apical dendrites; *p<0.05 vs CNT; §p<0.05 vs CMS-V. (c) Scholl analysis of apical dendrites; *p<0.05 vs CNT; #p<0.05 vs CMS-R; §p<0.05 vs CMS-V. (d) Representative drawings of CA3 pyramidal neurons reconstructed with Imaris software. Modified from Tornese et al., 2019

4.2 CMS and KET treatment alter the hippocampal expression of miRNAs

We measured the expression of 19 microRNAs, selected because of their known role in plasticity, stress response and depression (Giusti et al., 2014; Hu et al., 2014; Issler et al., 2014; Jasińska et al., 2016; Schratt et al., 2006; Song et al., 2015; Yu et al., 2008), using Real Time PCR in the HPC of rats subjected to CMS and treated with a single sub-anesthetic dose (10 mg/Kg) of KET 24 h before sacrifice. Ten of them were significantly modulated in the stressed animals (One-Way ANOVA of miR-124: $F_{3,30}$=3.669, p=0.0230; miR-let-7-d: $F_{3,33}$=5.067, p=0.0054; miR-132: $F_{3,29}$=4.241, p=0.0133; miR-34a: $F_{3,30}$=2.783, p=0.058; miR-135a-5p: $F_{3,24}$=10.96, p=0.001; miR-134: $F_{3,30}$=5.153, p=0.0054; miR-125a: $F_{3,30}$=5.335, p=0.0046; miR-9-5p: $F_{3,31}$=3.676, p=0.0225; miR-30a: $F_{3,31}$=6.339, p=0.0018; miR-210: $F_{3,32}$=3.218, p=0.0357) (Tab. 9). In particularly, miR-30a, miR-125a, miR-134, miR-135a and miR-let-7d were significantly reduced in all the stressed animals independently of the group (CMS-V, CMS-R and CMS-V+KET). miR-9-5p, miR-34a and miR-210 were reduced only in the CMS-V animals while miR-132 was reduced only in the CMS-R and miR-124 was reduced in CMS-V and CMS-V+KET. Interestingly, KET was able to revert the effect of stress on miRNAs expression only in the case of miR-9-5p by inducing an increase in its levels.

Table 9. miRNAs expression changes in the HPC of rats induced by chronic stress and ketamine

Changes in the expression of 19 selected miRNAs were measured in the HPC of adult rats after CMS and ketamine by qPCR. One-Way ANOVA followed by Newman-keuls post hoc test; *p < 0.05 vs CNT; **p < 0.01 vs CNT; ***p < 0.001 vs CNT; #p < 0.05 vs CMS-V. n= 7/10

	CNT	CMS-R	CMS-V	CMS-V+KET	ANOVA
miR-9-5p	1 ± 0.22	0.94 ± 0.17	**0,76 ± 0.12***	**1.03 ± 0.24#**	F(3, 31) = 3,676; **P<0.05**
miR-15a-5p	1 ± 0.24	0.78 ± 0.18	0.67 ± 0.18	0.84 ± 0.32	F(3, 28) = 2,258; P=0.1035
miR-16-5p	1 ± 0.20	0.83 ± 0.16	0.83 ± 0.20	0.80 ± 0.08	F(3, 31) = 2,183; P=0.1099
miR-26a-5p	1 ± 0.24	0.82 ± 0.11	0.81 ± 0.17	0.89 ± 0.15	F(3, 32) = 2,024; P=0.1302
miR-26b-5p	1 ± 0.22	0.93 ± 0.14	0.89 ± 0.18	0.90 ± 0.10	F(3, 34) = 0,846; P=0.4779
miR-29a-5p	1 ± 0.18	0.96 ± 0.21	0.98 ± 0.15	0.97 ± 0.17	F(3, 33) = 0,066; P=0.9771
miR-29b-5p	1 ± 0.19	0.96 ± 0.10	0.89 ± 0.06	0.86 ± 0.15	F(3, 30) = 1,903; P=0.1504
miR-30a-5p	1 ± 0.20	**0.74 ± 0.17****	**0.64 ± 0.15****	**0.72 ± 0.17****	F(3, 31) = 6,339; **P<0.01**
miR-34a-5p	1 ± 0.22	0.85 ± 0.28	0.68 ± 0.18	0.77 ± 0.18	F(3, 30) = 2,783; P=0.0580
miR-34c-5p	1 ± 0.37	0.78 ± 0.47	0.53 ± 0.18	0.66 ± 0.30	F(3, 31) = 2,366; P=0.0900
miR-124-5p	1 ± 0.17	0.88 ± 0.11	**0.81 ± 0.13***	**0.79 ± 0.16***	F(3, 30) = 3,669; **P<0.05**
miR-125a-5p	1 ± 0.17	**0.75 ± 0.09****	**0.84 ± 0.15***	**0.80 ± 0.10***	F(3, 30) = 5,335; **P<0.01**
miR-132-5p	1 ± 0.09	**0.80 ± 0.13****	0.85 ± 0.12	0.89 ± 0.12	F(3, 29) = 4,241; **P<0.05**
miR-134-5p	1 ± 0.29	**0.66 ± 0.07****	**0.79 ± 0.13***	**0.74 ± 0.19***	F(3, 30) = 5,153; **P<0.01**
miR-135a-5p	1 ± 0.12	**0.77 ± 0.10****	**0.62 ± 0.10*****	**0.76 ± 0.15****	F(3, 24) = 10,96; **P<0.001**
miR-137-5p	1 ± 0.23	0.85 ± 0.10	0.83 ± 0.11	0.80 ± 0.14	F(3, 31) = 2,674; P=0.0645
miR-195-5p	1 ± 0.33	0.77 ± 0.11	0.82 ± 0.14	0.77 ± 0.10	F(3, 32) = 2,756; P=0.0584
miR-210-5p	1 ± 0.18	0.82 ± 0.08	**0.79 ± 0.12***	0.83 ± 0.21	F(3, 32) = 3,218; **P<0.05**
let-7d-5p	1 ± 0.25	**0.74 ± 0.13****	**0.72 ± 0.14****	**0.80 ± 0.13***	F(3, 33) = 5,067; **P<0.01**

One-way ANOVA ($F_{3,31}$=3.676, p=0.0225) highlighted a peculiar expression pattern of miR-9-5p since, as reported, it is reduced selectively in the CMS-V (Newman-Keuls post-hoc test; $p < 0.05$ vs CNT) and not in the CMS-R (Newman-Keuls post-hoc test; $p = 0.7355$ vs CNT) and KET completely rescued the change (Newman-Keuls post-hoc test; $p < 0.05$ vs CMS-V) (Fig. 19a). This prompted us to consider this miRNA as a possible molecular determinant of the morphological and functional changes we have previously found restricted to the HPC of vulnerable animals (Tornese et al., 2019).

miR-135a-5p was another miRNA we focused our attention upon since it has been previously associated with stress response, with the mechanism of vulnerability and resilience to stress and with antidepressant response (Issler et al., 2014). In our model, miR-135a-5p is significantly modulated by stress (One-way ANOVA, $F_{3,24} = 10.96$, $p = 0.001$), both in CMS-V (Newman-Keuls post-hoc test; $p < 0.001$ vs CNT) and CMS-R (Newman-Keuls post-hoc test, $p < 0.01$ vs CNT). KET does not

exert a significant effect on miR-135a-5p expression as shown by a failure in rescuing the decrease caused by stress (Fig. 19b).

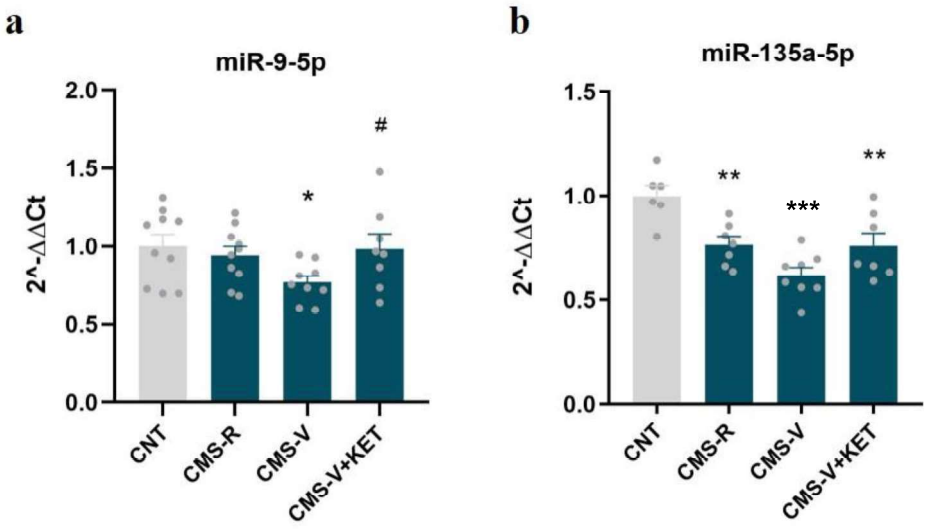

Figure 19. Hippocampal expression of miR-9-5p and miR-135a-5p measured with qPCR
One-way ANOVA followed by Newman-keuls post hoc test; *p < 0.05 vs CNT; **p < 0.01 vs CNT; ***p < 0.001 vs CNT; $^{\#}$p < 0.05 vs CMS-V. n= 7/10. Data are expressed as mean ± S.E.M

We further evaluated miR-9-5p and miR-135a-5p possible differential expression in the subregions of the hippocampus of rats CA3, CA1 and DG using in situ hybridization studies (Fig. 20-21). The expression of the microRNAs was measured as the optical density in a grey scale in the soma and along the dendrites at 20 µm and 40 µm from the soma. One-Way ANOVA revealed a significant effect of chronic stress on miR-9-5p expression in the soma of pyramidal neurons ($F_{3,21} = 30.78$, $p < 0.001$ in CA3; $F_{3,22} = 4.47$, $p = 0.0135$ in CA1 and $F_{3,22} = 6.868$, $p = 0.0020$ in DG). In particularly, miR-9-5p was selectively reduced in CMS-V animals (Tuckey's post-hoc test; $p < 0.001$ vs CNT in CA3, $p < 0.05$ vs CNT in CA1, and $p < 0.01$ vs CNT in the DG) (Fig. 20). Importantly, miR-9-5p expression was not changed in the CMS-R compared to the CNT. Ketamine treatment rescued the reduction in all three areas significantly increasing miR-9-5p somatic expression (Tuckey's post-hoc test; $p < 0.001$ vs CMS-V in CA3, $p < 0.05$ vs CMS-V in CA1, and $p < 0.01$ vs CMS-V in the DG). Along the proximal dendrites, miR-9-5p expression tended to decrease in CMS-V in all three areas CA3, CA1 and DG; KET seemed to reverse this reduction, however, only in CA3 KET completely rescued the decrease (Tuckey's post-hoc test, $p < 0.001$ vs CMS-V) (Fig. 20c).

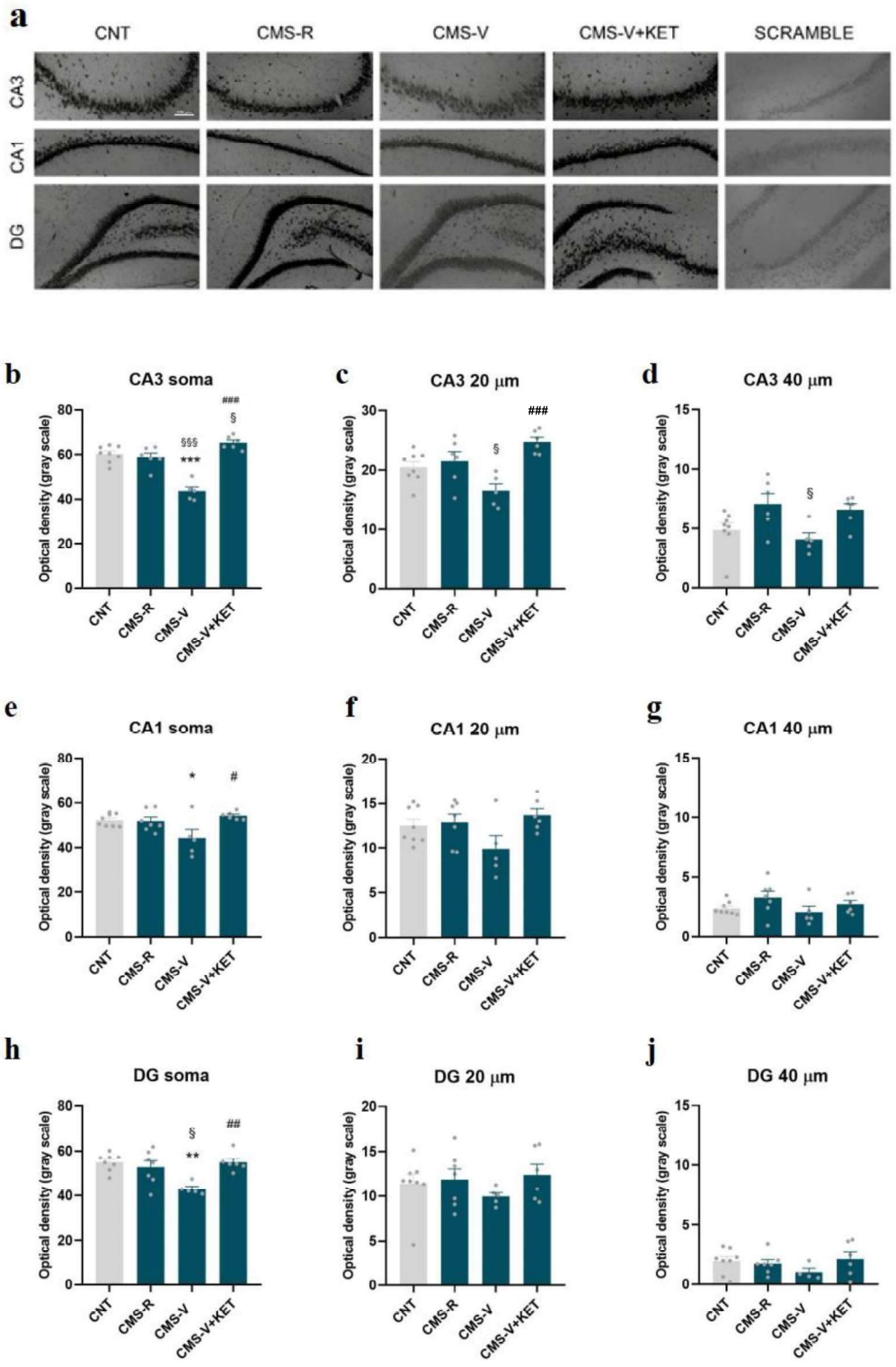

Figure 20. In situ hybridization analysis of miR-9-5p in coronal slices of the HPC of rats

(a) Representative images of hybridization signal in the different sub-regions of the HPC (CA3, CA1 and DG). (b,c,d) MiR-9-5p expression in CA3 measured in the soma, at 20 µm and at 40 µm from the soma, respectively. (e,f,g) MiR-9-5p expression in CA1 measured in the soma, at 20 µm and at 40 µm from the soma, respectively. (h,i,j) MiR-9-5p expression in DG measured in the soma, at 20 µm and at 40 µm from the soma, respectively. One-Way ANOVA followed by Tuckey's Multiple Comparison Test: *p<0.05 vs

CNT, **p<0.01 vs CNT, ***p<0.001 vs CNT, # p<0.05 vs CMS-V, ## p<0.01 vs CMS-V, ### p<0.001 vs CMS-V, §p< 0.05 vs CMS-R, §§§ p< 0.001 vs CMS-R. n= 3-4/group, 2-3 slices/rat. Data are expressed as mean ± S.E.M

Regarding miR-135a-5p (One-Way ANOVA; $F_{3,22}$=2.395, p=0.0957 in CA1; $F_{3,22}$=0.3821, p=0.7669 in CA3; $F_{3,22}$=4.132, p=0.0182 in DG), its somatic expression in CA3, CA1 and in the DG was mildly but non significantly reduced in the CMS-V animals and no changes were found in the CMS-R in all three areas (Fig. 21). In line with the results obtained from the qPCR, KET did not seem to have an effect in modulating miR-135a-5p expression except in the DG where in the CMS-V+KET group miR-135a-5p somatic expression was significantly lower (Tuckey's post-hoc test; p < 0.05 vs CNT). Further, the same trend of miR-135a-5p expression found in the soma was maintained also along the dendrites without any significant changes induced by chronic stress or KET.

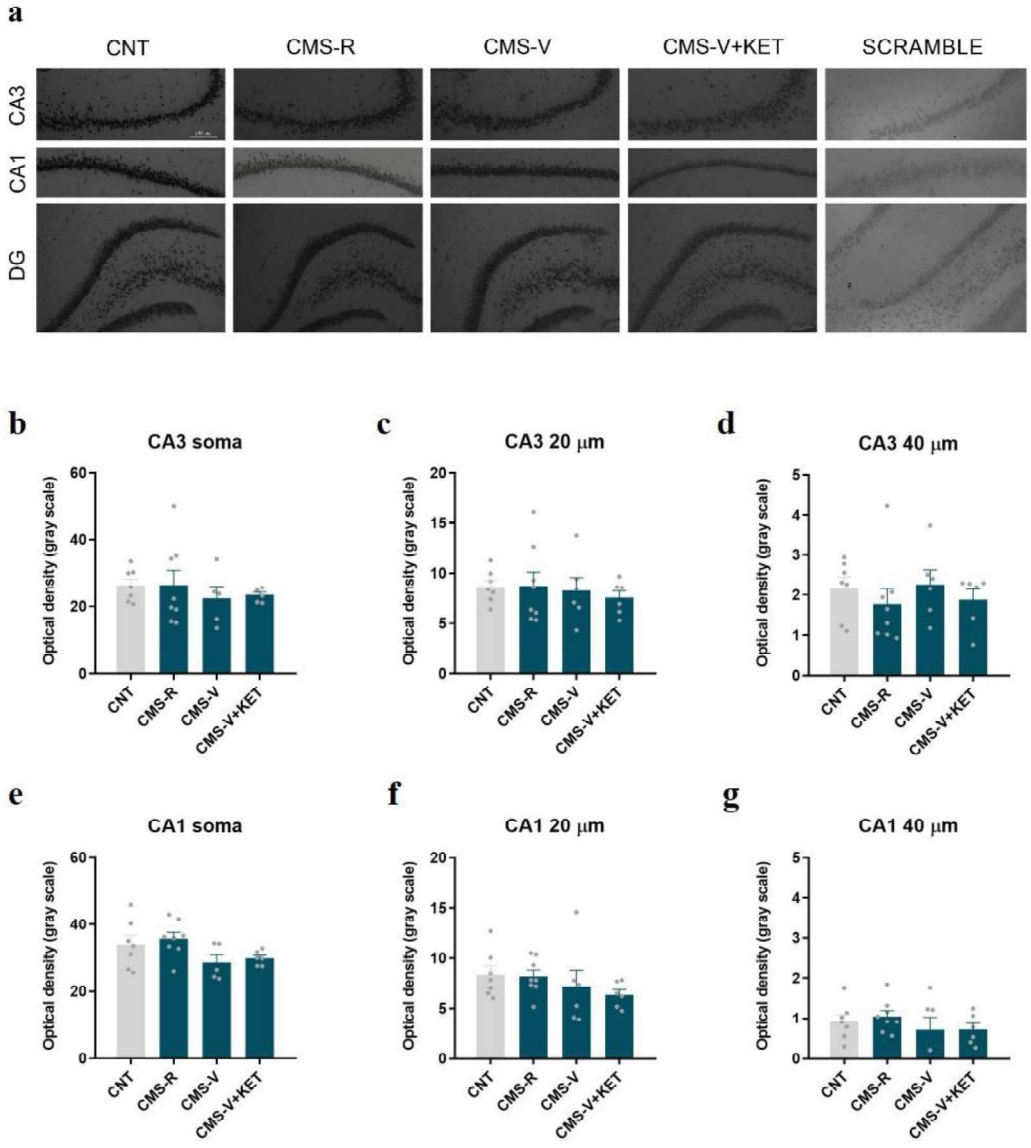

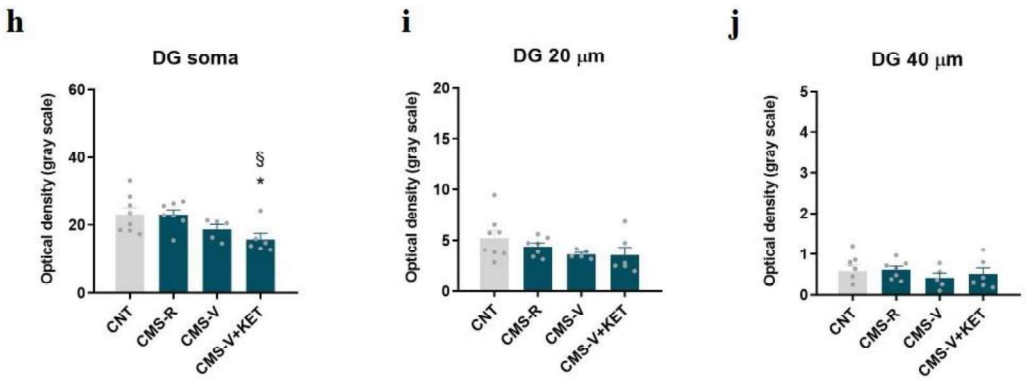

Figure 21. In situ hybridization analysis of miR-135a-5p in coronal slices of the HPC of rats

(a) Representative images of hybridization signal in the different sub-regions of the HPC (CA3, CA1 and DG). (b,c,d) MiR-135a-5p expression in CA3 measured in the soma, at 20 μm and at 40 μm from the soma, respectively (e,f,g) MiR-135a-5p expression in CA1 measured in the soma, at 20 μm and at 40 μm from the soma, respectively (h,i,j) MiR-135a-5p expression in CA1 measured in the soma, at 20 μm and at 40 μm from the soma, respectively. One-way ANOVA followed by Tuckey's Multiple Comparison Test: *p<0.05 vs CNT, §p< 0.05 vs CMS-R. n= 3-4/group, 2-3 slices/rat. Data are expressed as mean ± S.E.M

Together, these results show that chronic stress causes changes of miR-9-5p and miR-135a-5p expression in CA3, CA1 and DG of the HPC of rats. These variations are restricted to vulnerable animals for miR-9-5p while miR-135a-5p expression is modulated also in CMS-R. KET treatment exerts a restorative action only on miR-9-5p levels while failed to rescue the reduction of miR-135a-5p.

4.3 In vitro CORT treatment impairs dendritic morphology of primary hippocampal neurons and decreases the expression of miR-9-5p but not miR-135a-5p. KET rapidly rescues both changes

Stress in known to activate the HPA axis that eventually ends with the release from adrenal glands of glucocorticoids into the bloodstream (McEwen, 2017). In rodents, the major glucocorticoid is represented by corticosterone (CORT). Few works present in literature used this hormone *in vitro* to mimic stressful conditions in cellular cultures in order to study the molecular mechanisms underlying its actions (Groc et al., 2008; Yuen et al., 2011). Here we set up an *in vitro* model of chronic stress based on the repeated treatment of primary hippocampal cultures with 200 nM of CORT to test its direct effect on mediating the dendritic remodeling. We further evaluated acute KET action in reversing corticosterone-induced changes adding 1 μM KET to the cultured cells. One-Way ANOVA revealed a significant effect of CORT and KET on dendritic remodeling ($F_{2,38} = 5.595$, $p = 0.0074$). As reported in Fig. 22, repeated CORT significantly reduced total dendritic length of pyramidal neurons (Tuckey's post hoc test, $p < 0.05$ vs DMSO) mostly affecting apical dendrites (Tuckey's post hoc test, $p < 0.05$ vs DMSO). Importantly, KET completely rescued the retraction (Tuckey's post hoc

test, $p < 0.05$ vs CORT) with a more pronounced effect on basal dendrites (Tuckey's post hoc test, $p < 0.05$ vs CORT).

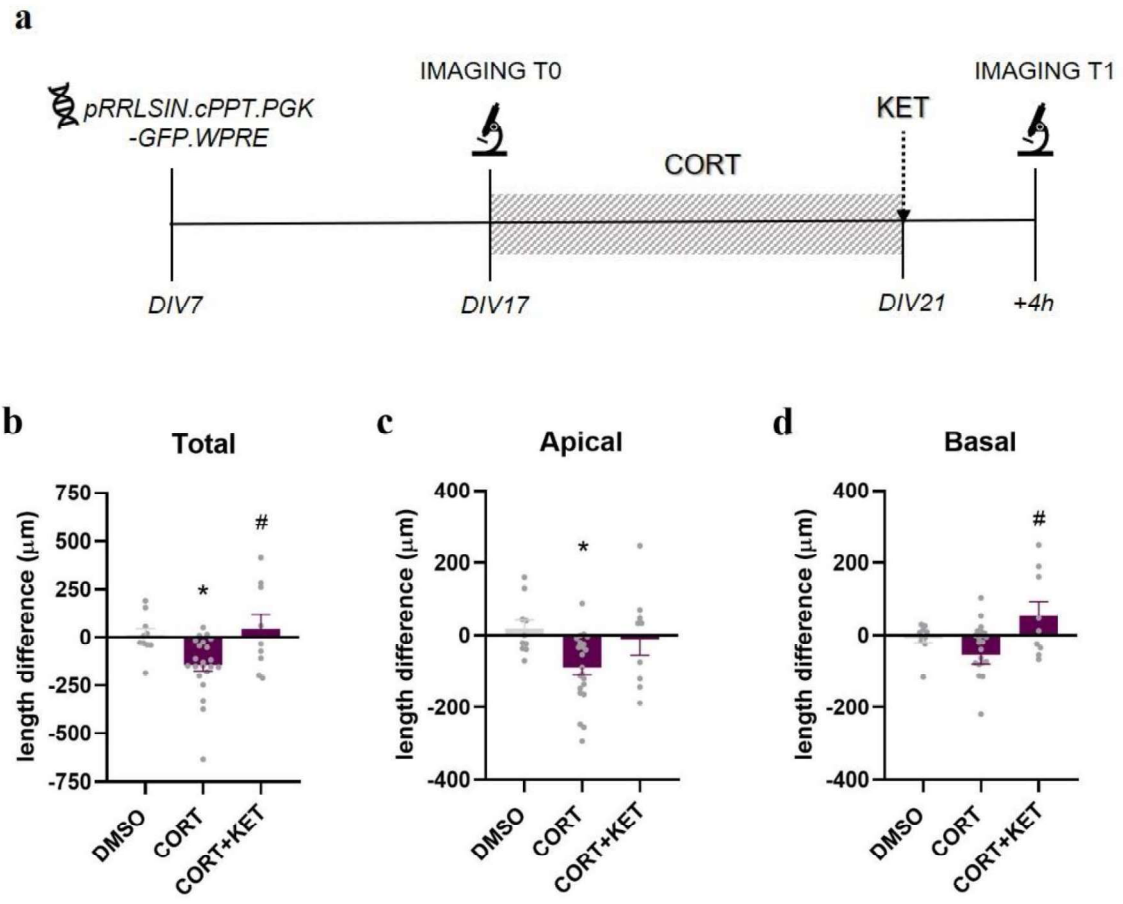

Figure 22. In vitro treatment with CORT and KET of primary hippocampal neurons

(a) Schematic protocol of repeated CORT and KET treatment. (b) Analysis of the variation of total, (c) apical and (d) basal, dendritic length after CORT and KET treatment. One-Way ANOVA followed by Tuckey's post hoc test: *p<0.05 vs DMSO, #p<0.05 vs CORT; n=10 (DMSO), n=22 (CORT), n=9 (CORT+KET). Data are expressed as mean ± S.E.M

qPCR analysis revealed a significant effect of stress and KET on miR-9-5p expression (One-Way ANOVA, $F_{3,34}$=5.997, p=0.0021) while the expression of miR-135a-5p was not changed (One-way ANOVA, $F_{3,14}$ = 0.1517; p = 0.9269) (Fig. 23). A reduction of miR-9-5p expression was found in cells treated with CORT (Tuckey's post-hoc test; $p < 0.01$ vs DMSO). The addiction of KET to the cells after the repeated CORT treatment, was able to completely rescue the reduction of miR-9-5p (Tuckey's post-hoc test; $p < 0.01$ vs CORT). KET alone did not seem to exert any effect on the expression of both miRNAs.

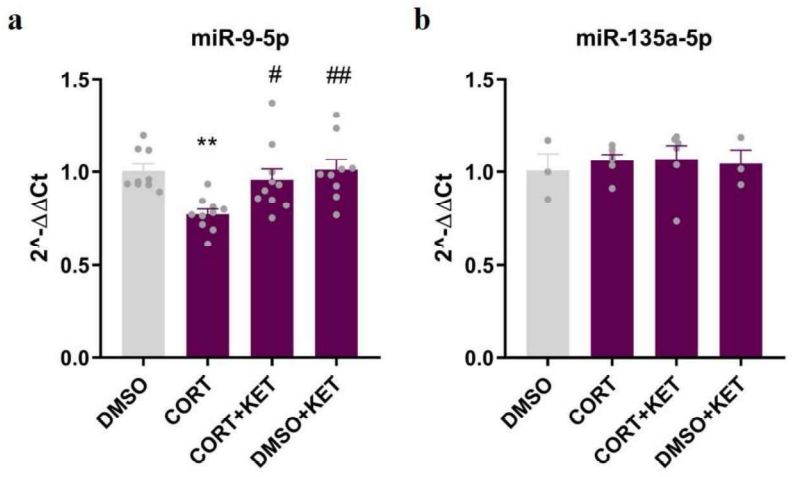

Figure 23. miR-9-5p and miR-135a-5p expression in primary neurons treated *in vitro* with CORT and KET
qPCR analysis of (a) miR-9-5p and (b) miR-135a-5p expression in primary neurons treated with CORT and KET. One-Way ANOVA followed by Tuckey's post hoc test; **p<0.01 vs DMSO; $^{\#}$p<0.05 vs CORT; $^{\#\#}$p<0.01 vs CORT. n=3-9. Data are expressed as mean ± S.E.M

4.4 *In vitro* modulation of miR-9-5p and miR-135a-5p expression using over-expression and down-regulation plasmids significantly change dendritic morphology and spine density of primary hippocampal neurons

In order to test whether miR-9-5p and miR-135a-5p could directly modulate the dendritic morphology of pyramidal neurons, specific plasmids to over-express or down-regulate the miRNAs were designed. The correct functioning of the down-regulation vectors was assessed evaluating the ability of mimics of miR-9-5p and miR-135a-5p to decrease the expression of the GFP fluorescence in HEK293T cells transduced with lentiviruses of Twl-sponge-miR-9-5p and Twl-sponge-miR-135a-5p. As Fig. 24a shows, miR-9-5p mimics significantly silenced the expression of the GFP only in the presence of Twl-sponge-miR-9-5p and not of the empty vector suggesting that the interaction between the mimic and its complementary sponge inserted in the vector induced a translational repression of the fluorescent protein. In the same way, mimics of miR-135a-5p reduced the expression of the GFP only in the presence of Twl-sponge-miR-135a-5p confirming the functioning of the vectors (Fig. 24b). No changes in the expression of the RFP were seen for both vectors to indicate that the effects described before were caused by the specific binding of the mimic to the sponge and not due to technical issues.

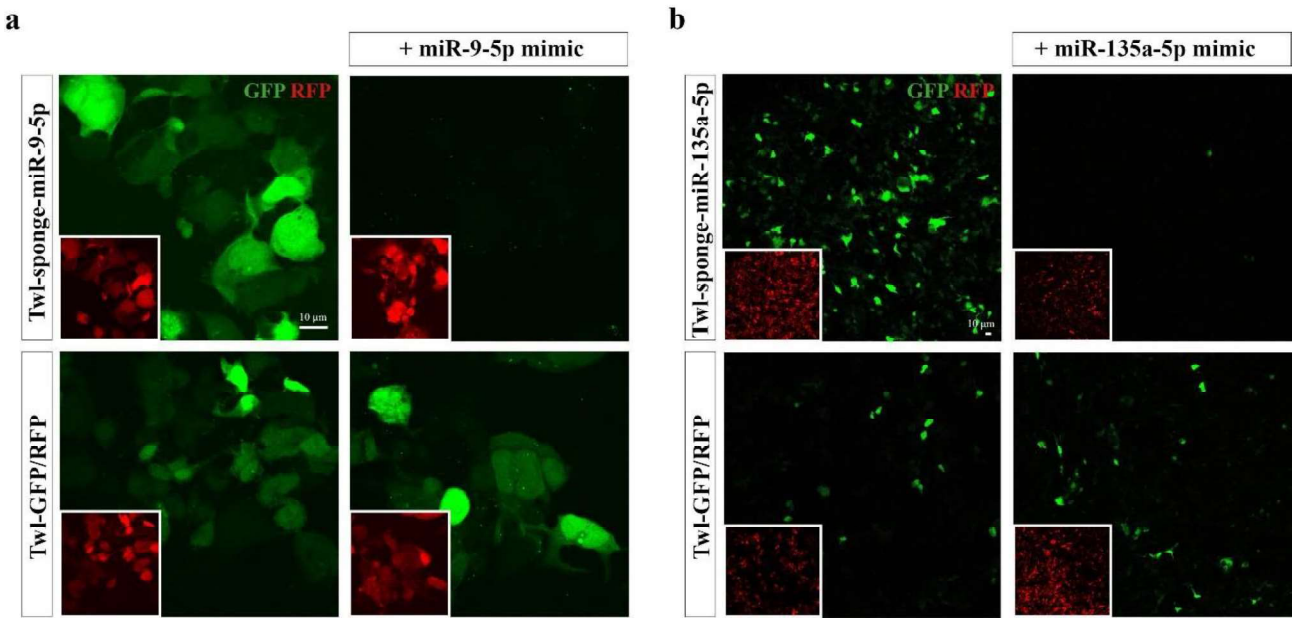

Figure 24. Evaluation of the functioning of miRNA down-regulation vectors, Twl-sponge-miR-9-5p and Twl-sponge-miR-135a-5p

(a) miR-9-5p mimics added to HEK293T cells transduced with the lentivirus of Twl-sponge-miR-9-5p effectively inhibited the expression of the GFP. No changes were seen in cells transduced with the lentivirus of the empty vector Twl-GFP/RFP. (b) miR-135a-5p mimics added to HEK293T cells transduced with the lentivirus of Twl-sponge-miR-135a-5p effectively inhibited the expression of the GFP. No changes were seen in cells transduced with the lentivirus of the empty vector Twl-GFP/RFP.

The plasmids were used to transfect hippocampal neurons at DIV11 to exogenously modulate the expression of miR-9-5p and miR-135a-5p for 72 h. After, pictures of fluorescent-labeled neurons were captured with a confocal microscope and the dendritic morphology and the number of spines have been analyzed manually with Fiji (Schindelin et al., 2012). The over-expression of miR-9-5p significantly increased the total dendritic length (Fig. 25a, Student's t test; $p < 0.05$ vs Twl-H1) and the number of branches of hippocampal neurons (Fig. 25d, Student's t test; $p < 0.05$ vs Twl-H1) together with an increase of the density of spines on secondary dendrites (Fig. 25e, Student's t test; $p < 0.0001$ vs Twl-H1). To note, the effect of miR-9-5p on the length of the dendrites mainly affected the apical dendrites (Fig. 25b, Student's t test; $p < 0.01$ vs Twl-H1) with no changes of the basal (Fig. 25c, Student's t test; $p = 0.200$).

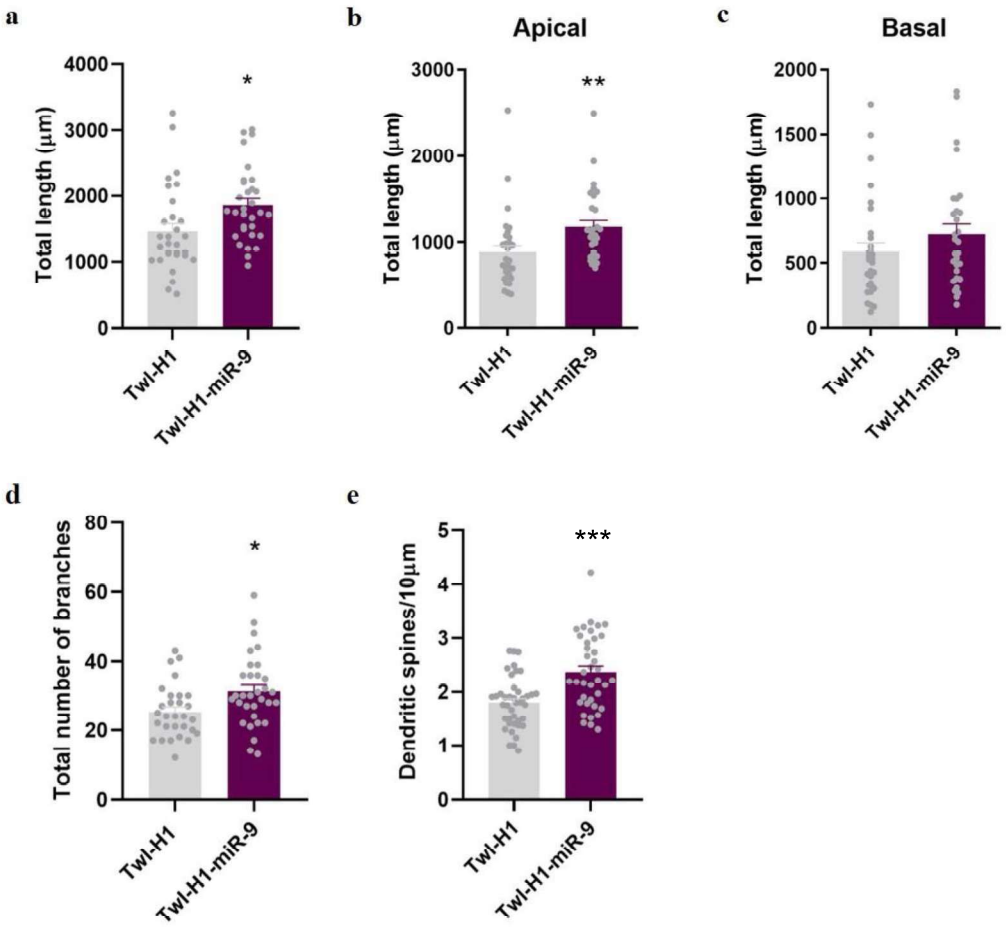

Figure 25. Morphological analysis of primary hippocampal neurons after 72 hours of miR-9-5p over-expression

(a) total dendritic length; n= 30, (b) apical dendritic length; n=30, (c) basal dendritic length; n=30, (d) total number of branches; n= 30, (e) dendritic spine density; n=40. Student's t test with Welch's correction: *p<0.05, **p<0.01, ***p<0.001. Data are expressed as mean ± S.E.M

Conversely, miR-9-5p down-regulation significantly decreases the total dendritic length (Fig. 26a, Student's t test; $p < 0.05$ vs Twl-GFP/RFP), especially of apical dendrites (Fig. 26b, Student's t test; $p < 0.05$ vs Twl-GFP/RFP), the total number of branches (Fig. 26d, Student's t test; $p < 0.05$ vs Twl-GFP/RFP) and the density of spines (Fig. 26e, Student's t test; $p < 0.001$ vs Twl-GFP/RFP).

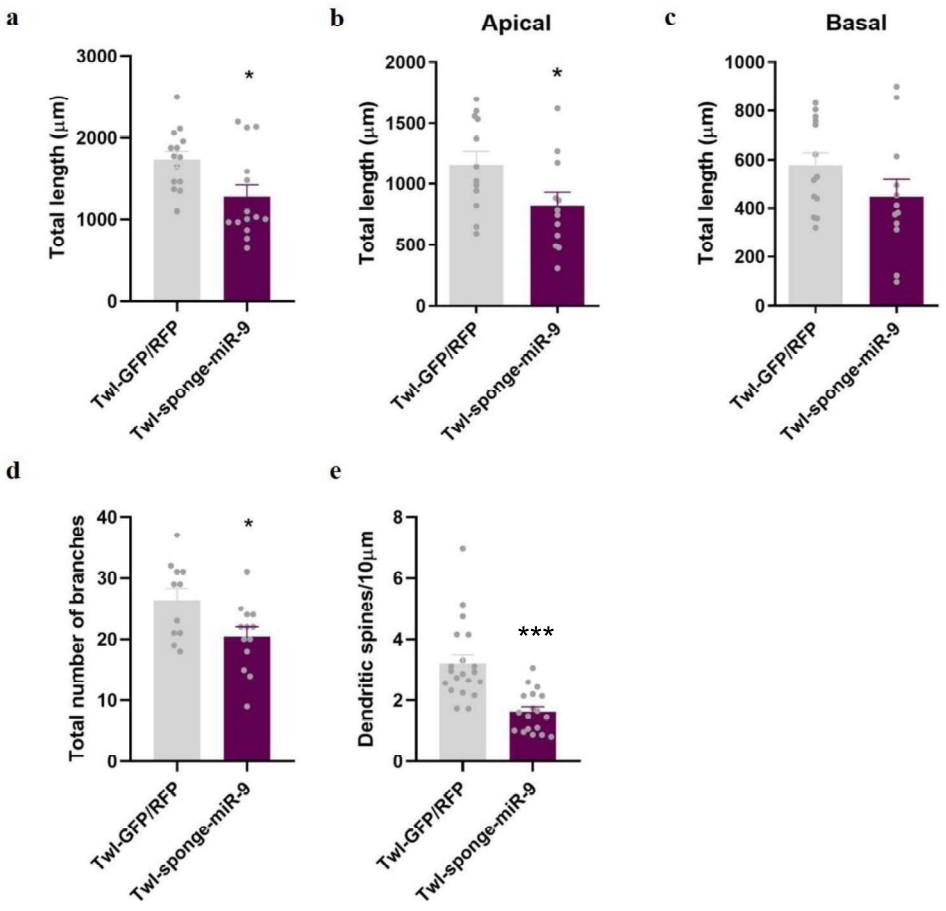

Figure 26. Morphological analysis of primary hippocampal neurons after 72 hours of miR-9-5p down-regulation

(a) total dendritic length; n= 15, (b) apical dendritic length; n=15, (c) basal dendritic length; n=15, (d) total number of branches; n= 15, (e) dendritic spine density; n=20. Student's t test with Welch's correction: *p<0.05, **p<0.01, ***p<0.001. Data are expressed as mean ± S.E.M

Regarding miR-135a-5p, the over-expression significantly increased the number of branches of hippocampal neurons (Fig. 27d, Student's t test; $p < 0.01$ vs Twl-H1) and the density of spines (Fig. 27e, Student's t test; $p < 0.05$ vs Twl-H1). The total dendritic length was not changed (Student's t test; $p = 0.0794$). Instead, the down-regulation of miR-135a-5p affected only the spine density (Student's t test; $p < 0.001$ vs Twl-GFP/RFP) (Fig. 28e) with no effect on the dendritic length (Student's t test; $p = 0.2155$) or arborization (Student's t test; $p = 0.0984$).

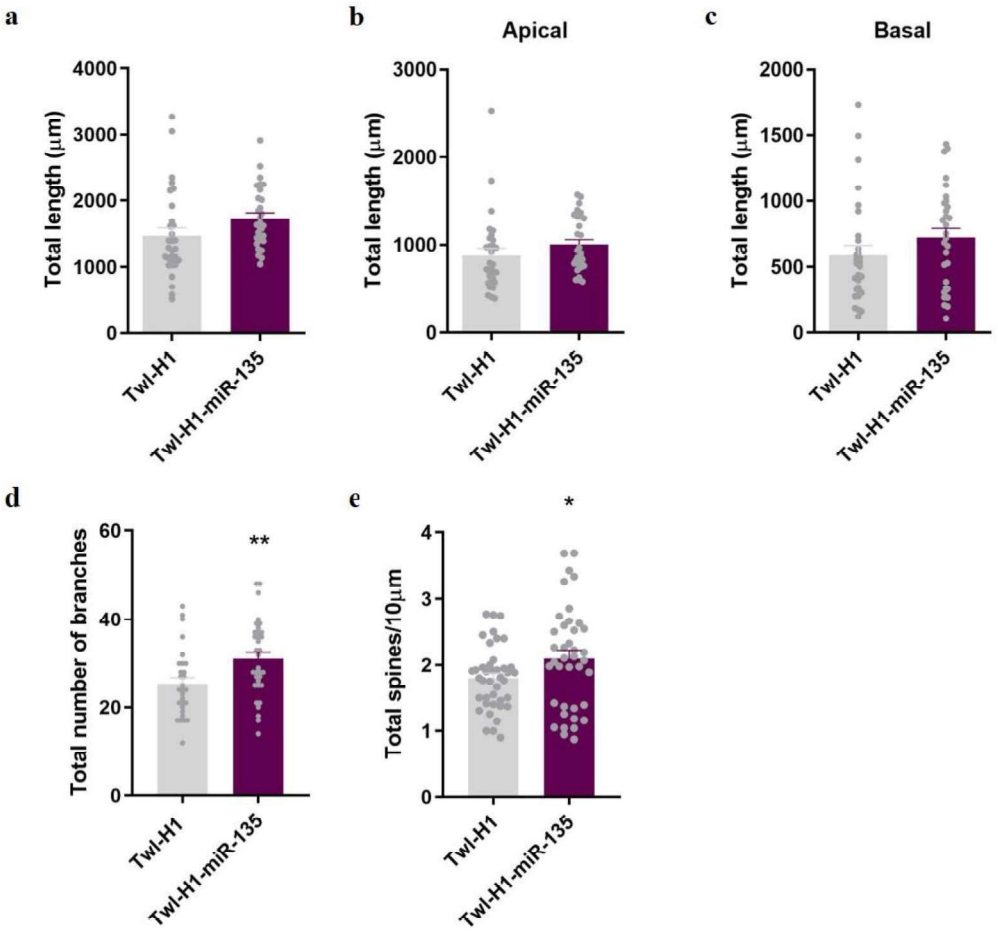

Figure 27. Morphological analysis of primary hippocampal neurons after 72 hours of miR-135a-5p over-expression

(a) total dendritic length; n= 30, (b) apical dendritic length; n=30, (c) basal dendritic length; n=30, (d) total number of branches; n= 30, (e) dendritic spine density; n=40. Student's t test with Welch's correction: *p<0.05, **p<0.01. Data are expressed as mean ± S.E.M

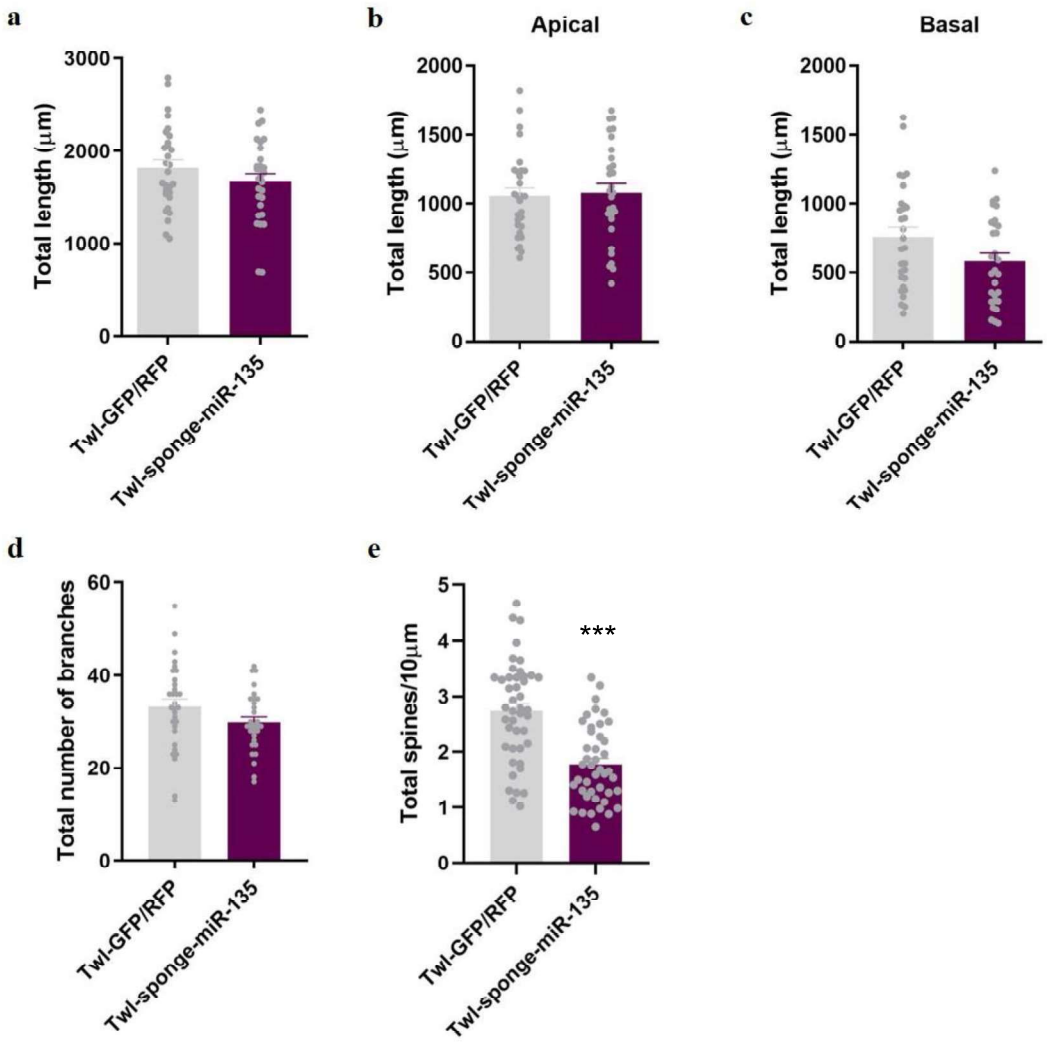

Figure 28. Morphological analysis of primary hippocampal neurons after 72 hours of miR-135a-5p down-regulation
(a) total dendritic length; n= 30, (b) apical dendritic length; n=30, (c) basal dendritic length; n=30, (d) total number of branches; n= 30, (e) dendritic spine density; n=40. Student's t test with Welch's correction: ***p<0.001. Data are expressed as mean ± S.E.M

Taken together, these results suggest a clear role of miR-9-5p in regulating the morphology of pyramidal neurons while the role of miR-135a-5p in the dendritic remodeling is not well defined and mostly regards the dendritic spine dynamics. Considering this evaluation, we assumed that studying the function of miR-9-5p in the regulation of morphological changes following chronic stress and KET would have given us more insights in the underneath mechanisms compared to miR-135a-5p.

4.5 Bioinformatic analysis of miR-9-5p target genes and *in vitro* validation using Luciferase assay revealed two candidate genes: SIRT1 and REST

The bioinformatic prediction tools TargetScan, mirDB and microT-CDS were used to identify miR-9-5p target genes. Among the more than hundreds of genes, we initially selected seven genes: DRD2 (Dopamine Receptor D2; binding position 285-292 of DRD2 3'UTR), ELAVL1 (ELAV like RNA

binding protein 1; binding position 788-795 of ELAVL1 3'UTR), GSK-3β (Glycogen Synthase Kinase 3, beta; binding position 3565-3571 of GSK-3β 3'UTR), NTRK3 (Neurotrophic Receptor Tyrosine Kinase 3; binding position 1741-1749 of NTRK3 3'UTR), REST (RE-1 Silencing Transcription Factor; binding position 1749-1755 and 3207-3213 of REST 3'UTR), SIRT1 (Sirtuin 1; binding position 335-342 of SIRT1 3'UTR) and SORT1 (Sortilin 1; binding position 3274-3280 of SORT1 3'UTR) (Table 10).

Table 10. List of targets of miR-9-5p selected after the bioinformatic analysis

Gene	Representative transcript	Prediction databases			Prior evidence
		TargetScan v.7	MirDB	microT-CDS	
Drd2	ENSMUST00000075764.6	x			(Mavrikaki et al., 2019; Zhang et al., 2015)
Elavl1	ENSMUST00000098950.4	x	x	x	(Chi et al., 2009)
Gsk-3β	ENSMUST00000023507.7	x			(Dong et al., 2018)
Ntrk3	ENSMUST00000039431.8	x			
Rest	ENSMUST00000080359.6	x		x	(Giusti et al., 2014; Packer et al., 2008)
Sirt1	ENSMUST00000120239.2	x	x	x	(Delaloy et al., 2010; Schonrock et al., 2012)
Sort1	ENSMUST00000102632.5	x	x	x	(Chi et al., 2009)

The interaction between miR-9-5p and its complementary binding site present within the 3'UTR of the genes was tested with the Luciferase assay. The use of a dual-reporter vector allows to assess the interaction miRNA-target gene by measuring the change in the luminescence produced by the *Firefly* luciferase with or without the presence of miR-9-5p mimics. Student's t test revealed that miR-9-5p mimics significantly decreased the *Firefly* luciferase activity only when co-transfected in HEK293T cells with pmirGLO-GSK-3β ($p < 0.01$ vs NEG mimic) (Fig. 29c), pmirGLO-SIRT1 ($p < 0.05$ vs NEG mimic) (Fig. 29f) and pmirGLO-REST ($p < 0.05$ vs NEG mimic) (Fig. 29e). The reduction observed is the result of the interaction between miR-9-5p and its complementary sites and suggests that GSK-3β, SIRT1 and REST may be confirmed targets of miR-9-5p. No changes in the *Firefly* luciferase activity were found after pmirGLO-NTRK3 ($p = 0.4700$), pmirGLO-DRD2 ($p = 0.4474$), pmirGLO-SORT1 ($p = 0.0525$), pmirGLO-ELAVL1 ($p = 0.3582$) were co-transfected with miR-9-5p mimics, indicating that the miRNA and these genes do not interact and thus are not confirmed targets (Fig. 29).

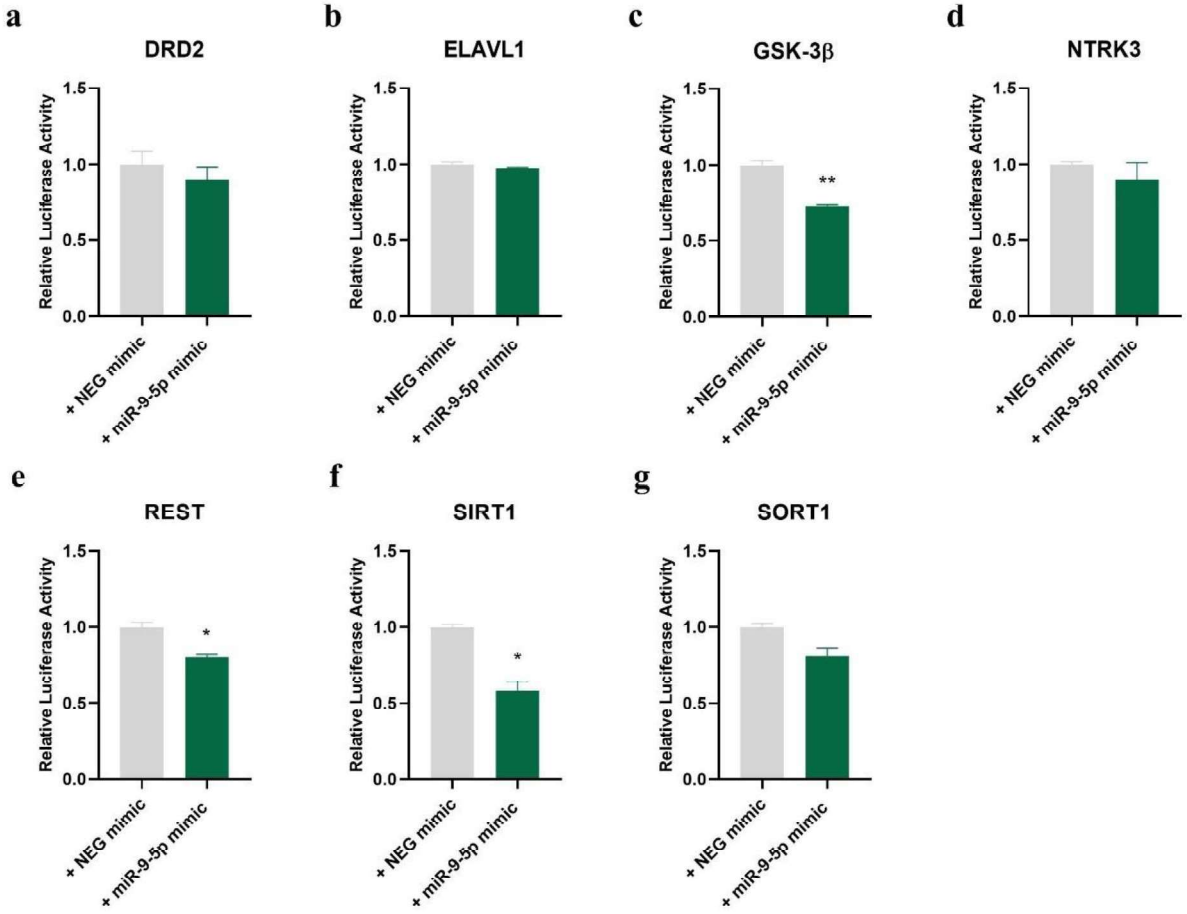

Figure 29. Analysis of miR-9-5p interaction with predicted target genes using Luciferase assay

(a) DRD2 (b) ELAVL1 (c) GSK-3β (d) NTRK3 (e) REST (f) SIRT1 (g) SORT1. Unpaired Student's test with Welch's correction: p* < 0.05, p** < 0.01. n=3; all experiments were repeated 3 times

In order to evaluate the interaction between miR-9-5p and GSK-3β, REST and SIRT1 in a way that takes into account the biological context in which the interaction would take place, we decided to repeat the Luciferase assay this time cloning into the pmirGLO vector a longer segment of the 3'UTR of the three genes containing the binding site for miR-9-5p. Student's t test highlighted no interaction between GSK-3β 3'UTR and miR-9-5p, as showed in Fig. 30a, by no changes in the activity of *Firefly* luciferase ($p = 0.2994$ vs NEG mimic). Instead, co-transfection of HEK293T cells with miR-9-5p mimics and pmirGLO-SIRT1-UTR or pmirGLO-REST-UTR produced a significant decrease in the *Firefly* luciferase activity of the 40 % ($p < 0.05$ vs NEG mimic) (Fig. 30b) and of the 60 % ($p < 0.001$ vs NEG mimic) (Fig. 30c), respectively. The results confirmed the interaction between miR-9-5p and the 3'UTR of REST and SIRT1.

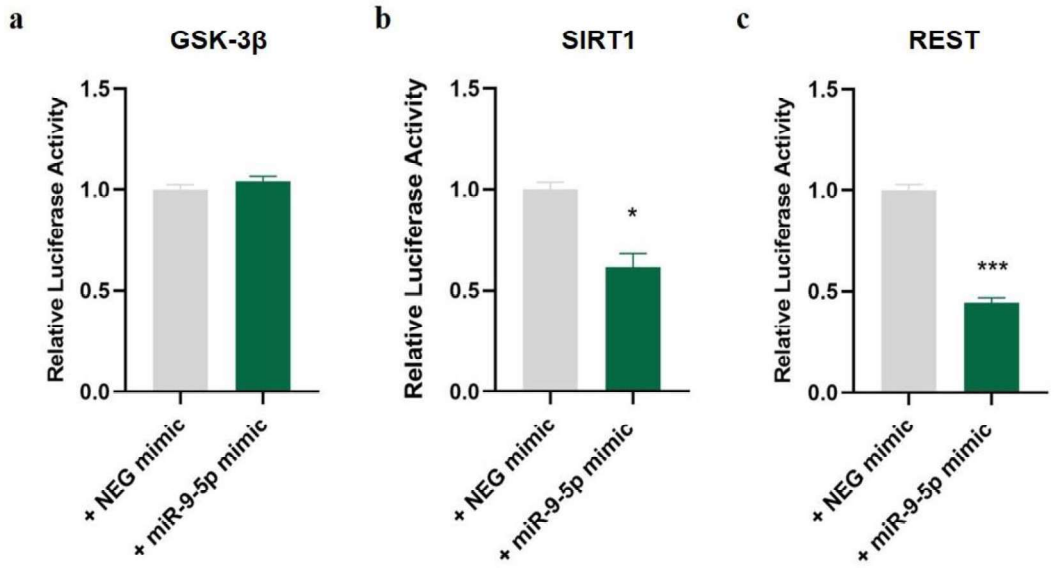

Figure 30. Analysis of miR-9-5p interaction with GSK-3β, SIRT1 and REST 3'UTRs using Luciferase assay
(a) GSK-3β (b) SIRT1 (c) REST. Unpaired Student's t test with Welch's correction: p* < 0.05, p*** < 0.001. n=3; all experiments were repeated 3 times

Interestingly, studying the 3'UTR of SIRT1 and GSK-3β we found in both a sequence complementary to miR-135a-5p. With the purpose of testing a synergic effect of miR-9-5p and miR-135a-5p on SIRT1 and GSK-3β, the Luciferase assay was repeated co-transfecting pmirGLO-SIRT1-UTR and pmirGLO-GSK-3β-UTR with miR-135a-5p mimics alone or together with miR-9-5p mimics. As reported in Fig. 31a, the mimics of miR-135a-5p alone did not change the *Firefly* luciferase activity of pmirGLO-GSK3-β-UTR (Student's t test, $p = 0.1546$ vs NEG mimic) while the combination of miR-135a-5p and miR-9-5p (Fig. 31b) produced a significant but modest (approx. -10 %) decrease of the enzymatic activity ($p < 0.05$ vs NEG mimic). Regarding SIRT1, the *Firefly* luciferase activity was reduced of the 30 % ($p < 0.01$ vs NEG mimic; Fig. 31c) when pmirGLO-SIRT1-UTR was co-transfected with miR-135a-5p mimics alone and approximately of the 40 % ($p < 0.05$ vs NEG mimic; Fig. 31d) when miR-135a-5p was used together with mir-9-5p.

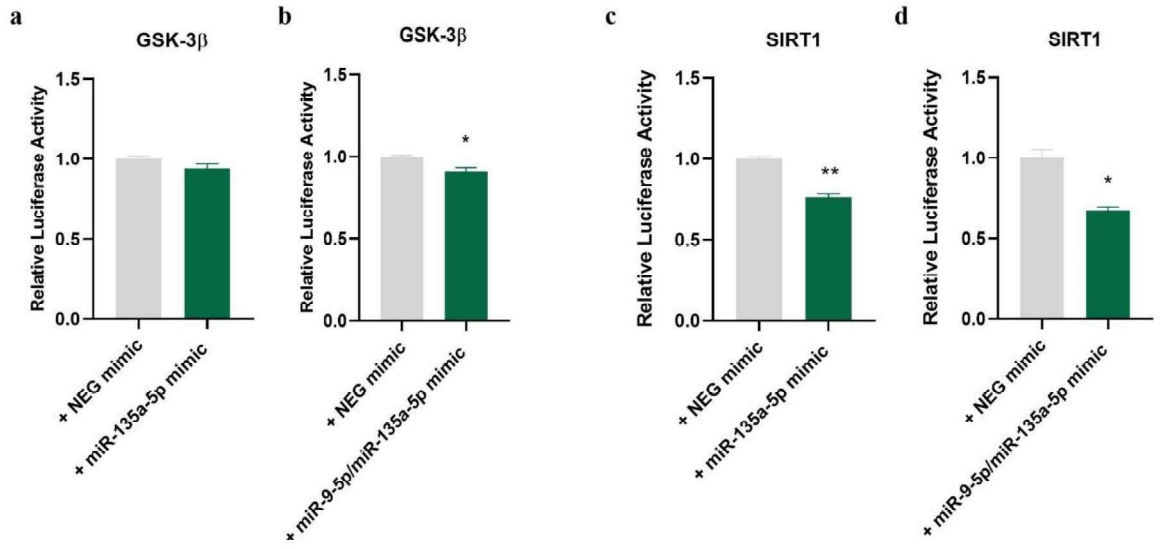

Figure 31. Analysis of miR-135a-5p interaction with GSK-3β and SIRT1 3'UTRs alone or in combination with miR-9-5p using Luciferase assay

(a) GSK-3β with miR-135a-5p mimics (b) GSK-3β with miR-135a-5p plus miR-9-5p mimics (c) SIRT1 with miR-135a-5p mimics (d) SIRT1 with miR-135a-5p plus miR-9-5p mimics. Unpaired t test with Welch's correction: p* < 0.05, p** < 0.01. n=3; all experiments were repeated 3 times

4.6 *In vitro* modulation of miR-9-5p expression levels in primary hippocampal cultures modulates the protein expression of its target genes

DIV11 primary hippocampal neurons were transfected with mimics of miR-9-5p and after 72 hours the expression of SIRT1, GSK-3β and REST was evaluated in total cell lysates using Western-blotting. As reported in Fig. 32, the overexpression of miR-9-5p significantly decreased the expression of GSK-3β (-33,7 %; Student's t test, $p < 0.01$ vs NEG CNT), SIRT1 (-32,1 %; Student's t test, $p < 0.01$ vs NEG CNT) and REST (-37,7 %; Student's t test, $p < 0.01$ vs NEG CNT).

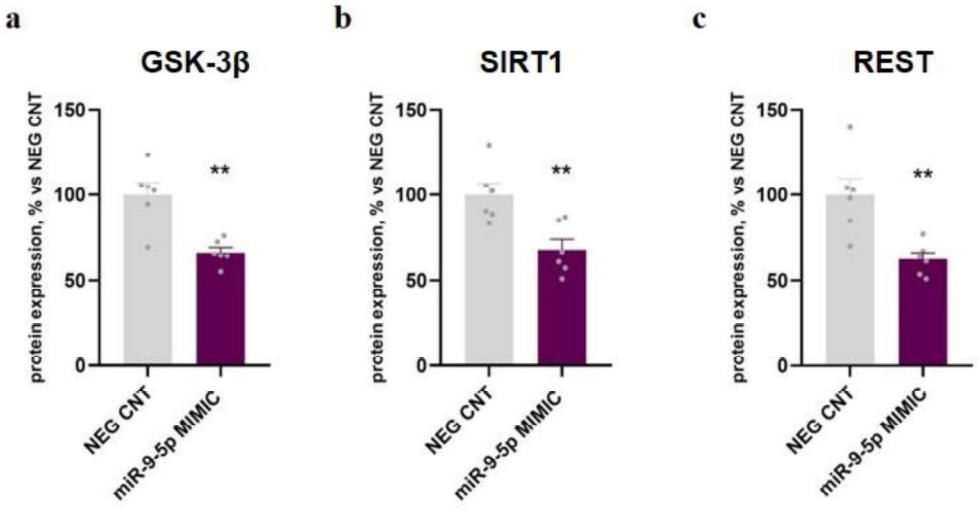

Figure 32. GSK-3β, SIRT1 and REST expression in cell lysates after modulation of miR-9-5p in primary neurons
(a) GSK-3β, (b) SIRT1, (c) REST protein expression after miR-9-5p overexpression. Unpaired Student's t test with Welch's correction. **p < 0.01. n=6. Data are expressed as mean ± S.E.M

4.7 Analysis of the expression of GSK-3β, SIRT1 and REST in the HPC of rats subjected to CMS and KET

In order to test whether the changes in miR-9-5p expression in the HPC of CMS animals caused also alterations in the expression of its predicted target genes (GSK-3β, SIRT1, REST), we performed Real-Time PCR and Western-blotting experiments on total homogenate of HPC from CMS rats (Fig. 33). One-Way ANOVA revealed no changes of GSK-3β mRNA in all the treated groups compared to CNT ($F_{3,24}$ = 2.190; p = 0.1154) (Fig. 33a); however, GSK-3β protein expression was affected ($F_{3,21}$ = 4.080; p = 0.0198) as demonstrated by a significant increase only in the CMS-V+KET group (Tuckey's post-hoc test; p < 0.05 vs CNT) (Fig. 33d). On the other end, SIRT1 mRNA ($F_{3,23}$ = 5.011; p = 0.0081) but not the protein ($F_{3,21}$ = 2.771; p = 0.0669) was significantly changed after CMS (Fig. 33b,e). Indeed, CMS-V animals showed increased levels of SIRT1 (Tuckey's post-hoc test; p < 0.05 vs CNT) although for the protein we found only a trend. In both cases, the treatment with KET seemed to modestly revert the increase in the expression without reaching a statistical significance. As expected, REST expression was significantly changed ($F_{3,21}$ = 5.796, p = 0.0047) (Fig. 33f); in particularly, REST was increased only in CMS-V animals compared to both CNT (Tuckey's post-hoc test; p < 0.01) and CMS-R (Tuckey's post-hoc test; p < 0.01). The treatment with KET completely rescued the increase (p < 0.05 vs CMS-V). No significant changes were found in REST mRNA expression ($F_{3,21}$ = 2.345, p = 0.1020) (Fig. 33c).

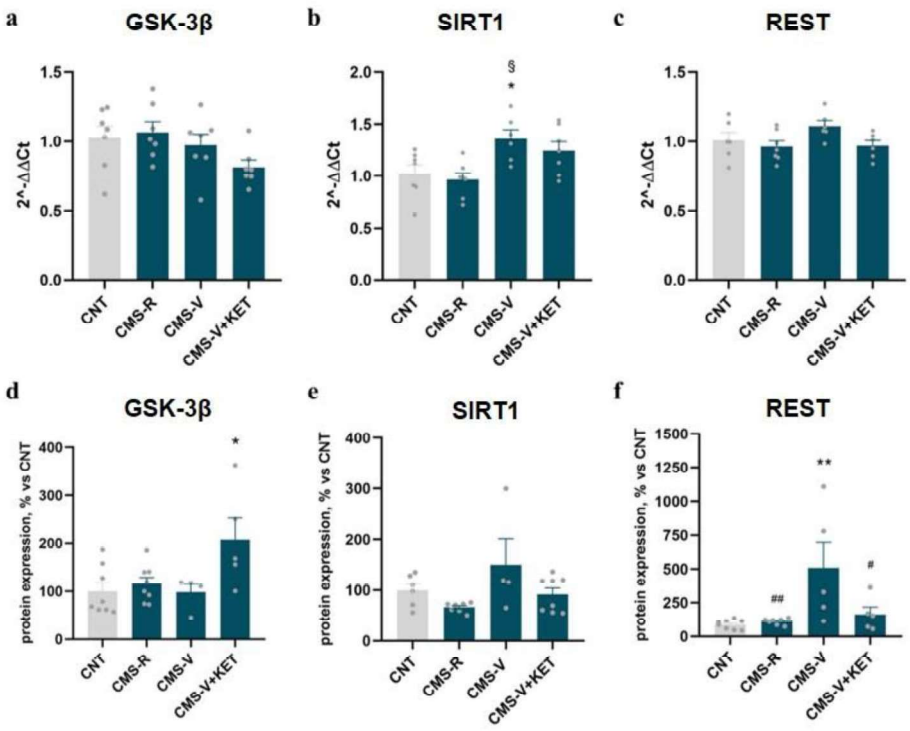

Figure 33. GSK-3β, SIRT1 and REST expression in the HPC of rats subjected to CMS and KET

(a) GSK-3β mRNA (b) SIRT1 mRNA (c) REST mRNA (d) GSK-3β protein (e) SIRT1 protein (f) REST protein. One-Way ANOVA followed by Tuckey's post hoc test; n=7 (mRNA), n=4-8 (protein). *p < 0.05 vs CNT; **p < 0.01 vs CNT; $^{\#}$p < 0.05 vs CMS-V; $^{\#\#}$p < 0.01 vs CMS-V; §p < 0.05 vs CMS-R. Data are expressed as mean ± S.E.M

4.8 Analysis of the expression of GSK-3β, SIRT1 and REST in cell lysates from primary hippocampal neurons treated with CORT and KET

We previously demonstrated that repeated CORT treatment of primary hippocampal neurons was able to negatively modulate miR-9-5p expression levels. On the other end, acute KET rapidly reverted the decrease. With the purpose to test whether this change reflected in a modulation of miR-9-5p targets expression, we performed Western-blotting on whole cell lysates from primary hippocampal neurons treated with 200 nM CORT and 1 μM KET. As Fig. 34a shows, GSK-3β was modestly reduced by CORT and KET did not exert any effect on its expression levels (One-Way ANOVA; $F_{3,32}$ = 0.9883; p = 0.4107). Further, KET alone did not change GSK-3β expression. Regarding SIRT1, the treatment with CORT induced a small decrease in its expression that was not rescued by KET (Fig. 34b, One-Way ANOVA; $F_{3,13}$ = 2.046; p = 0.1571). No changes were found in the group treated only with KET. On the contrary, REST showed a trend of increase after CORT treatment that was not reverted by KET; KET alone followed the same pattern (Fig. 34c, One-Way ANOVA; $F_{3,31}$ = 0.4; p = 0.7540).

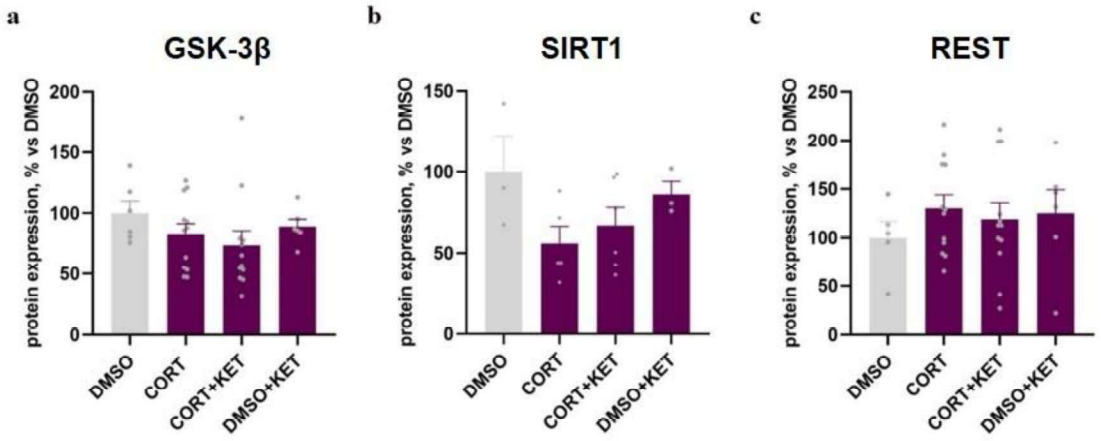

Figure 34. GSK-3β, SIRT1 and REST expression in cell lysates after treatment of primary neurons with CORT and KET
(a) GSK-3β, (b) SIRT1, (c) REST protein expression. One-way ANOVA; n=6-12 (GSK-3β, REST), n=3-6 (SIRT1). Data are expressed as mean ± S.E.M

4.9 Modulation of REST neuronal targets in the HPC of rats subjected to CMS and KET

REST is a transcriptional repressor with a primary role in regulating the expression of numerous neuronal genes thus exerting a key role in regulating brain development, function and synaptic plasticity. qPCR was performed to measure the expression of some of the targets of REST known to be involved in synaptic function and transmission (SYN1 (Synapsin I), NPTX2 (Neuronal pentraxin 2), SHANK2 (SH3 And Multiple Ankyrin Repeat Domains 2)), neurite outgrowth (L1CAM (L1 cell adhesion molecule), ARC (Activity Regulated Cytoskeleton Associated Protein), EXTL3 (Exostosin Like Glycosyltransferase 3)), signal transduction (AKT1 (RAC-alpha serine/threonine-protein kinase 1), CTNND2 (Catenin Delta 2)), and neurotrophic factor (BDNF).

One-Way ANOVA revealed that there was a significant effect of both stress and KET on the expression of SYN1 ($F_{3,21}$ = 9.519; p = 0.0004) (Fig. 35a). In particularly, Tuckey's post-hoc test showed a significant decrease in SYN1 both in CMS-R ($p < 0.05$ vs CNT) and with a bigger extent in CMS-V ($p < 0.001$ vs CNT). KET treatment completely reversed the decrease ($p < 0.01$ vs CMS-V). Instead, there were no evident changes in NPTX2 expression ($F_{3,24}$ = 1.534; p = 0.2325) (Fig. 35b). SHANK2 expression was affected by stress ($F_{3,24}$=4.635; p=0.0108) (Fig. 35c) as shown by a significant increase of its expression in the CMS-V animals (Tuckey's post-hoc test; $p < 0.01$ vs CMS-R), independently of the treatment with KET ($p < 0.05$ vs CMS-R) but not different from the CNT. One-Way ANOVA did not highlight any changes in the expression of L1CAM ($F_{3,24}$ = 1.554; p = 0.2264), EXTL3 ($F_{3,24}$ = 1.327; p = 0.2889), ARC ($F_{3,23}$ = 2.139; p = 0.1230), AKT1 ($F_{3,23}$ = 2.185; p = 0.1172), CTNND2 (F3,24 = 0.5242; p = 0.6698) (Fig. 35d-h). However, we saw a trend of decrease of ARC expression in CMS-R and CMS-V that was not present in the group treated with

KET. Regarding BDNF (Fig. 35i; One-Way ANOVA, $F_{3,21} = 4.832$; $p = 0.0104$), there was a significant decrease in CMS-R (Tuckey's post-hoc test; $p < 0.05$ vs CNT) and especially in CMS-V (Tuckey's post-hoc test; $p < 0.01$ vs CNT); in this case KET was not able to revert the change.

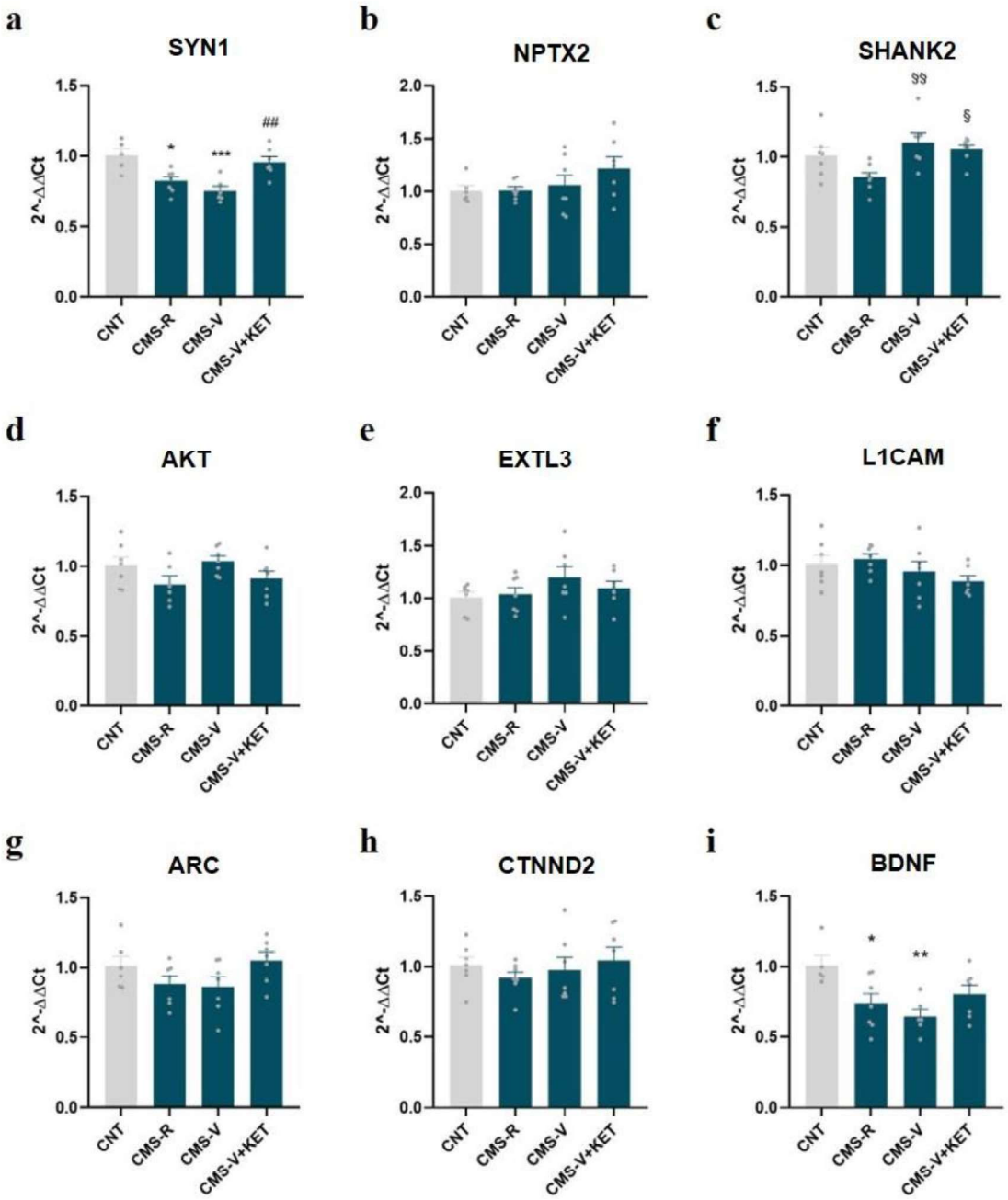

Figure 35. Analysis of the expression of REST target genes in the HPC of CMS rats

qPCR analysis of the expression of (a) SYN1, (b) NPTX2, (c) SHANK2, (d) AKT, (e) EXTL3, (f) L1CAM, (g) ARC, (h) CTNND2, (i) BDNF, One-Way ANOVA followed by Tuckey's post hoc test; *$p < 0.05$ vs CNT, **$p < 0.01$ vs CNT, ***$p < 0.001$ vs CNT, $^{\#\#}p < 0.01$ vs CMS-V, $^{\S}p < 0.05$ vs CMS-R, $^{\S\S}p < 0.01$ vs CMS-R. n=5-7. Data are expressed as mean ± S.E.M

5. DISCUSSION

5.1 Hippocampal changes in the expression of miRNAs following CMS and KET

We have previously demonstrated that the CMS animal model of depression significantly reduced dendritic length of hippocampal neurons selectively in the CA3 of the hippocampus (HPC) of CMS-V rats (Tornese et al., 2019). A single sub-anesthetic dose (10 mg/Kg) of KET completely rescued this change together with a rescue of the anhedonic behavior suggesting a primary role of the hippocampal structural changes in the pathophysiology of depression. As a matter of fact, several works are present in literature that underlie changes in structural plasticity of specific brain areas both in stress-based preclinical models of depression and in depressed patients (Drevets, 2001; Krishnan & Nestler, 2008). The HPC is one of these areas and its involvement in stress-dependent pathological consequences has been studied since the discovery that glucocorticoid receptors are expressed in the HPC (Joëls & Baram, 2009). Indeed, it is involved in memory formation, learning and emotional behavior; all processes that were shown to be somehow altered in depressed patients and in animals expressing a depressive-like phenotype. With my thesis project we decided to look at the molecular determinants of these changes in order to shed light onto new major players in the stress response and possibly find new mechanisms by which KET exerts its fast antidepressant effect. Given that it is conceivable that multiple genes are involved in these processes, we thought that molecules such as miRNAs, able to specifically regulate the expression of multitudes of genes, could have been promising. Moreover, many works demonstrated their involvement in stress-response, depression and in the action of antidepressant drugs. Based on the findings present in literature, we decided to focus on 20 miRNAs that were previously associated with these processes (Giusti et al., 2014; Hu et al., 2014; Issler et al., 2014; Jasińska et al., 2016; Schratt et al., 2006; Song et al., 2015; Yu et al., 2008) and analyze their expression in the HPC of CMS rats. Our analysis revealed that chronic stress was able to modify the expression of ten of them. However, they showed different expression patterns since for some of them there was a general effect of stress and for some other the expression was selective for resilient or vulnerable animals. There was only one miRNA whose expression was modulated by KET, namely miR-9-5p. We considered this miRNA particularly interesting since its expression was selectively reduced in vulnerable animals but not in resilient animals and KET completely rescued the reduction suggesting that a decrease in miR-9-5p could have a role in the morphological impairments found in the HPC of vulnerable animals. Further, the ability of KET to restore its levels might underline a new mechanism of action for this drug. Interestingly, miR-9-5p has been demonstrated to exert a key role during neuronal development, directing neural precursors differentiation, cell-type specification and migration. Further, it is involved also in axons formation

and elongation (Dajas-bailador et al., 2012) and in dendritic development and branching (Giusti et al., 2014; Xue et al., 2016). miR-9-5p is widely conserved among species and abundantly expressed in the brain suggesting that its roles are evolutionarily essential for the proper functioning of the brain. There are also evidences of alteration of miR-9-5p levels in stress-based animal models (Buran et al., 2017; Rinaldi et al., 2010; Zhang et al., 2015) and in the blood of depressed patients. Together these data made miR-9-5p a valuable target for my research project.

miR-135a-5p was the second miRNA that we selected because of its well-known role in the mechanism of stress resiliency/vulnerability as elegantly showed in mice by Issler and colleagues (Issler et al., 2014) who also found a reduction of miR-135a-5p expression in the blood and brain of depressed patients. In our model, miR-135a-5p was significantly altered by chronic stress that produced a decrease of its levels in all stressed animals; however, KET did not exert any effect on its expression. The analysis of miR-9-5p and miR-135a-5p expression using Real-Time PCR on HPC samples measures the levels of the miRNAs in the whole HPC with no distinction for the sub-regions. With the purpose of elucidating possible different expression patterns in CA3, CA1 and DG we performed in situ hybridization studies that allow to quantify the signal belonging to each sub-region. This experiment confirmed a decrease for miR-9-5p selectively in the vulnerable animals that affected all the sub-regions and KET completely rescued miR-9-5p levels. Interestingly, the persistence of the signal along the dendrites suggests that miR-9-5p might be active in the dendritic compartment and regulate gene expression locally (Siegel et al., 2009). Interestingly, the reduction of miR-9-5p in vulnerable animals was present also in the proximal dendrites of CA3 neurons. To note, increase of miR-9-5p levels were seen after acute stress in the frontal cortex (Rinaldi et al., 2010) or after CMS in the prefrontal cortex of mice (Buran et al., 2017). Another report showed alterations of miR-9-5p in the striatum and in the Nucleus Accumbens of rats, respectively after maternal deprivation or chronic unpredictable stress (Zhang et al., 2015). The different findings might depend on the fact that different types of stressors have been used and different brain regions were investigated. Regarding miR-135a-5p, in situ hybridization analysis showed a trend of expression similar in CA3, CA1 and DG suggesting that all three areas contribute to the expression alterations.

5.2 Repeated treatment with CORT of primary hippocampal neurons impairs dendritic morphology and modulates miR-9-5p expression. KET exerts a restorative action

Glucocorticoids play a key role in mediating the response to stress as downstream effectors of the HPA axis activation. Their actions in the brain, and specifically in the HPC, are involved in the functional and morphological rearrangements that follow stress experiences. Several works are present in literature in which the authors used corticosterone (CORT), the mostly abundant

glucocorticoid in rodents, to study directly *in vitro* the effect of its modulation on neuronal function and morphology (Alfarez et al., 2009; Donoso et al., 2019), synaptic transmission and excitability (Chatterjee & Sikdar, 2014). Here, we used low (200 nM) and repeated (6 times) doses of CORT on primary hippocampal neurons aiming at reproducing a "chronic stressful environment" and study its direct effect on the morphology of hippocampal neurons and on the expression of miR-9-5p and miR-135a-5p. One issue about the use of primary cultures for cell morphological analysis would be the high rate of variability of cell shape within the same culture due to the fact that neurons are growing in 2D. To overcome this problem, we set up a model in which we were able to measure every cell before and after the treatments thanks to the use of live-imaging acquisitions. This method allowed us to analyze morphological changes within the same cell avoiding any biases due to cell variability. The repeated exposure of mature neurons (DIV17 to DIV20) to CORT significantly reduced the total dendritic length of pyramidal neurons together with a reduction of miR-9-5p expression. These data strength the association between dendritic remodeling and miR-9-5p activity. We observed the main changes at apical dendrites without significant modification of basal arborization. However, considering that neurons *in vitro* do not have the underneath structures that are present in tissues and the connections with other cell types, it is reasonable to be careful with this distinction. To test the effect of KET in reverting the morphological and molecular changes, we exposed neuronal cells to KET after three days of treatments with CORT. We found that after 4 h of KET treatment, the reduction of miR-9-5p levels was completely rescued together with a full recovery of dendritic length suggesting that KET could positively regulate both miR-9-5p expression and dendritic remodeling. Instead, miR-135a-5p expression was not changed neither by CORT nor by KET treatment. Here we show that chronic CORT, similarly to CMS in vulnerable rats, impairs both the dendritic arborization and the expression of miR-9-5p in primary hippocampal neurons suggesting a direct role of stress in these alterations. Importantly, we found that KET ability to reverse the morphological changes induced by CORT may depend at least in part on modulation of miR-9-5p. Other works already looked at alterations of this miRNA as a possible mechanism in response to antidepressant treatment (Zhang et al., 2015), but to our knowledge it is the first time that it has been studied in relation to the fast-acting antidepressant KET.

5.3 Direct modulation of miR-9-5p in primary hippocampal neurons is sufficient to regulate dendritic remodeling. Both miR-9-5p and miR-135a-5p regulate spine density

In order to assess whether miR-9-5p and miR-135a-5p exerted a direct effect on dendritic remodeling of primary hippocampal neurons, specific vectors designed to overexpress or downregulate the two miRNAs were used. The presence within the vectors of fluorescent reporters allowed us to analyze

only transfected cells eliminating any bias from other cells in the cultures. We found that 72 h of overexpression of miR-9-5p significantly increased total dendritic length, especially of apical dendrites, total number of branches and the density of dendritic spines. Oppositely, the downregulation of miR-9-5p negatively affected total dendritic length, total number of branches and spine density. Together, these results confirmed our hypothesis that miR-9-5p modulation could regulate dendritic remodeling. To note, there are evidences that report a role of miR-9-5p in dendritic development and branching (Giusti et al., 2014; Xue et al., 2016). Regarding miR-135a-5p, we found minor changes after its modulation and mostly involving dendritic spines. Indeed, the overexpression of miR-135a-5p significantly increased only the number of branches and the density of spines. The downregulation, instead, decreased the number of spines without modifying the dendritic arborization. It has been previously shown that miR-135a-5p is involved in spine plasticity throughout the targeting of Complexin I and II (Hu et al., 2014). Other miRNAs have been linked to changes in axonal/dendritic remodeling by regulating the expression of target genes involved in synaptic plasticity (Li et al., 2014; Schratt et al., 2006). Importantly, we found an impairment in dendritic morphology when miR-9-5p was downregulated that is the same pattern that we have seen both in vulnerable animals after CMS and in primary neurons after CORT treatment. Moreover, KET was shown to revert this change in both cases inducing an increase of miR-9-5p levels which, as demonstrated here, is associated with a positive regulation of dendritic arborization. The effect on synaptic plasticity is extremely important considering the role that it plays in stress-induced disorders such as depression. How stress and KET are able to increase miR-9-5p levels is still unknown but it is noteworthy a work of 2006 (Wu & Xie, 2006) where a cAMP response element (CRE) recognized by CREB was computationally identified nearby ten miRNA genes, including miR-9. Upon phosphorylation (p-CREB), p-CREB acts as a transcription factor for genes involved in growth and survival, neuroprotection and synaptic plasticity (Duman et al., 1999). Interestingly, it was shown that p-CREB is upregulated after chronic antidepressant treatment, including KET (Dwivedi, 2008; Wray et al., 2019). Further studies are required to investigate possible undelying mechanisms. In conclusion, our results confirmed an important role for miR-9-5p, more than for miR-135a-5p, on mediating the morphological effect on pyramidal neuron of chronic stress and KET. Considering that our primary interest was to find molecular determinants of the cytoarchitectural modification we decided to focus our attention on miR-9-5p and its downstream pathways.

5.4 Bioinformatic analysis of miR-9-5p target genes and their validation with Luciferase assay and Western-blotting identified REST and SIRT1 as biological targets of miR-9-5p

Since miRNAs mostly act by negatively controlling the expression of their target genes, we conducted a bioinformatic research to identify miR-9-5p targets that may be of our interest to explain the role of this miRNA on dendritic remodeling. The prediction tools rely on algorithms that predict the probability that the seed sequence of a specific miRNA recognize a complementary sequence in the 3'UTR of all the genes annotated in the database. This interaction should be considered putative until it is validated *in vitro* but still could give important insights in the target genes of the miRNAs and their relative pathways. Our analysis revealed more than one thousand transcripts with predicted binding sites for miR-9-5p and most of them were conserved. After applying selection requirements to narrow down the number of targets we selected seven genes: DRD2, ELAVL1, GSK-3β, NTRK3, SIRT1, SORT1 and REST. Most of them are involved in neuronal plasticity and are modulated in response to stress (Bradley et al., 2012; Chen, 2005; Farhang et al., 2014; Gao et al., 2010; He et al., 2019; Mampay & Sheridan, 2019; Quattrone et al., 2001; Skliris et al., 2015; Żurawek et al., 2013). Further, some of them have also been associated with depression and with antidepressant activity (Athanasiu et al., 2011; Beurel et al., 2011; Buttenschøn et al., 2015; Duman et al., 2017; Otnæss et al., 2009; Polter et al., 2010; Zhou et al., 2013).

Luciferase assay was used to validate the interaction between miR-9-5p and its predicted targets using HEK293T cells. Firstly, we assessed the interaction of miR-9-5p with a shorter sequence of the 3'UTR of the targets spanning 30 bp before and after the binding site of miR-9-5p. Accordingly, only three (GSK-3β, SIRT1 and REST) of the selected genes interacted with miR-9-5p mimics as demonstrated by the reduced production of *Firefly* luciferase-dependent luminescence. Considering that in a biological system we would not find a fragment of the 3'UTR of GSK-3β, SIRT1 and REST but the whole region, we repeated the experiment cloning approximately the whole 3'UTR of these genes. This time we found that only the interaction between SIRT1 and REST 3'UTRs with miR-9-5p mimics was able to reduce the luminescence produced by *Firefly* luciferase confirming that miR-9-5p effectively binds to these mRNAs. Evidences are present in literature that confirmed that REST is a target of miR-9-5p (Giusti et al., 2014; Wu & Xie, 2006). On the contrary, GSK-3β 3'UTR did not seem to interact to miR-9-5p suggesting that possible structural rearrangements of the 3'UTR might prevent the recognition of the binding site. To note, other works previously obtained different results from ours demonstrating an interaction between miR-9-5p and GSK-3β (Dong et al., 2018). Interestingly, both GSK-3β and SIRT1 3'UTRs contain also a complementary sequence to miR-135a-5p. Thus, we investigated the interaction between miR-135a-5p and those genes alone or together

with miR-9-5p to evaluate synergistic effect. Regarding GSK-3β, we did not find any interaction with miR-135a-5p alone but together with miR-9-5p it induced a slight decrease in the *firefly* luciferase activity. However, the extent of the reduction was too small to possibly produce a biological effect. On the other hand, miR-135a-5p produced a significant decrease in the *firefly* luciferase activity by its interaction with SIRT1 3'UTR; the effect was more pronounced when miR-135a-5p and miR-9-5p where used together. This might suggest that the two miRNAs can contribute together to the regulation of SIRT1 gene expression. With the purpose of testing whether the modulation of miR-9-5p in neuronal cultures produced related changes in the target genes that we validated, we over-expressed miR-9-5p using mimics in primary hippocampal neurons and measured the expression of GSK-3β, SIRT1 and REST with Western blotting. We found that the increase of miR-9-5p led to a significant reduction of the expression of GSK-3β, SIRT1 and REST. While this result was expected for SIRT1 and REST since we validated their interaction with miR-9-5p, we did not expect to see changes in GSK-3β expression after modulating miR-9-5p. However, the reduction of REST and SIRT1 confirmed their interaction with miR-9-5p suggesting considering their role in mediating miR-9-5p effect on neuronal morphology. SIRT1 belongs to the family of sirtuins that are histone deacetylases associated with transcriptional silencing, aging, cell differentiation, stress response and inflammation (Lu et al., 2018). SIRT1 is abundantly expressed in the brain where throughout the epigenetic control of plasticity-associated genes it has been shown to regulate synaptic plasticity, memory formation and cognitive function (Gao et al., 2010; Michan et al., 2010). SIRT1 has also been associated with depression in both stress-based animal models and in humans (Lu et al., 2018). The repressor element 1 silencing transcription factor (REST), also known as neuron-restrictive silencer factor (NRSF), is a transcription repressor of more than 2000 neuron-specific target genes, encoding proteins involved in synaptic plasticity, neurotransmitter receptors, ion channel proteins and adhesion molecules (Mampay & Sheridan, 2019). REST expression changes during neuronal maturation: during embryogenesis is highly expressed in neuronal stem cells while in the last phases of neuronal differentiation its downregulation is critical for the acquisition of neuronal phenotype and allowing important processes such as axonal growth, synaptic signaling and membrane excitability (Baldelli & Meldolesi, 2015; Johnson et al., 2008). Although REST expression is low in mature neurons, it can be reactivated during specific moments of synaptic remodeling to fine tune genes involved in these processes. For example, neuronal insults such as ischemia and seizure were shown to increase REST expression to promote neuronal death (Mampay & Sheridan, 2019). Further, both physical and psychological stress cause an upregulation of REST levels in various rodent brain regions (Mampay & Sheridan, 2019; Soga et al., 2021). Numerous works showed that REST levels are highly responsive to stressful stimuli and implicate the control of genes involved in the

neuroendocrine stress response such as Crh, 5htr1a, Tph2 and Bdnf (Lemonde et al., 2004; Patel et al., 2007; Uchida et al., 2010; Zuccato et al., 2007). Moreover, REST has the ability to control neuronal excitability preserving the intrinsic homeostatic plasticity (Pozzi et al., 2013).

5.5 Effect of CORT and KET treatment on the expression of GSK-3β, SIRT1 and REST in primary hippocampal cultures

We have shown in this study that the treatment of primary neurons with CORT negatively affected dendritic arborisation of pyramidal neurons together with a reduction in miR-9-5p expression. Acute treatment with KET was able to rescue the morphological impairment and to restore miR-9-5p levels. After validating SIRT1 and REST as biological targets of miR-9-5p, we analysed their expression in primary neurons treated with CORT and KET to assess whether the changes described could be explained by modulation of SIRT1 and REST expression. No significative changes were found although we could observe for REST a trend of increase in cells treated with CORT but this was not reverted by KET. SIRT1 expression slightly decreased after CORT without being changed by KET. We also looked at GSK-3β and did not observe important changes. Taken together, these results may be influenced by the high variability within the experimental groups that is an issue that may occur using *in vitro* neuronal cultures. The analysis of protein expression has been made immediately at the end of the repeated CORT treatment; this period of time was enough to detect changes in miR-9-5p expression but maybe it would require a longer time to see changes in protein levels. Further, the use of CORT directly on neurons produces diverse effects beyond the modulation of miRNAs and those activated pathways could involve the modulation of our targets thus masking the miRNA-mediated alterations.

5.6 Modulation of REST and SIRT1 expression in CMS rats is a putative mechanism of miR-9-5p effect on neuronal morphology and is regulated by KET

We measured the expression of SIRT1, REST and GSK-3β in the HPC of CMS rats to assess whether the changes that we previously found in the expression of miR-9-5p are associated with alterations of its validated targets. GSK-3β was not changed, neither at transcript nor at protein level. However, we found an increase of its expression in vulnerable animals that received KET which may seem odd considering that KET has been demonstrated to inhibit the activity of this enzyme (Zarate & Machado-Vieira, 2016). To note, we did not look at the level of phosphorylated GSK-3β-Ser9, that is the inactive form, because we were not able to validate GSK-3β as a target of miR-9-5p and thus it seemed not relevant for our study. Further, the variability within the CMS-V+KET group may have influenced this result. Regarding SIRT1, we found a selective increase in vulnerable animals although

it did not always reach a statistical significance. This would fit with a reduction of miR-9-5p expression in CMS-V animals. KET seemed to partially revert this increase as shown by a lower expression of SIRT1 in vulnerable rats treated with KET. SIRT1 expression in resilient animals was not different from the controls suggesting that elevation of its levels specifically in vulnerable animals may underpin the changes found in those animals. Conflicting opinions are present in literature about the role of SIRT1 in the response to stress and in depression. It has been demonstrated that SIRT1 expression in the peripheral blood of depressed individuals is lower than in healthy subjects (Kishi et al., 2010) and that mutations within SIRT1 gene contribute to increased risk of depression (CONVERGE Consortium, 2015). Using animal models of depression, it was found a decreased SIRT1 activity in the dentate gyrus of mice after chronic stress and an elevation of depressive-like behaviors after pharmacologic or genetic ablation of hippocampal SIRT1 (Abe-Higuchi et al., 2016). However, other groups found that mice with brain-specific SIRT1 knockout decreased anxiety and developed a resilient phenotype to depression induced by social defeat stress (Libert et al., 2011). Moreover, increased SIRT1 levels and activity were found in hippocampal CA3 and DG regions following chronic stress in rats (Ferland & Schrader, 2011). These incongruities may depend on the use of animals with a different genetic background or different stress protocols. According to our data, stress induces an increase in SIRT1 expression in the HPC of rats vulnerable to CMS due to a down-regulation of miR-9-5p. This could induce an alteration of the expression of genes that are targets of SIRT1, including those plasticity-associated genes, resulting in an impairment of synaptic remodeling. The role of SIRT1 in the morphological changes that we found after stress and in response to KET should be further addressed to better elucidate the specific mechanism.

The analysis of REST revealed a robust increase of its expression only in CMS vulnerable animals with no changes in the resilient. This result is consistent with other findings in which REST protein expression was elevated after stress (Chen et al., 2016; Mou & Zhao, 2016) and could be explained by the concurrent reduction of miR-9-5p found both in CMS vulnerable animals and in CORT-treated primary neurons. Interestingly, Giusti and collaborators (Giusti et al., 2014) have shown that miR-9-5p controls dendritic growth in developing mouse primary hippocampal neurons by targeting REST. Accordingly, the transfection of neural precursors with shRNA against REST strongly rescued the dendritic growth defects in neurons with conditional downregulation of miR-9-5p confirming that increase in REST levels is a major mediator of miR-9-5p effect on dendritic growth. In line with this, our data suggest that miR-9-5p-mediated control of REST expression is implicated in dendritic remodeling of hippocampal neurons and is regulated by stress. We also found that defects in this pathway can be reversed by KET. Indeed, KET completely restore miR-9-5p levels either in stressed

animals or in primary neurons treated with CORT. However, few is known about the exact mechanism by which REST directly modulate dendritic morphology. Given that miR-9-5p is abundantly expressed in the adult brain while REST is downregulated, except in areas involved in neurogenesis processes, it is reasonable to think that miR-9-5p may function to keep low REST levels during maturation. This activity may be necessary to avoid REST-dependent inhibition of expression of plasticity-associated genes. Many genes that are targets of REST are in fact involved in vesicular transport, signal transduction, neurite outgrowth and cell adhesion (Sun et al., 2005). We hypothesize that in the absence of miR-9-5p, REST upregulation could inhibit the transcription of genes involved in synaptic plasticity and negatively affect dendritic morphology. Therefore, we looked at the expression of several targets of REST in the hippocampus of CMS animals and noticed that some of them (i.e. SYN1, BDNF, ARC) were downregulated in stressed animals where REST levels where higher. Interestingly, SYN1 expression was restored by KET. Overall, this approach may not be enough to prove a molecular responsible for the morphological changes but still can suggest that upon the increase of REST expression many other genes are modulated that can play a role in the structural rearrangements. This highlights a key role for REST as an epigenetic regulator of synaptic and dendritic plasticity especially in response to stress.

It would be of primary importance in future studies to determine whether the overexpression of miR-9-5p, whose role in dendritic remodeling has been elucidated here, will prevent the morphological impairments induced by stress. The corroboration of the protective role of miR-9-5p against neuronal dendrites retraction would further support our hypothesis that this miRNA plays a fundamental role in maintaining a functional structure of the hippocampal neurons. Further, a more in-depth study of the molecular mechanisms activated by REST and SIRT1 would provide details on how their increase, induced by a stress-dependent downregulation of miR-9-5p, negatively affect dendritic arborization.

6. CONCLUSIONS

We have investigated the role of miRNAs in the functional and morphological changes induced by chronic stress and ketamine (KET) both in the hippocampus of rats subjected to Chronic Mild Stress (CMS) and in primary hippocampal cultures.

Stress is considered a risk factor for the pathogenesis of neuropsychiatric disorders such as depression and thus elucidating the molecular mechanisms that are activated in response to stressful events and that become dysfunctional in individuals that fail to copy with them is crucial to the development of new pharmacological strategies to treat stress-induced disorders, including depression. Here, we

showed that CMS alters the hippocampal expression of several miRNAs; among them we focused our attention on miR-9-5p and miR-135a-5p. Those miRNAs are abundantly expressed in the brain and have been demonstrated to exert important role in neurodevelopment, axonal and dendritic extension and remodeling, synaptic function and stress response. We found that miR-9-5p expression was reduced selectively in animals vulnerable to CMS in which we previously demonstrated that chronic stress impaired dendritic arborization of CA3 pyramidal neurons (Tornese et al., 2019). Importantly, acute KET was able to rapidly rescue both the dendritic retraction and miR-9-5p levels. Using repeated corticosterone (CORT) treatments in primary hippocampal neurons, we demonstrated that miR-9-5p expression is directly controlled by stress. Indeed, pyramidal neurons treated with CORT presented lower levels of miR-9-5p and reduced dendritic length. KET completely reverted these changes. With the purpose of studying whether miR-9-5p directly regulate dendritic remodeling of hippocampal neurons, we cloned vectors to modulate the expression of the miRNA in primary cultures. We observed a significant impairment in dendritic length, arborization and spine density in neurons where miR-9-5p was down-regulated while its over-expression exerted the opposite effect, increasing dendritic length, arborization and spine density. We further studied putative target genes of miR-9-5p that could mediate the morphological effects and validated them with Luciferase assay. We demonstrated that both SIRT1 and REST are targets of miR-9-5p as verified by the analysis of their expression after miR-9-5p modulation in hippocampal neurons. Importantly, SIRT1 and REST were also modulated in the HPC of CMS rats where they were both increased selectively in vulnerable animals and a subanesthetic dose of KET rescued the change.

In the present work, we demonstrated that morphological changes induced by chronic stress and KET are accompanied by a modulation of miR-9-5p levels both in the hippocampus of CMS rats and in primary neuronal cultures. This alteration prevents miR-9-5p regulation of the expression of SIRT1 and REST that therefore negatively influence neuronal dendritic morphology presumably by controlling the expression of synaptic plasticity-associated genes.

7. BIBLIOGRAPHY

Abe-Higuchi, N., Uchida, S., Yamagata, H., Higuchi, F., Hobara, T., Hara, K., Kobayashi, A., & Watanabe, Y. (2016). Hippocampal Sirtuin 1 Signaling Mediates Depression-like Behavior. *Biological Psychiatry*, *80*(11), 815–826. https://doi.org/10.1016/j.biopsych.2016.01.009

Alfarez, D. N., De Simoni, A., Velzing, E. H., Bracey, E., Joëls, M., Edwards, F. A., & Krugers, H. J. (2009). Corticosterone reduces dendritic complexity in developing hippocampal CA1 neurons. *Hippocampus*, *19*(9), 828–836. https://doi.org/10.1002/hipo.20566

American Psychiatric Association. (2013). *Diagnostic and Statistical Manual of Mental Disorders: DSM-5*. American Psychiatric Publishing.

Anacker, C., Zunszain, P. A., Carvalho, L. A., & Pariante, C. M. (2011). The glucocorticoid receptor: Pivot of depression and of antidepressant treatment? *Psychoneuroendocrinology*, *36*(3), 415–425. https://doi.org/10.1016/j.psyneuen.2010.03.007

Athanasiu, L., Mattingsdal, M., Melle, I., Inderhaug, E., Lien, T., Agartz, I., Lorentzen, S., Morken, G., Andreassen, O. A., & Djurovic, S. (2011). Intron 12 in NTRK3 is associated with bipolar disorder. *Psychiatry Research*, *185*(3), 358–362. https://doi.org/10.1016/j.psychres.2010.05.011

Autry, A. E., Adachi, M., Nosyreva, E., Na, E. S., Los, M. F., Cheng, P., Kavalali, E. T., & Monteggia, L. M. (2011). NMDA receptor blockade at rest triggers rapid behavioural antidepressant responses. *Nature*, *475*(7354), 91–95. https://doi.org/10.1038/nature10130

Autry, A. E., & Monteggia, L. M. (2012). Brain-Derived Neurotrophic Factor and Neuropsychiatric Disorders. *Pharmacological Reviews*, *64*(2), 238–258. https://doi.org/10.1124/pr.111.005108

Baj, G., Leone, E., Chao, M. V., & Tongiorgi, E. (2011). Spatial segregation of BDNF transcripts enables BDNF to differentially shape distinct dendritic compartments. *Proceedings of the National Academy of Sciences of the United States of America*, *108*(40), 16813–16818. https://doi.org/10.1073/pnas.1014168108

Baldelli, P., & Meldolesi, J. (2015). The transcription repressor REST in adult neurons: Physiology, pathology, and diseases. *ENeuro*, *2*(4). https://doi.org/10.1523/ENEURO.0010-15.2015

Ballard, E. D., Lally, N., Nugent, A. C., Furey, M. L., Luckenbaugh, D. A., & Zarate, C. A. (2014). Neural correlates of suicidal ideation and its reduction in depression. *The International Journal of Neuropsychopharmacology*, *18*(1). https://doi.org/10.1093/ijnp/pyu069

Banasr, M., Valentine, G. W., Li, X.-Y., Gourley, S. L., Taylor, J. R., & Duman, R. S. (2007). Chronic Unpredictable Stress Decreases Cell Proliferation in the Cerebral Cortex of the Adult Rat. *Biological Psychiatry*, *62*(5), 496–504. https://doi.org/10.1016/j.biopsych.2007.02.006

Bartel, D. P., Lee, R., & Feinbaum, R. (2004). MicroRNAs : Genomics , Biogenesis , Mechanism , and Function Genomics : The miRNA Genes. *Cell*, *116*, 281–297.

Bech, P. (2006). Rating scales in depression: limitations and pitfalls. *Dialogues in Clinical Neuroscience*, *8*(2), 207–215. http://www.ncbi.nlm.nih.gov/pubmed/16889106

Berman, R. M., Cappiello, A., Anand, A., Oren, D. A., Heninger, G. R., Charney, D. S., & Krystal, J. H. (2000). *Antidepressant Effects of Ketamine in Depressed Patients*. *3223*(99).

Beurel, E., Song, L., & Jope, R. S. (2011). Inhibition of glycogen synthase kinase-3 is necessary for the rapid antidepressant effect of ketamine in mice. *Molecular Psychiatry*, *16*(11), 1068–1070.

https://doi.org/10.1038/mp.2011.47

Beveridge, N. J., Tooney, P. A., Carroll, A. P., Tran, N., & Cairns, M. J. (2009). Down-regulation of miR-17 family expression in response to retinoic acid induced neuronal differentiation. *Cellular Signalling*, *21*(12), 1837–1845. https://doi.org/10.1016/j.cellsig.2009.07.019

Bloss, E. B., Janssen, W. G., McEwen, B. S., & Morrison, J. H. (2010). Interactive Effects of Stress and Aging on Structural Plasticity in the Prefrontal Cortex. *Journal of Neuroscience*, *30*(19), 6726–6731. https://doi.org/10.1523/JNEUROSCI.0759-10.2010

Bonev, B., Pisco, A., & Papalopulu, N. (2011). MicroRNA-9 reveals regional diversity of neural progenitors along the anterior-posterior axis. *Developmental Cell*, *20*(1), 19–32. https://doi.org/10.1016/j.devcel.2010.11.018

Bonini, D., Mora, C., Tornese, P., Sala, N., Filippini, A., La Via, L., Milanese, M., Calza, S., Bonanno, G., Racagni, G., Gennarelli, M., Popoli, M., Musazzi, L., & Barbon, A. (2016). Acute Footshock Stress Induces Time-Dependent Modifications of AMPA/NMDA Protein Expression and AMPA Phosphorylation. *Neural Plasticity*, *2016*, 1–10. https://doi.org/10.1155/2016/7267865

Bradley, C. A., Peineau, S., Taghibiglou, C., Nicolas, C. S., Whitcomb, D. J., Bortolotto, Z. A., Kaang, B.-K., Cho, K., Wang, Y. T., & Collingridge, G. L. (2012). A pivotal role of GSK-3 in synaptic plasticity. *Frontiers in Molecular Neuroscience*, *5*. https://doi.org/10.3389/fnmol.2012.00013

Braun, I., Genius, J., Grunze, H., Bender, A., Möller, H.-J., & Rujescu, D. (2007). Alterations of hippocampal and prefrontal GABAergic interneurons in an animal model of psychosis induced by NMDA receptor antagonism. *Schizophrenia Research*, *97*(1–3), 254–263. https://doi.org/10.1016/j.schres.2007.05.005

Brunson, K. L. (2005). Mechanisms of Late-Onset Cognitive Decline after Early-Life Stress. *Journal of Neuroscience*, *25*(41), 9328–9338. https://doi.org/10.1523/JNEUROSCI.2281-05.2005

Buran, İ., Etem, E. Ö., Tektemur, A., & Elyas, H. (2017). Treatment with TREK1 and TRPC3/6 ion channel inhibitors upregulates microRNA expression in a mouse model of chronic mild stress. *Neuroscience Letters*, *656*, 51–57. https://doi.org/10.1016/j.neulet.2017.07.017

Buttenschøn, H. N., Demontis, D., Kaas, M., Elfving, B., Mølgaard, S., Gustafsen, C., Kaerlev, L., Petersen, C. M., Børglum, A. D., Mors, O., & Glerup, S. (2015). Increased serum levels of sortilin are associated with depression and correlated with BDNF and VEGF. *Translational Psychiatry*, *5*(11), e677–e677. https://doi.org/10.1038/tp.2015.167

Castrén, E., & Rantamäki, T. (2010). The role of BDNF and its receptors in depression and antidepressant drug action: Reactivation of developmental plasticity. *Developmental Neurobiology*, *70*(5), 289–297. https://doi.org/10.1002/dneu.20758

Caudy, A. A., Myers, M., Hannon, G. J., & Hammond, S. M. (2002). Fragile X-related protein and VIG associate with the RNA interference machinery. *Genes & Development*, *16*(19), 2491–2496. https://doi.org/10.1101/gad.1025202

Chatterjee, S., & Sikdar, S. K. (2014). Corticosterone targets distinct steps of synaptic transmission via concentration specific activation of mineralocorticoid and glucocorticoid receptors. *Journal of Neurochemistry*, *128*(4), 476–490. https://doi.org/10.1111/jnc.12478

Chen, C.-C., Huang, C.-C., & Hsu, K.-S. (2016). Chronic Social Stress Affects Synaptic Maturation

of Newly Generated Neurons in the Adult Mouse Dentate Gyrus. *International Journal of Neuropsychopharmacology*, *19*(3), pyv097. https://doi.org/10.1093/ijnp/pyv097

Chen, Y., & Wang, X. (2020). miRDB: an online database for prediction of functional microRNA targets. *Nucleic Acids Research*, *48*(D1), D127–D131. https://doi.org/10.1093/nar/gkz757

Chen, Z.-Y. (2005). Sortilin Controls Intracellular Sorting of Brain-Derived Neurotrophic Factor to the Regulated Secretory Pathway. *Journal of Neuroscience*, *25*(26), 6156–6166. https://doi.org/10.1523/JNEUROSCI.1017-05.2005

Chi, S. W., Zang, J. B., Mele, A., & Darnell, R. B. (2009). Ago HITS-CLIP decodes miRNA-mRNA interaction maps. *Nature*, *460*(7254), 479–486. https://doi.org/10.1038/nature08170.Ago

CONVERGE Consortium. (2015). Sparse whole-genome sequencing identifies two loci for major depressive disorder. *Nature*, *523*(7562), 588–591. https://doi.org/10.1038/nature14659

Dajas-bailador, F., Bonev, B., Garcez, P., Stanley, P., Guillemot, F., & Papalopulu, N. (2012). microRNA-9 regulates axon extension and branching by targeting Map1b in mouse cortical neurons. *Nature Neuroscience*, *15*(5). https://doi.org/10.1038/nn.3082

Delaloy, C., Liu, L., Lee, J.-A., Su, H., Shen, F., Yang, G.-Y., Young, W. L., Ivey, K. N., & Gao, F.-B. (2010). MicroRNA-9 Coordinates Proliferation and Migration of Human Embryonic Stem Cell-Derived Neural Progenitors. *Cell Stem Cell*, *6*(4), 323–335. https://doi.org/10.1016/j.stem.2010.02.015

Diamond, P. R., Farmery, A. D., Atkinson, S., Haldar, J., Williams, N., Cowen, P. J., Geddes, J. R., & McShane, R. (2014). Ketamine infusions for treatment resistant depression: a series of 28 patients treated weekly or twice weekly in an ECT clinic. *Journal of Psychopharmacology*, *28*(6), 536–544. https://doi.org/10.1177/0269881114527361

Dias, C., Feng, J., Sun, H., Shao, N. yi, Mazei-Robison, M. S., Damez-Werno, D., Scobie, K., Bagot, R., LaBonté, B., Ribeiro, E., Liu, X., Kennedy, P., Vialou, V., Ferguson, D., Peña, C., Calipari, E. S., Koo, J. W., Mouzon, E., Ghose, S., … Nestler, E. J. (2014). β-catenin mediates stress resilience through Dicer1/microRNA regulation. *Nature*, *516*(7529), 51–55. https://doi.org/10.1038/nature13976

Domino, E. F., Chodoff, P., & Corssen, G. (1965). Pharmacologic effects of CI-581, a new dissociative anesthetic, in man. *Clinical Pharmacology & Therapeutics*, *6*(3), 279–291. https://doi.org/10.1002/cpt196563279

Dong, Z. C., Zhang, D., Wang, S. B., & Lin, Z. Q. (2018). Target Inhibition on GSK-3β by miR-9 to modulate proliferation and apoptosis of bladder cancer cells. *European Review for Medical and Pharmacological Sciences*, *22*(10), 3018–3026. https://doi.org/10.26355/eurrev_201805_15059

Donoso, F., Ramírez, V. T., Golubeva, A. V, Moloney, G. M., Stanton, C., Dinan, T. G., & Cryan, J. F. (2019). Naturally Derived Polyphenols Protect Against Corticosterone-Induced Changes in Primary Cortical Neurons. *International Journal of Neuropsychopharmacology*, *22*(12), 765–777. https://doi.org/10.1093/ijnp/pyz052

Douglas, R. J., & Martin, K. A. C. (2007). Recurrent neuronal circuits in the neocortex. *Current Biology*, *17*(13), R496–R500. https://doi.org/10.1016/j.cub.2007.04.024

Drevets, W. C. (2001). Neuroimaging and neuropathological studies of depression: implications for the cognitive-emotional features of mood disorders. *Current Opinion in Neurobiology*, *11*(2),

240–249. https://doi.org/10.1016/S0959-4388(00)00203-8

Duman, R. S., Aghajanian, G. K., Sanacora, G., Krystal, J. H., & Haven, N. (2017). Synaptic plasticity and depression: New insights from stress and rapid-acting antidepressants. *Nature Medicine*, *22*(3), 238–249. https://doi.org/10.1038/nm.4050.Synaptic

Duman, R. S., Malberg, J., & Thome, J. (1999). Neural plasticity to stress and antidepressant treatment. *Biological Psychiatry*, *46*(9), 1181–1191. https://doi.org/10.1016/S0006-3223(99)00177-8

Duman, R. S., & Monteggia, L. M. (2006). A Neurotrophic Model for Stress-Related Mood Disorders. *Biological Psychiatry*, *59*(12), 1116–1127. https://doi.org/10.1016/j.biopsych.2006.02.013

Dundee, J. W., Bovill, J., Knox, J. W. D., Clarke, R. S. J., Black, G. W., Love, S. H. S., Moore, J., Elliott, J., Pandit, S. K., & Coppel, D. L. (1970). KETAMINE AS AN INDUCTION AGENT IN ANÆSTHETICS. *The Lancet*, *295*(7661), 1370–1371. https://doi.org/10.1016/S0140-6736(70)91273-0

Dwivedi, Y, Roy, B., Lugli, G., Rizavi, H., Zhang, H., & Smalheiser, N. R. (2015). Chronic corticosterone-mediated dysregulation of microRNA network in prefrontal cortex of rats: relevance to depression pathophysiology. *Translational Psychiatry*, *5*(11), e682–e682. https://doi.org/10.1038/tp.2015.175

Dwivedi, Yogesh. (2008). Adenylyl cyclase-cyclicAMP signaling in mood disorders: Role of the crucial phosphorylating enzyme protein kinase A. *Neuropsychiatric Disease and Treatment*, 161. https://doi.org/10.2147/NDT.S2380

Edbauer, D., Neilson, J. R., Foster, K. A., Wang, C.-F., Seeburg, D. P., Batterton, M. N., Tada, T., Dolan, B. M., Sharp, P. A., & Sheng, M. (2010). Regulation of synaptic structure and function by FMRP-associated microRNAs miR-125b and miR-132. *Neuron*, *65*(3), 373–384. https://doi.org/10.1016/j.neuron.2010.01.005

Farhang, S., Barar, J., Fakhari, A., Mesgariabbasi, M., Khani, S., Omidi, Y., & Farnam, A. (2014). Asymmetrical expression of BDNF and NTRK3 genes in frontoparietal cortex of stress-resilient rats in an animal model of depression. *Synapse*, *68*(9), 387–393. https://doi.org/10.1002/syn.21746

Ferland, C. L., & Schrader, L. A. (2011). Regulation of histone acetylation in the hippocampus of chronically stressed rats: a potential role of sirtuins. *Neuroscience*, *174*, 104–114. https://doi.org/10.1016/j.neuroscience.2010.10.077

Filippini, A., Bonini, D., Lacoux, C., Pacini, L., Zingariello, M., Sancillo, L., Bosisio, D., Salvi, V., Mingardi, J., La Via, L., Zalfa, F., Bagni, C., & Barbon, A. (2017). Absence of the Fragile X Mental Retardation Protein results in defects of RNA editing of neuronal mRNAs in mouse. *RNA Biology*, *14*(11), 1580–1591. https://doi.org/10.1080/15476286.2017.1338232

Fiore, R., Khudayberdiev, S., Christensen, M., Siegel, G., Flavell, S. W., Kim, T.-K., Greenberg, M. E., & Schratt, G. (2009). Mef2-mediated transcription of the miR379-410 cluster regulates activity-dependent dendritogenesis by fine-tuning Pumilio2 protein levels. *The EMBO Journal*, *28*(6), 697–710. https://doi.org/10.1038/emboj.2009.10

Fiori, L. M., Lopez, J. P., Richard-Devantoy, S., Berlim, M., Chachamovich, E., Jollant, F., Foster, J., Rotzinger, S., Kennedy, S. H., & Turecki, G. (2017). Investigation of miR-1202, miR-135a, and miR-16 in Major Depressive Disorder and Antidepressant Response. *International Journal*

of Neuropsychopharmacology, *20*(8), 619–623. https://doi.org/10.1093/ijnp/pyx034

Franke, K., Otto, W., Johannes, S., Baumgart, J., Nitsch, R., & Schumacher, S. (2012). miR-124-regulated RhoG reduces neuronal process complexity via ELMO/Dock180/Rac1 and Cdc42 signalling. *The EMBO Journal*, *31*(13), 2908–2921. https://doi.org/10.1038/emboj.2012.130

Frazer, A. (1997). Pharmacology of Antidepressants. *Journal of Clinical Psychopharmacology*, *17*, 2S-18S. https://doi.org/10.1097/00004714-199704001-00002

Gadad, B. S., Jha, M. K., Czysz, A., Furman, J. L., Mayes, T. L., Emslie, M. P., & Trivedi, M. H. (2018). Peripheral biomarkers of major depression and antidepressant treatment response: Current knowledge and future outlooks. *Journal of Affective Disorders*, *233*, 3–14. https://doi.org/10.1016/j.jad.2017.07.001

Gao, J., Wang, W.-Y., Mao, Y.-W., Gräff, J., Guan, J.-S., Pan, L., Mak, G., Kim, D., Su, S. C., & Tsai, L.-H. (2010). A novel pathway regulates memory and plasticity via SIRT1 and miR-134. *Nature*, *466*(7310), 1105–1109. https://doi.org/10.1038/nature09271

Gaughwin, P., Ciesla, M., Yang, H., Lim, B., & Brundin, P. (2011). Stage-Specific Modulation of Cortical Neuronal Development by Mmu-miR-134. *Cerebral Cortex*, *21*(8), 1857–1869. https://doi.org/10.1093/cercor/bhq262

Gaynes, B. N. (2009). Identifying Difficult-to-Treat Depression. *The Journal of Clinical Psychiatry*, *70*(suppl 6), 10–15. https://doi.org/10.4088/JCP.8133su1c.02

Gelenberg, A., Freeman, M., Markowitz, J., Rosenbaum, J., Thase, M., Trivedi, M., & Schneck, C. (2010). *Practice guideline for the treatment of patients with major depressive disorder* (Am J Psychiatry. (ed.); Third).

Ghosh, T., Aprea, J., Nardelli, J., Engel, H., Selinger, C., Mombereau, C., Lemonnier, T., Moutkine, I., Schwendimann, L., Dori, M., Irinopoulou, T., Henrion-Caude, A., Benecke, A. G., Arnold, S. J., Gressens, P., Calegari, F., & Groszer, M. (2014). MicroRNAs Establish Robustness and Adaptability of a Critical Gene Network to Regulate Progenitor Fate Decisions during Cortical Neurogenesis. *Cell Reports*, *7*(6), 1779–1788. https://doi.org/10.1016/j.celrep.2014.05.029

Giusti, S. A., Vogl, A. M., Brockmann, M. M., Vercelli, C. A., Rein, M. L., Trümbach, D., Wurst, W., Cazalla, D., Stein, V., Deussing, J. M., & Refojo, D. (2014). MicroRNA-9 controls dendritic development by targeting REST. *ELIFE*, 1–22. https://doi.org/10.7554/eLife.02755

Gomez-Sanchez, E. P. (2014). Brain mineralocorticoid receptors in cognition and cardiovascular homeostasis. *Steroids*, *91*, 20–31. https://doi.org/10.1016/j.steroids.2014.08.014

Goslin, K., & Banker, G. (1991). Rat hippocampal neurons in low density culture. In *Culturing nerve cells* (pp. 251–282). Cambridge, Massachusets: The MIT press.

Gould, E., McEwen, B. S., Tanapat, P., Galea, L. A. M., & Fuchs, E. (1997). Neurogenesis in the Dentate Gyrus of the Adult Tree Shrew Is Regulated by Psychosocial Stress and NMDA Receptor Activation. *The Journal of Neuroscience*, *17*(7), 2492–2498. https://doi.org/10.1523/JNEUROSCI.17-07-02492.1997

Grieco, S. F., Velmeshev, D., Magistri, M., Eldar-Finkelman, H., Faghihi, M. A., Jope, R. S., & Beurel, E. (2017). Ketamine up-regulates a cluster of intronic miRNAs within the serotonin receptor 2C gene by inhibiting glycogen synthase kinase-3. *The World Journal of Biological Psychiatry : The Official Journal of the World Federation of Societies of Biological Psychiatry*, *18*(6), 445–456. https://doi.org/10.1080/15622975.2016.1224927

Griffiths-Jones, S. (2004). The microRNA Registry. *Nucleic Acids Research*, *32*(Database issue), D109-11. https://doi.org/10.1093/nar/gkh023

Groc, L., Choquet, D., & Chaouloff, F. (2008). The stress hormone corticosterone conditions AMPAR surface trafficking and synaptic potentiation. *Nature Neuroscience*, *11*(8), 868–870. https://doi.org/10.1038/nn.2150

Gururajan, A., Reif, A., Cryan, J. F., & Slattery, D. A. (2019). The future of rodent models in depression research. *Nature Reviews Neuroscience*, *20*(11), 686–701. https://doi.org/10.1038/s41583-019-0221-6

Han, M.-H., & Nestler, E. J. (2017). Neural Substrates of Depression and Resilience. *Neurotherapeutics*, *14*(3), 677–686. https://doi.org/10.1007/s13311-017-0527-x

Harris, E. W., Ganong, A. H., & Cotman, C. W. (1984). Long-term potentiation in the hippocampus involves activation of N-methyl-D-aspartate receptors. *Brain Research*, *323*(1), 132–137. https://doi.org/10.1016/0006-8993(84)90275-0

He, Y., Zhou, Y., Xi, Q., Cui, H., Luo, T., Song, H., Nie, X., Wang, L., & Ying, B. (2012). Genetic Variations in MicroRNA Processing Genes Are Associated with Susceptibility in Depression. *DNA and Cell Biology*, *31*(9), 1499–1506. https://doi.org/10.1089/dna.2012.1660

He, Z. X., Song, H. F., Liu, T. Y., Ma, J., Xing, Z. K., Yin, Y. Y., Liu, L., Zhang, Y. N., Zhao, Y. F., Yu, H. L., He, X. X., Guo, W. X., & Zhu, X. J. (2019). HuR in the Medial Prefrontal Cortex is Critical for Stress-Induced Synaptic Dysfunction and Depressive-Like Symptoms in Mice. *Cerebral Cortex*, *29*(6), 2737–2747. https://doi.org/10.1093/cercor/bhz036

Heim, C., Newport, D. J., Mletzko, T., Miller, A. H., & Nemeroff, C. B. (2008). The link between childhood trauma and depression: Insights from HPA axis studies in humans. *Psychoneuroendocrinology*, *33*(6), 693–710. https://doi.org/10.1016/j.psyneuen.2008.03.008

Heinrichs, S. C., & Koob, G. F. (2004). Corticotropin-Releasing Factor in Brain: A Role in Activation, Arousal, and Affect Regulation. *Journal of Pharmacology and Experimental Therapeutics*, *311*(2), 427–440. https://doi.org/10.1124/jpet.103.052092

Hollins, S. L., & Cairns, M. J. (2016). MicroRNA: Small RNA mediators of the brains genomic response to environmental stress. *Progress in Neurobiology*, *143*, 61–81. https://doi.org/10.1016/j.pneurobio.2016.06.005

Horowitz, M. A., Cattaneo, A., Cattane, N., Lopizzo, N., Tojo, L., Bakunina, N., Musaelyan, K., Borsini, A., Zunszain, P. A., & Pariante, C. M. (2020). Glucocorticoids prime the inflammatory response of human hippocampal cells through up-regulation of inflammatory pathways. *Brain, Behavior, and Immunity*, *87*, 777–794. https://doi.org/10.1016/j.bbi.2020.03.012

Hu, Z., Yu, D., Gu, Q., Yang, Y., Tu, K., Zhu, J., & Li, Z. (2014). miR-191 and miR-135 are required for long-lasting spine remodelling associated with synaptic long-term depression. *Nature Communications*, *5*(1), 3263. https://doi.org/10.1038/ncomms4263

Huang, E. J., & Reichardt, L. F. (2001). Neurotrophins: roles in neuronal development and function. *Annual Review of Neuroscience*, *24*, 677–736. https://doi.org/10.1146/annurev.neuro.24.1.677

Huizink, A. C., Mulder, E. J. H., & Buitelaar, J. K. (2004). Prenatal Stress and Risk for Psychopathology: Specific Effects or Induction of General Susceptibility? *Psychological Bulletin*, *130*(1), 115–142. https://doi.org/10.1037/0033-2909.130.1.115

Ieraci, A., Mallei, A., & Popoli, M. (2016). Social Isolation Stress Induces Anxious-Depressive-Like Behavior and Alterations of Neuroplasticity-Related Genes in Adult Male Mice. *Neural Plasticity*, *2016*, 6212983. https://doi.org/10.1155/2016/6212983

Issler, O., Haramati, S., Paul, E. D., Maeno, H., Navon, I., Zwang, R., Gil, S., Mayberg, H. S., Dunlop, B. W., Menke, A., Awatramani, R., Binder, E. B., Deneris, E. S., Lowry, C. A., & Chen, A. (2014). MicroRNA 135 is essential for chronic stress resiliency, antidepressant efficacy, and intact serotonergic activity. *Neuron*, *83*(2), 344–360. https://doi.org/10.1016/j.neuron.2014.05.042

Jacobson, L., & Sapolsky, R. M. (1991). The Role of the Hippocampus in Feedback Regulation of the Hypothalamic-Pituitary-Adrenocortical Axis*. *Endocrine Reviews*, *12*(2), 118–134. https://doi.org/10.1210/edrv-12-2-118

Jasińska, M., Miłek, J., Cymerman, I. A., Łęski, S., Kaczmarek, L., & Dziembowska, M. (2016). miR-132 Regulates Dendritic Spine Structure by Direct Targeting of Matrix Metalloproteinase 9 mRNA. In *Molecular Neurobiology* (Vol. 53, Issue 7, pp. 4701–4712). https://doi.org/10.1007/s12035-015-9383-z

Joëls, M., & Baram, T. Z. (2009). The neuro-symphony of stress. *Nature Reviews. Neuroscience*, *10*(6), 459–466. https://doi.org/10.1038/nrn2632

Joëls, M., Sarabdjitsingh, R. A., & Karst, H. (2012). Unraveling the Time Domains of Corticosteroid Hormone Influences on Brain Activity: Rapid, Slow, and Chronic Modes. *Pharmacological Reviews*, *64*(4), 901–938. https://doi.org/10.1124/pr.112.005892

Johnson, R., Teh, C. H., Kunarso, G., Wong, K. Y., Srinivasan, G., Cooper, M. L., Volta, M., Chan, S. S., Lipovich, L., Pollard, S. M., Karuturi, R. K. M., Wei, C., Buckley, N. J., & Stanton, L. W. (2008). REST Regulates Distinct Transcriptional Networks in Embryonic and Neural Stem Cells. *PLoS Biology*, *6*(10), e256. https://doi.org/10.1371/journal.pbio.0060256

Jovicic, A., Roshan, R., Moisoi, N., Pradervand, S., Moser, R., Pillai, B., & Luthi-Carter, R. (2013). Comprehensive Expression Analyses of Neural Cell-Type-Specific miRNAs Identify New Determinants of the Specification and Maintenance of Neuronal Phenotypes. *Journal of Neuroscience*, *33*(12), 5127–5137. https://doi.org/10.1523/JNEUROSCI.0600-12.2013

Kadriu, B., Musazzi, L., Henter, I. D., Graves, M., Popoli, M., & Zarate, C. A. (2019). Glutamatergic Neurotransmission: Pathway to Developing Novel Rapid-Acting Antidepressant Treatments. *International Journal of Neuropsychopharmacology*, *22*(2), 119–135. https://doi.org/10.1093/ijnp/pyy094

Kang, H. J., Voleti, B., Hajszan, T., Rajkowska, G., Stockmeier, C. A., Licznerski, P., Lepack, A., Majik, M. S., Jeong, L. S., Banasr, M., Son, H., & Duman, R. S. (2012). Decreased expression of synapse-related genes and loss of synapses in major depressive disorder. *Nature Medicine*, *18*(9), 1413–1417. https://doi.org/10.1038/nm.2886

Karege, F., Vaudan, G., Schwald, M., Perroud, N., & La Harpe, R. (2005). Neurotrophin levels in postmortem brains of suicide victims and the effects of antemortem diagnosis and psychotropic drugs. *Molecular Brain Research*, *136*(1–2), 29–37. https://doi.org/10.1016/j.molbrainres.2004.12.020

Kennedy, S. H. (2008). Core symptoms of major depressive disorder: relevance to diagnosis and treatment. *Dialogues in Clinical Neuroscience*, *10*(3), 271–277. https://doi.org/10.31887/DCNS.2008.10.3/shkennedy

Kim, J., Inoue, K., Ishii, J., Vanti, W. B., Voronov, S. V, Murchison, E., Hannon, G., & Abeliovich, A. (2007). A MicroRNA feedback circuit in midbrain dopamine neurons. *Science (New York, N.Y.)*, *317*(5842), 1220–1224. https://doi.org/10.1126/science.1140481

Kishi, T., Yoshimura, R., Kitajima, T., Okochi, T., Okumura, T., Tsunoka, T., Yamanouchi, Y., Kinoshita, Y., Kawashima, K., & Fukuo, Y. (2010). SIRT1 gene is associated with major depressive disorder in the Japanese population. *Journal of Affective Disorders*, *126*(1–2), 167–173. https://doi.org/10.1016/j.jad.2010.04.003

Kohrs, R., & Durieux, M. E. (1998). Ketamine: teaching an old drug new tricks. *Anesthesia and Analgesia*, *87*(5), 1186–1193. https://doi.org/10.1097/00000539-199811000-00039

Kos, A., Klein-Gunnewiek, T., Meinhardt, J., Loohuis, N. F. M. O., van Bokhoven, H., Kaplan, B. B., Martens, G. J., Kolk, S. M., & Aschrafi, A. (2017). MicroRNA-338 Attenuates Cortical Neuronal Outgrowth by Modulating the Expression of Axon Guidance Genes. *Molecular Neurobiology*, *54*(5), 3439–3452. https://doi.org/10.1007/s12035-016-9925-z

Kos, A., Olde Loohuis, N., Meinhardt, J., van Bokhoven, H., Kaplan, B. B., Martens, G. J., & Aschrafi, A. (2016). MicroRNA-181 promotes synaptogenesis and attenuates axonal outgrowth in cortical neurons. *Cellular and Molecular Life Sciences*, *73*(18), 3555–3567. https://doi.org/10.1007/s00018-016-2179-0

Krishnan, V., & Nestler, E. J. (2008). The molecular neurobiology of depression. *Nature*, *455*(7215), 894–902. https://doi.org/10.1038/nature07455

Krishnan, V., & Nestler, E. J. (2011). *Animal Models of Depression: Molecular Perspectives* (pp. 121–147). https://doi.org/10.1007/7854_2010_108

Kurdi, M. S., Theerth, K. A., & Deva, R. S. (2014). Ketamine: Current applications in anesthesia, pain, and critical care. *Anesthesia, Essays and Researches*, *8*(3), 283–290. https://doi.org/10.4103/0259-1162.143110

La Via, L., Bonini, D., Russo, I., Orlandi, C., Barlati, S., & Barbon, A. (2013). Modulation of dendritic AMPA receptor mRNA trafficking by RNA splicing and editing. *Nucleic Acids Research*, *41*(1), 617–631. https://doi.org/10.1093/nar/gks1223

Lagos-Quintana, M. (2001). Identification of Novel Genes Coding for Small Expressed RNAs. *Science*, *294*(5543), 853–858. https://doi.org/10.1126/science.1064921

Lagos-quintana, M., Rauhut, R., Yalcin, A., Meyer, J., Lendeckel, W., & Tuschl, T. (2002). Identification of Tissue-Specific MicroRNAs from Mouse. *Current Biology*, *12*(02), 735–739.

Lahti, A. C., Warfel, D., Michaelidis, T., Weiler, M. A., Frey, K., & Tamminga, C. A. (2001). Long-term outcome of patients who receive ketamine during research. *Biological Psychiatry*, *49*(10), 869–875. https://doi.org/10.1016/S0006-3223(00)01037-4

Lai, E. C. (2002). Micro RNAs are complementary to 3 ′ UTR sequence motifs that mediate negative post-transcriptional. *Nature Genetics*, *30*(april), 363–364. https://doi.org/10.1038/ng865

Laje, G., Lally, N., Mathews, D., Brutsche, N., Chemerinski, A., Akula, N., Kelmendi, B., Simen, A., McMahon, F. J., Sanacora, G., & Zarate, C. (2012). Brain-Derived Neurotrophic Factor Val66Met Polymorphism and Antidepressant Efficacy of Ketamine in Depressed Patients. *Biological Psychiatry*, *72*(11), e27–e28. https://doi.org/10.1016/j.biopsych.2012.05.031

Lally, N., Nugent, A. C., Luckenbaugh, D. A., Ameli, R., Roiser, J. P., & Zarate, C. A. (2014).

Anti-anhedonic effect of ketamine and its neural correlates in treatment-resistant bipolar depression. *Translational Psychiatry*, *4*, e469. https://doi.org/10.1038/tp.2014.105

Launay, J. M., Mouillet-Richard, S., Baudry, A., Pietri, M., & Kellermann, O. (2011). Raphe-mediated signals control the hippocampal response to SRI antidepressants via miR-16. *Translational Psychiatry*, *1*, e56. https://doi.org/10.1038/tp.2011.54

Lee, R. C., Feinbaum, R. L., & Ambros, V. (1993). The C. elegans heterochronic gene lin-4 encodes small RNAs with antisense complementarity to lin-14. *Cell*, *75*(5), 843–854. https://doi.org/10.1016/0092-8674(93)90529-y

Lee, Y., Ahn, C., Han, J., Choi, H., Kim, J., Yim, J., Lee, J., Provost, P., Kim, S., & Kim, V. N. (2003). The nuclear RNase III Drosha initiates microRNA processing. *Nature*, *425*(September), 1–5.

Lee, Y., Jeon, K., Lee, J.-T., Kim, S., & Kim, V. N. (2002). MicroRNA maturation: stepwise processing and subcellular localization. *The EMBO Journal*, *21*(17), 4663–4670. https://doi.org/10.1093/emboj/cdf476

Lemonde, S., Rogaeva, A., & Albert, P. R. (2004). Cell type-dependent recruitment of trichostatin A-sensitive repression of the human 5-HT1A receptor gene. *Journal of Neurochemistry*, *88*(4), 857–868. https://doi.org/10.1046/j.1471-4159.2003.02223.x

Lepack, A. E., Fuchikami, M., Dwyer, J. M., Banasr, M., & Duman, R. S. (2015). BDNF Release Is Required for the Behavioral Actions of Ketamine. *International Journal of Neuropsychopharmacology*, *18*(1), pyu033–pyu033. https://doi.org/10.1093/ijnp/pyu033

Lewis, B. P., Burge, C. B., & Bartel, D. P. (2005). Conserved Seed Pairing, Often Flanked by Adenosines, Indicates that Thousands of Human Genes are MicroRNA Targets. *Cell*, *120*(1), 15–20. https://doi.org/10.1016/j.cell.2004.12.035

Lewis, B. P., Shih, I., Jones-rhoades, M. W., Bartel, D. P., & Burge, C. B. (2003). Prediction of Mammalian MicroRNA Targets. *Cell*, *115*, 787–798.

Li, H., Mao, S., Wang, H., Zen, K., Zhang, C., & Li, L. (2014). MicroRNA-29a modulates axon branching by targeting doublecortin in primary neurons. *Protein & Cell*, *5*(2), 160–169. https://doi.org/10.1007/s13238-014-0022-7

Li, N., Lee, B., Liu, R.-J., Banasr, M., Dwyer, J. M., Iwata, M., Li, X.-Y., Aghajanian, G., & Duman, R. S. (2010). mTOR-Dependent Synapse Formation Underlies the Rapid Antidepressant Effects of NMDA Antagonists. *Science*, *329*(5994), 959–964. https://doi.org/10.1126/science.1190287

Li, Nanxin, Liu, R.-J., Dwyer, J. M., Banasr, M., Lee, B., Son, H., Li, X.-Y., Aghajanian, G., & Duman, R. S. (2011). Glutamate N-methyl-D-aspartate Receptor Antagonists Rapidly Reverse Behavioral and Synaptic Deficits Caused by Chronic Stress Exposure. *Biological Psychiatry*, *69*(8), 754–761. https://doi.org/10.1016/j.biopsych.2010.12.015

Libert, S., Pointer, K., Bell, E. L., Das, A., Cohen, D. E., Asara, J. M., Kapur, K., Bergmann, S., Preisig, M., Otowa, T., Kendler, K. S., Chen, X., Hettema, J. M., van den Oord, E. J., Rubio, J. P., & Guarente, L. (2011). SIRT1 Activates MAO-A in the Brain to Mediate Anxiety and Exploratory Drive. *Cell*, *147*(7), 1459–1472. https://doi.org/10.1016/j.cell.2011.10.054

Lindert, J., von Ehrenstein, O. S., Grashow, R., Gal, G., Braehler, E., & Weisskopf, M. G. (2014). Sexual and physical abuse in childhood is associated with depression and anxiety over the life course: systematic review and meta-analysis. *International Journal of Public Health*, *59*(2),

359–372. https://doi.org/10.1007/s00038-013-0519-5

Lippi, G., Fernandes, C. C., Ewell, L. A., John, D., Romoli, B., Curia, G., Taylor, S. R., Frady, E. P., Jensen, A. B., Liu, J. C., Chaabane, M. M., Belal, C., Nathanson, J. L., Zoli, M., Leutgeb, J. K., Biagini, G., Yeo, G. W., & Berg, D. K. (2016). MicroRNA-101 Regulates Multiple Developmental Programs to Constrain Excitation in Adult Neural Networks. *Neuron*, *92*(6), 1337–1351. https://doi.org/10.1016/j.neuron.2016.11.017

Lipton, J. O., & Sahin, M. (2014). The Neurology of mTOR. *Neuron*, *84*(2), 275–291. https://doi.org/10.1016/j.neuron.2014.09.034

Liston, C., Miller, M. M., Goldwater, D. S., Radley, J. J., Rocher, A. B., Hof, P. R., Morrison, J. H., & McEwen, B. S. (2006). Stress-Induced Alterations in Prefrontal Cortical Dendritic Morphology Predict Selective Impairments in Perceptual Attentional Set-Shifting. *Journal of Neuroscience*, *26*(30), 7870–7874. https://doi.org/10.1523/JNEUROSCI.1184-06.2006

Liu, R.-J., Fuchikami, M., Dwyer, J. M., Lepack, A. E., Duman, R. S., & Aghajanian, G. K. (2013). GSK-3 Inhibition Potentiates the Synaptogenic and Antidepressant-Like Effects of Subthreshold Doses of Ketamine. *Neuropsychopharmacology*, *38*(11), 2268–2277. https://doi.org/10.1038/npp.2013.128

Liu, R.-J., Lee, F. S., Li, X.-Y., Bambico, F., Duman, R. S., & Aghajanian, G. K. (2012). Brain-Derived Neurotrophic Factor Val66Met Allele Impairs Basal and Ketamine-Stimulated Synaptogenesis in Prefrontal Cortex. *Biological Psychiatry*, *71*(11), 996–1005. https://doi.org/10.1016/j.biopsych.2011.09.030

Lopez, J. P., Lim, R., Cruceanu, C., Crapper, L., Fasano, C., Labonte, B., Maussion, G., Yang, J. P., Yerko, V., Vigneault, E., El Mestikawy, S., Mechawar, N., Pavlidis, P., & Turecki, G. (2014). miR-1202 is a primate-specific and brain-enriched microRNA involved in major depression and antidepressant treatment. *Nature Medicine*, *20*(7), 764–768. https://doi.org/10.1038/nm.3582

Lopizzo, N., Zonca, V., Cattane, N., Pariante, C. M., & Cattaneo, A. (2019). miRNAs in depression vulnerability and resilience: novel targets for preventive strategies. *Journal of Neural Transmission (Vienna, Austria : 1996)*, *126*(9), 1241–1258. https://doi.org/10.1007/s00702-019-02048-2

Lu, G., Li, J., Zhang, H., Zhao, X., Yan, L. J., & Yang, X. (2018). Role and possible mechanisms of sirt1 in depression. *Oxidative Medicine and Cellular Longevity*, *2018*. https://doi.org/10.1155/2018/8596903

Lucassen, P. J., Pruessner, J., Sousa, N., Almeida, O. F. X. X., Van Dam, A. M., Rajkowska, G., Swaab, D. F., & Czéh, B. (2014). Neuropathology of stress. *Acta Neuropathologica*, *127*(1), 109–135. https://doi.org/10.1007/s00401-013-1223-5

Machado-Vieira, R., Henter, I. D., & Zarate Jr., C. A. (2017). New targets for rapid antidepressant action. *Progress in Neurobiology*, *152*, 21–37. https://doi.org/10.1016/j.pneurobio.2015.12.001

Machado-Vieira, R., Salvadore, G., Diazgranados, N., & Zarate, C. A. (2009). Ketamine and the next generation of antidepressants with a rapid onset of action. *Pharmacology & Therapeutics*, *123*(2), 143–150. https://doi.org/10.1016/j.pharmthera.2009.02.010

Maeng, S., Zarate, C. A., Du, J., Schloesser, R. J., McCammon, J., Chen, G., & Manji, H. K. (2008). Cellular Mechanisms Underlying the Antidepressant Effects of Ketamine: Role of α-Amino-3-Hydroxy-5-Methylisoxazole-4-Propionic Acid Receptors. *Biological Psychiatry*,

63(4), 349–352. https://doi.org/10.1016/j.biopsych.2007.05.028

Magill, S. T., Cambronne, X. A., Luikart, B. W., Lioy, D. T., Leighton, B. H., Westbrook, G. L., Mandel, G., & Goodman, R. H. (2010). microRNA-132 regulates dendritic growth and arborization of newborn neurons in the adult hippocampus. *Proceedings of the National Academy of Sciences*, *107*(47), 20382–20387. https://doi.org/10.1073/pnas.1015691107

Mampay, M., & Sheridan, G. K. (2019). REST: An epigenetic regulator of neuronal stress responses in the young and ageing brain. *Frontiers in Neuroendocrinology*, *53*(April), 100744. https://doi.org/10.1016/j.yfrne.2019.04.001

Mannironi, C., Camon, J., De Vito, F., Biundo, A., De Stefano, M. E., Persiconi, I., Bozzoni, I., Fragapane, P., Mele, A., & Presutti, C. (2013). Acute stress alters amygdala microRNA miR-135a and miR-124 expression: inferences for corticosteroid dependent stress response. *PloS One*, *8*(9), e73385. https://doi.org/10.1371/journal.pone.0073385

Maras, P. M., Molet, J., Chen, Y., Rice, C., Ji, S. G., Solodkin, A., & Baram, T. Z. (2014). Preferential loss of dorsal-hippocampus synapses underlies memory impairments provoked by short, multimodal stress. *Molecular Psychiatry*, *19*(7), 811–822. https://doi.org/10.1038/mp.2014.12

Mattson, M. P. (2008). Glutamate and Neurotrophic Factors in Neuronal Plasticity and Disease. *Annals of the New York Academy of Sciences*, *1144*(1), 97–112. https://doi.org/10.1196/annals.1418.005

Mavrikaki, M., Anastasiadou, E., Ozdemir, R. A., Potter, D., Helmholz, C., Slack, F. J., & Chartoff, E. H. (2019). Overexpression of miR-9 in the Nucleus Accumbens Increases Oxycodone Self-Administration. *International Journal of Neuropsychopharmacology*, *22*(6), 383–393. https://doi.org/10.1093/ijnp/pyz015

Mazzelli, M., Maj, C., Mariani, N., Mora, C., Begni, V., Pariante, C. M., Riva, M. A., Cattaneo, A., & Cattane, N. (2020). The Long-Term Effects of Early Life Stress on the Modulation of miR-19 Levels. *Frontiers in Psychiatry*, *11*. https://doi.org/10.3389/fpsyt.2020.00389

McEwen, B. S. (1993). Stress and the Individual. *Archives of Internal Medicine*, *153*(18), 2093. https://doi.org/10.1001/archinte.1993.00410180039004

McEwen, B. S. (2007). Physiology and Neurobiology of Stress and Adaptation: Central Role of the Brain. *Physiological Reviews*, *87*(3), 873–904. https://doi.org/10.1152/physrev.00041.2006

McEwen, B. S. (2017). Neurobiological and Systemic Effects of Chronic Stress. *Chronic Stress (Thousand Oaks, Calif.)*, *1*. https://doi.org/10.1177/2470547017692328

McEwen, B. S., & Akil, H. (2020). Revisiting the Stress Concept: Implications for Affective Disorders. *The Journal of Neuroscience*, *40*(1), 12–21. https://doi.org/10.1523/JNEUROSCI.0733-19.2019

McEwen, B. S., Bowles, N. P., Gray, J. D., Hill, M. N., Hunter, R. G., Karatsoreos, I. N., & Nasca, C. (2015). McEwen. Stress Mechanisms Brain. 2015. *Nature Neuroscience*, *18*(10), 1353–1363. https://doi.org/10.1038/nn.4086

McEwen, B. S., Nasca, C., & Gray, J. D. (2016). Stress Effects on Neuronal Structure: Hippocampus, Amygdala, and Prefrontal Cortex. *Neuropsychopharmacology*, *41*(1), 3–23. https://doi.org/10.1038/npp.2015.171

Meerson, A., Cacheaux, L., Goosens, K. A., Sapolsky, R. M., Soreq, H., & Kaufer, D. (2010).

Changes in brain MicroRNAs contribute to cholinergic stress reactions. *Journal of Molecular Neuroscience : MN*, *40*(1–2), 47–55. https://doi.org/10.1007/s12031-009-9252-1

Meyer, J. H., Ginovart, N., Boovariwala, A., Sagrati, S., Hussey, D., Garcia, A., Young, T., Praschak-Rieder, N., Wilson, A. A., & Houle, S. (2006). Elevated Monoamine Oxidase A Levels in the Brain. *Archives of General Psychiatry*, *63*(11), 1209. https://doi.org/10.1001/archpsyc.63.11.1209

Michan, S., Li, Y., Chou, M. M.-H., Parrella, E., Ge, H., Long, J. M., Allard, J. S., Lewis, K., Miller, M., Xu, W., Mervis, R. F., Chen, J., Guerin, K. I., Smith, L. E. H., McBurney, M. W., Sinclair, D. A., Baudry, M., de Cabo, R., & Longo, V. D. (2010). SIRT1 Is Essential for Normal Cognitive Function and Synaptic Plasticity. *Journal of Neuroscience*, *30*(29), 9695–9707. https://doi.org/10.1523/JNEUROSCI.0027-10.2010

Miller, O. H., Bruns, A., Ben Ammar, I., Mueggler, T., & Hall, B. J. (2017). Synaptic Regulation of a Thalamocortical Circuit Controls Depression-Related Behavior. *Cell Reports*, *20*(8), 1867–1880. https://doi.org/10.1016/j.celrep.2017.08.002

Miller, O. H., Yang, L., Wang, C.-C., Hargroder, E. A., Zhang, Y., Delpire, E., & Hall, B. J. (2014). GluN2B-containing NMDA receptors regulate depression-like behavior and are critical for the rapid antidepressant actions of ketamine. *ELife*, *3*. https://doi.org/10.7554/eLife.03581

Mion, G., & Villevieille, T. (2013). *Ketamine Pharmacology : An Update (Pharmacodynamics and Molecular Aspects , Recent Findings)*. *19*, 370–380. https://doi.org/10.1111/cns.12099

Moghaddam, B., Adams, B., Verma, A., & Daly, D. (1997). Activation of Glutamatergic Neurotransmission by Ketamine: A Novel Step in the Pathway from NMDA Receptor Blockade to Dopaminergic and Cognitive Disruptions Associated with the Prefrontal Cortex. *The Journal of Neuroscience*, *17*(8), 2921–2927. https://doi.org/10.1523/JNEUROSCI.17-08-02921.1997

Mou, H., & Zhao, X. (2016). NRSF and CCR5 Established Neuron-glia Communication during Acute and Chronic Stresses. *Journal of Drug Metabolism & Toxicology*, *7*(1). https://doi.org/10.4172/2157-7609.1000197

Mourelatos, Z., Dostie, J., S, P., Sharma, A., Charroux, B., Abel, L., Rappsilber, J., Mann, M., & Dreyfuss, G. (2002). miRNPs: a novel class of ribonucleoproteins containing numerous microRNAs. *Genes & Development*, *16*(6), 720–728. https://doi.org/10.1101/gad.974702

Murrough, J. W., Perez, A. M., Pillemer, S., Stern, J., Parides, M. K., aan het Rot, M., Collins, K. A., Mathew, S. J., Charney, D. S., & Iosifescu, D. V. (2013). Rapid and longer-term antidepressant effects of repeated ketamine infusions in treatment-resistant major depression. *Biological Psychiatry*, *74*(4), 250–256. https://doi.org/10.1016/j.biopsych.2012.06.022

Musazzi, L, Tornese, P., Sala, N., & Popoli, M. (2017). Acute stress is not acute: sustained enhancement of glutamate release after acute stress involves readily releasable pool size and synapsin I activation. *Molecular Psychiatry*, *22*(9), 1226–1227. https://doi.org/10.1038/mp.2016.175

Musazzi, Laura, Treccani, G., Mallei, A., & Popoli, M. (2013). The action of antidepressants on the glutamate system: regulation of glutamate release and glutamate receptors. *Biological Psychiatry*, *73*(12), 1180–1188. https://doi.org/10.1016/j.biopsych.2012.11.009

Natera-Naranjo, O., Aschrafi, A., Gioio, A. E., & Kaplan, B. B. (2010). Identification and quantitative analyses of microRNAs located in the distal axons of sympathetic neurons. *RNA*,

16(8), 1516–1529. https://doi.org/10.1261/rna.1833310

National Institute of Mental Health. (2018). *Depression*. https://www.nimh.nih.gov/health/topics/depression/index.shtml#part_145398

Neill, J. C., Barnes, S., Cook, S., Grayson, B., Idris, N. F., McLean, S. L., Snigdha, S., Rajagopal, L., & Harte, M. K. (2010). Animal models of cognitive dysfunction and negative symptoms of schizophrenia: Focus on NMDA receptor antagonism. *Pharmacology & Therapeutics*, *128*(3), 419–432. https://doi.org/10.1016/j.pharmthera.2010.07.004

Nestler, E. J., Barrot, M., Dileone, R. J., Eisch, A. J., Gold, S. J., & Monteggia, L. M. (2002). *Neurobiology of Depression Review*. *34*, 13–25.

Olde Loohuis, N. F. M., Ba, W., Stoerchel, P. H., Kos, A., Jager, A., Schratt, G., Martens, G. J. M., van Bokhoven, H., Nadif Kasri, N., & Aschrafi, A. (2015). MicroRNA-137 Controls AMPA-Receptor-Mediated Transmission and mGluR-Dependent LTD. *Cell Reports*, *11*(12), 1876–1884. https://doi.org/10.1016/j.celrep.2015.05.040

Otnæss, M. K., Djurovic, S., Rimol, L. M., Kulle, B., Kähler, A. K., Jönsson, E. G., Agartz, I., Sundet, K., Hall, H., Timm, S., Hansen, T., Callicott, J. H., Melle, I., Werge, T., & Andreassen, O. A. (2009). Evidence for a possible association of neurotrophin receptor (NTRK-3) gene polymorphisms with hippocampal function and schizophrenia. *Neurobiology of Disease*, *34*(3), 518–524. https://doi.org/10.1016/j.nbd.2009.03.011

Otte, C., Gold, S. M., Penninx, B. W., Pariante, C. M., Etkin, A., Fava, M., Mohr, D. C., & Schatzberg, A. F. (2016). Major depressive disorder. *Nature Reviews. Disease Primers*, *2*, 16065. https://doi.org/10.1038/nrdp.2016.65

Packer, A. N., Xing, Y., Harper, S. Q., Jones, L., & Davidson, B. L. (2008). The Bifunctional microRNA miR-9/miR-9* Regulates REST and CoREST and Is Downregulated in Huntington's Disease. *Journal of Neuroscience*, *28*(53), 14341–14346. https://doi.org/10.1523/JNEUROSCI.2390-08.2008

Paridaen, J. T., & Huttner, W. B. (2014). Neurogenesis during development of the vertebrate central nervous system. *EMBO Reports*, *15*(4), 351–364. https://doi.org/10.1002/embr.201438447

Pasquinelli, A. E., Reinhart, B. J., Slack, F., Martindale, M. Q., Kuroda, M. I., Maller, B., Hayward, D. C., Ball, E. E., Degnan, B., Müller, P., Spring, J., Srinivasan, A., Fishman, M., Finnerty, J., Corbo, J., Levine, M., Leahy, P., Davidson, E., & Ruvkun, G. (2000). Conservation of the sequence and temporal expression of let-7 heterochronic regulatory RNA. *Nature*, *408*(6808), 86–89. https://doi.org/10.1038/35040556

Patel, P. D., Bochar, D. A., Turner, D. L., Meng, F., Mueller, H. M., & Pontrello, C. G. (2007). Regulation of Tryptophan Hydroxylase-2 Gene Expression by a Bipartite RE-1 Silencer of Transcription/Neuron restrictive Silencing Factor (REST/NRSF) Binding Motif. *Journal of Biological Chemistry*, *282*(37), 26717–26724. https://doi.org/10.1074/jbc.M705120200

Pawlak, R., Rao, B. S. S., Melchor, J. P., Chattarji, S., McEwen, B., & Strickland, S. (2005). Tissue plasminogen activator and plasminogen mediate stress-induced decline of neuronal and cognitive functions in the mouse hippocampus. *Proceedings of the National Academy of Sciences*, *102*(50), 18201–18206. https://doi.org/10.1073/pnas.0509232102

Pena, J. T. G., Sohn-Lee, C., Rouhanifard, S. H., Ludwig, J., Hafner, M., Mihailovic, A., Lim, C., Holoch, D., Berninger, P., Zavolan, M., & Tuschl, T. (2009). miRNA in situ hybridization in formaldehyde and EDC–fixed tissues. *Nature Methods*, *6*(2), 139–141.

https://doi.org/10.1038/nmeth.1294

Perry, E. B., Cramer, J. A., Cho, H.-S., Petrakis, I. L., Karper, L. P., Genovese, A., O'Donnell, E., Krystal, J. H., D'Souza, D. C., & Yale Ketamine Study Group. (2007). Psychiatric safety of ketamine in psychopharmacology research. *Psychopharmacology*, *192*(2), 253–260. https://doi.org/10.1007/s00213-007-0706-2

Pettersson, A., Boström, K. B., Gustavsson, P., & Ekselius, L. (2015). Which instruments to support diagnosis of depression have sufficient accuracy? A systematic review. *Nordic Journal of Psychiatry*, *69*(7), 497–508. https://doi.org/10.3109/08039488.2015.1008568

Polter, A., Beurel, E., Yang, S., Garner, R., Song, L., Miller, C. A., Sweatt, J. D., McMahon, L., Bartolucci, A. A., Li, X., & Jope, R. S. (2010). Deficiency in the Inhibitory Serine-Phosphorylation of Glycogen Synthase Kinase-3 Increases Sensitivity to Mood Disturbances. *Neuropsychopharmacology*, *35*(8), 1761–1774. https://doi.org/10.1038/npp.2010.43

Popoli, M., Yan, Z., McEwen, B. S., & Sanacora, G. (2011). The stressed synapse: the impact of stress and glucocorticoids on glutamate transmission. *Nature Reviews. Neuroscience*, *13*(1), 22–37. https://doi.org/10.1038/nrn3138

Pozzi, D., Lignani, G., Ferrea, E., Contestabile, A., Paonessa, F., D'Alessandro, R., Lippiello, P., Boido, D., Fassio, A., Meldolesi, J., Valtorta, F., Benfenati, F., & Baldelli, P. (2013). REST/NRSF-mediated intrinsic homeostasis protects neuronal networks from hyperexcitability. *The EMBO Journal*, *32*(22), 2994–3007. https://doi.org/10.1038/emboj.2013.231

Price, J. L., & Drevets, W. C. (2010). Neurocircuitry of Mood Disorders. *Neuropsychopharmacology*, *35*(1), 192–216. https://doi.org/10.1038/npp.2009.104

Qi, A.-Q., Qiu, J., Xiao, L., & Chen, Y.-Z. (2005). Rapid activation of JNK and p38 by glucocorticoids in primary cultured hippocampal cells. *Journal of Neuroscience Research*, *80*(4), 510–517. https://doi.org/10.1002/jnr.20491

Quattrone, A., Pascale, A., Nogues, X., Zhao, W., Gusev, P., Pacini, A., & Alkon, D. L. (2001). Posttranscriptional regulation of gene expression in learning by the neuronal ELAV-like mRNA-stabilizing proteins. *Proceedings of the National Academy of Sciences*, *98*(20), 11668–11673. https://doi.org/10.1073/pnas.191388398

Racagni, G., & Popoli, M. (2008). Cellular and molecular mechanisms in the long-term action of antidepressants. *Dialogues in Clinical Neuroscience*, *10*(4), 385–400. https://doi.org/10.31887/DCNS.2008.10.4/gracagni

Rago, L., Beattie, R., Taylor, V., & Winter, J. (2014). miR379-410 cluster miRNAs regulate neurogenesis and neuronal migration by fine-tuning N-cadherin. *The EMBO Journal*, *33*(8), 906–920. https://doi.org/10.1002/embj.201386591

Rajman, M., & Schratt, G. (2017). MicroRNAs in neural development: from master regulators to fine-tuners. *Development (Cambridge, England)*, *144*(13), 2310–2322. https://doi.org/10.1242/dev.144337

Reczko, M., Maragkakis, M., Alexiou, P., Grosse, I., & Hatzigeorgiou, A. G. (2012). Functional microRNA targets in protein coding sequences. *Bioinformatics*, *28*(6), 771–776. https://doi.org/10.1093/bioinformatics/bts043

Reinhart, B. J., Slack, F. J., Basson, M., Pasquinelli, A. E., Bettinger, J. C., Rougvie, A. E., Horvitz, H. R., & Ruvkun, G. (2000). The 21-nucleotide let-7 RNA regulates developmental timing in

Caenorhabditis elegans. *Nature*, *403*(6772), 901–906. https://doi.org/10.1038/35002607

Reinhart, B. J., Weinstein, E. G., Rhoades, M. W., Bartel, B., & Bartel, D. P. (2002). MicroRNAs in plants. *Genes & Development*, *16*(13), 1616–1626. https://doi.org/10.1101/gad.1004402

Rhoades, M. W., Reinhart, B. J., Lim, L. P., Burge, C. B., Bartel, B., & Bartel, D. P. (2002). Prediction of Plant MicroRNA Targets. *Cell*, *110*(4), 513–520. https://doi.org/10.1016/S0092-8674(02)00863-2

Rinaldi, A., Vincenti, S., De Vito, F., Bozzoni, I., Oliverio, A., Presutti, C., Fragapane, P., & Mele, A. (2010). Stress induces region specific alterations in microRNAs expression in mice. *Behavioural Brain Research*, *208*(1), 265–269. https://doi.org/10.1016/j.bbr.2009.11.012

Rodgers, A B, Morgan, C. P., Bronson, S. L., Revello, S., & Bale, T. L. (2013). Paternal Stress Exposure Alters Sperm MicroRNA Content and Reprograms Offspring HPA Stress Axis Regulation. *Journal of Neuroscience*, *33*(21), 9003–9012. https://doi.org/10.1523/JNEUROSCI.0914-13.2013

Rodgers, Ali B, Morgan, C. P., Leu, N. A., & Bale, T. L. (2015). Transgenerational epigenetic programming via sperm microRNA recapitulates effects of paternal stress. *Proceedings of the National Academy of Sciences*, *112*(44), 13699–13704. https://doi.org/10.1073/pnas.1508347112

Rose, C. R., Blum, R., Kafitz, K. W., Kovalchuk, Y., & Konnerth, A. (2004). From modulator to mediator: rapid effects of BDNF on ion channels. *BioEssays : News and Reviews in Molecular, Cellular and Developmental Biology*, *26*(11), 1185–1194. https://doi.org/10.1002/bies.20118

Russo, S. J., Murrough, J. W., Han, M.-H., Charney, D. S., & Nestler, E. J. (2012). Neurobiology of resilience. *Nature Neuroscience*, *15*(11), 1475–1484. https://doi.org/10.1038/nn.3234

Sambandan, S., Akbalik, G., Kochen, L., Rinne, J., Kahlstatt, J., Glock, C., Tushev, G., Alvarez-Castelao, B., Heckel, A., & Schuman, E. M. (2017). Activity-dependent spatially localized miRNA maturation in neuronal dendrites. *Science*, *355*(6325), 634–637. https://doi.org/10.1126/science.aaf8995

Sanacora, G., Treccani, G., & Popoli, M. (2012). Towards a glutamate hypothesis of depression: an emerging frontier of neuropsychopharmacology for mood disorders. *Neuropharmacology*, *62*(1), 63–77. https://doi.org/10.1016/j.neuropharm.2011.07.036

Schindelin, J., Arganda-Carreras, I., Frise, E., Kaynig, V., Longair, M., Pietzsch, T., Preibisch, S., Rueden, C., Saalfeld, S., Schmid, B., Tinevez, J.-Y., White, D. J., Hartenstein, V., Eliceiri, K., Tomancak, P., & Cardona, A. (2012). Fiji: an open-source platform for biological-image analysis. *Nature Methods*, *9*(7), 676–682. https://doi.org/10.1038/nmeth.2019

Schonrock, N., Humphreys, D. T., Preiss, T., & Götz, J. (2012). Target gene repression mediated by miRNAs miR-181c and miR-9 both of which are down-regulated by amyloid-β. *Journal of Molecular Neuroscience : MN*, *46*(2), 324–335. https://doi.org/10.1007/s12031-011-9587-2

Schratt, G. M., Tuebing, F., Nigh, E. A., Kane, C. G., Sabatini, M. E., Kiebler, M., & Greenberg, M. E. (2006). A brain-specific microRNA regulates dendritic spine development. *Nature*, *439*(7074), 283–289. https://doi.org/10.1038/nature04367

Selye, H. (1936). A Syndrome produced by Diverse Nocuous Agents. *Nature*, *138*(3479), 32–32. https://doi.org/10.1038/138032a0

Selye, H. (1956). *The Stress of Life* (THE MCGRAW-HILL COMPANIES (ed.)).

Sen, S., Duman, R., & Sanacora, G. (2008). Serum Brain-Derived Neurotrophic Factor, Depression, and Antidepressant Medications: Meta-Analyses and Implications. *Biological Psychiatry*, *64*(6), 527–532. https://doi.org/10.1016/j.biopsych.2008.05.005

Shors, T. J., Seib, T. B., Levine, S., & Thompson, R. F. (1989). Inescapable versus escapable shock modulates long-term potentiation in the rat hippocampus. *Science (New York, N.Y.)*, *244*(4901), 224–226. https://doi.org/10.1126/science.2704997

Siegel, G., Obernosterer, G., Fiore, R., Oehmen, M., Bicker, S., Christensen, M., Khudayberdiev, S., Leuschner, P. F., Busch, C. J. L., Kane, C., Hübel, K., Dekker, F., Hedberg, C., Rengarajan, B., Drepper, C., Waldmann, H., Kauppinen, S., Greenberg, M. E., Draguhn, A., … Schratt, G. M. (2009). A functional screen implicates microRNA-138-dependent regulation of the depalmitoylation enzyme APT1 in dendritic spine morphogenesis. *Nature Cell Biology*, *11*(6), 705–716. https://doi.org/10.1038/ncb1876

Skliris, A., Papadaki, O., Kafasla, P., Karakasiliotis, I., Hazapis, O., Reczko, M., Grammenoudi, S., Bauer, J., & Kontoyiannis, D. L. (2015). Neuroprotection requires the functions of the RNA-binding protein HuR. *Cell Death & Differentiation*, *22*(5), 703–718. https://doi.org/10.1038/cdd.2014.158

Skolnick, Layer, R. T., Popik, P., Nowak, G., Paul, I. A., & Trullas, R. (1996). Adaptation of N-methyl-D-aspartate (NMDA) receptors following antidepressant treatment: implications for the pharmacotherapy of depression. *Pharmacopsychiatry*, *29*(1), 23–26. https://doi.org/10.1055/s-2007-979537

Skolnick, P., Popik, P., & Trullas, R. (2009). Glutamate-based antidepressants: 20 years on. *Trends in Pharmacological Sciences*, *30*(11), 563–569. https://doi.org/10.1016/j.tips.2009.09.002

Smalheiser, N. R., Lugli, G., Rizavi, H. S., Torvik, V. I., Turecki, G., & Dwivedi, Y. (2012). MicroRNA expression is down-regulated and reorganized in prefrontal cortex of depressed suicide subjects. *PloS One*, *7*(3), e33201. https://doi.org/10.1371/journal.pone.0033201

Smalheiser, N. R., Lugli, G., Rizavi, H. S., Zhang, H., Torvik, V. I., Pandey, G. N., Davis, J. M., & Dwivedi, Y. (2011). MicroRNA expression in rat brain exposed to repeated inescapable shock: differential alterations in learned helplessness vs. non-learned helplessness. *The International Journal of Neuropsychopharmacology*, *14*(10), 1315–1325. https://doi.org/10.1017/S1461145710001628

Soga, T., Nakajima, S., Kawaguchi, M., & Parhar, I. S. (2021). Repressor element 1 silencing transcription factor /neuron-restrictive silencing factor (REST/NRSF) in social stress and depression. *Progress in Neuro-Psychopharmacology and Biological Psychiatry*, *104*, 110053. https://doi.org/10.1016/j.pnpbp.2020.110053

Song, M.-F., Dong, J.-Z., Wang, Y.-W., He, J., Ju, X., Zhang, L., Zhang, Y.-H., Shi, J.-F., & Lv, Y.-Y. (2015). CSF miR-16 is decreased in major depression patients and its neutralization in rats induces depression-like behaviors via a serotonin transmitter system. *Journal of Affective Disorders*, *178*, 25–31. https://doi.org/10.1016/j.jad.2015.02.022

Souery, D., Oswald, P., Massat, I., Bailer, U., Bollen, J., Demyttenaere, K., Kasper, S., Lecrubier, Y., Montgomery, S., Serretti, A., Zohar, J., & Mendlewicz, J. (2007). Clinical Factors Associated With Treatment Resistance in Major Depressive Disorder. *The Journal of Clinical Psychiatry*, *68*(07), 1062–1070. https://doi.org/10.4088/JCP.v68n0713

Southwick, S. M., Vythilingam, M., & Charney, D. S. (2005). The Psychobiology of Depression and Resilience to Stress: Implications for Prevention and Treatment. *Annual Review of Clinical*

Psychology, *1*(1), 255–291. https://doi.org/10.1146/annurev.clinpsy.1.102803.143948

Strekalova, T., Couch, Y., Kholod, N., Boyks, M., Malin, D., Leprince, P., & Steinbusch, H. M. W. (2011). Update in the methodology of the chronic stress paradigm: Internal control matters. *Behavioral and Brain Functions*, *7*(1), 9. https://doi.org/10.1186/1744-9081-7-9

Sun, Y.-M., Greenway, D. J., Johnson, R., Street, M., Belyaev, N. D., Deuchars, J., Bee, T., Wilde, S., & Buckley, N. J. (2005). Distinct Profiles of REST Interactions with Its Target Genes at Different Stages of Neuronal Development. *Molecular Biology of the Cell*, *16*(12), 5630–5638. https://doi.org/10.1091/mbc.e05-07-0687

Thiebes, K. P., Nam, H., Cambronne, X. A., Shen, R., Glasgow, S. M., Cho, H.-H., Kwon, J.-S., Goodman, R. H., Lee, J. W., Lee, S., & Lee, S.-K. (2015). miR-218 is essential to establish motor neuron fate as a downstream effector of Isl1-Lhx3. *Nature Communications*, *6*, 7718. https://doi.org/10.1038/ncomms8718

Thomas, A. M., & Duman, R. S. (2017). Novel rapid-acting antidepressants: molecular and cellular signaling mechanisms. *Neuronal Signaling*, *1*(4). https://doi.org/10.1042/NS20170010

Tornese, P., Sala, N., Bonini, D., Bonifacino, T., La Via, L., Milanese, M., Treccani, G., Seguini, M., Ieraci, A., Mingardi, J., Nyengaard, J. R., Calza, S., Bonanno, G., Wegener, G., Barbon, A., Popoli, M., & Musazzi, L. (2019). Chronic mild stress induces anhedonic behavior and changes in glutamate release, BDNF trafficking and dendrite morphology only in stress vulnerable rats. The rapid restorative action of ketamine. *Neurobiology of Stress*, *10*(March), 100160. https://doi.org/10.1016/j.ynstr.2019.100160

Torres-Berrío, A., Lopez, J. P., Bagot, R. C., Nouel, D., Dal Bo, G., Cuesta, S., Zhu, L., Manitt, C., Eng, C., Cooper, H. M., Storch, K.-F., Turecki, G., Nestler, E. J., & Flores, C. (2017). DCC Confers Susceptibility to Depression-like Behaviors in Humans and Mice and Is Regulated by miR-218. *Biological Psychiatry*, *81*(4), 306–315. https://doi.org/10.1016/j.biopsych.2016.08.017

Toth, E., Gersner, R., Wilf-Yarkoni, A., Raizel, H., Dar, D. E., Richter-Levin, G., Levit, O., & Zangen, A. (2008). Age-dependent effects of chronic stress on brain plasticity and depressive behavior. *Journal of Neurochemistry*, *107*(2), 522–532. https://doi.org/10.1111/j.1471-4159.2008.05642.x

Trullas, R., & Skolnick, P. (1990). Functional antagonists at the NMDA receptor complex exhibit antidepressant actions. *European Journal of Pharmacology*, *185*(1), 1–10. https://doi.org/10.1016/0014-2999(90)90204-j

Tyler, M. W., Yourish, H. B., Ionescu, D. F., & Haggarty, S. J. (2017). Classics in Chemical Neuroscience: Ketamine. *ACS Chemical Neuroscience*, *8*(6), 1122–1134. https://doi.org/10.1021/acschemneuro.7b00074

U.S. Food and Drug Administration. (2019). *FDA approves new nasal spray medication for treatment-resistant depression; available only at a certified doctor's office or clinic*. https://www.fda.gov/news-events/press-announcements/fda-approves-new-nasal-spray-medication-treatment-resistant-depression-available-only-certified

Uchida, S., Hara, K., Kobayashi, A., Funato, H., Hobara, T., Otsuki, K., Yamagata, H., McEwen, B. S., & Watanabe, Y. (2010). Early life stress enhances behavioral vulnerability to stress through the activation of REST4-mediated gene transcription in the medial prefrontal cortex of rodents. *Journal of Neuroscience*, *30*(45), 15007–15018. https://doi.org/10.1523/JNEUROSCI.1436-10.2010

Uchida, S., Nishida, A., Hara, K., Kamemoto, T., Suetsugi, M., Fujimoto, M., Watanuki, T., Wakabayashi, Y., Otsuki, K., McEwen, B. S., & Watanabe, Y. (2008). Characterization of the vulnerability to repeated stress in Fischer 344 rats: Possible involvement of microRNA-mediated down-regulation of the glucocorticoid receptor. *European Journal of Neuroscience*, *27*(9), 2250–2261. https://doi.org/10.1111/j.1460-9568.2008.06218.x

Verpelli, C., Piccoli, G., Zibetti, C., Zanchi, A., Gardoni, F., Huang, K., Brambilla, D., Di Luca, M., Battaglioli, E., & Sala, C. (2010). Synaptic activity controls dendritic spine morphology by modulating eEF2-dependent BDNF synthesis. *The Journal of Neuroscience : The Official Journal of the Society for Neuroscience*, *30*(17), 5830–5842. https://doi.org/10.1523/JNEUROSCI.0119-10.2010

Vreugdenhil, E., Verissimo, C. S. L., Mariman, R., Kamphorst, J. T., Barbosa, J. S., Zweers, T., Champagne, D. L., Schouten, T., Meijer, O. C., de Kloet, E. R., & Fitzsimons, C. P. (2009). MicroRNA 18 and 124a down-regulate the glucocorticoid receptor: implications for glucocorticoid responsiveness in the brain. *Endocrinology*, *150*(5), 2220–2228. https://doi.org/10.1210/en.2008-1335

Vyas, A., Mitra, R., Shankaranarayana Rao, B. S., & Chattarji, S. (2002). Chronic Stress Induces Contrasting Patterns of Dendritic Remodeling in Hippocampal and Amygdaloid Neurons. *The Journal of Neuroscience*, *22*(15), 6810–6818. https://doi.org/10.1523/JNEUROSCI.22-15-06810.2002

Wan, Y.-Q., Feng, J.-G., Li, M., Wang, M.-Z., Liu, L., Liu, X., Duan, X.-X., Zhang, C.-X., & Wang, X.-B. (2018). Prefrontal cortex miR-29b-3p plays a key role in the antidepressant-like effect of ketamine in rats. *Experimental & Molecular Medicine*, *50*(10), 1–14. https://doi.org/10.1038/s12276-018-0164-4

Waterhouse, E. G., & Xu, B. (2009). New insights into the role of brain-derived neurotrophic factor in synaptic plasticity. *Molecular and Cellular Neurosciences*, *42*(2), 81–89. https://doi.org/10.1016/j.mcn.2009.06.009

Willner, P. (2017). The chronic mild stress (CMS) model of depression: History, evaluation and usage. *Neurobiology of Stress*, *6*, 78–93. https://doi.org/10.1016/j.ynstr.2016.08.002

Winter, J., Jung, S., Keller, S., Gregory, R. I., & Diederichs, S. (2009). Many roads to maturity: microRNA biogenesis pathways and their regulation. *Nature Cell Biology*, *11*(3), 228–234. https://doi.org/10.1038/ncb0309-228

World Health Organization. (2017). *Depression and Other Common Mental Disorders: Global Health Estimates*.

Wray, N. H., Schappi, J. M., Singh, H., Senese, N. B., & Rasenick, M. M. (2019). NMDAR-independent, cAMP-dependent antidepressant actions of ketamine. *Molecular Psychiatry*, *24*(12), 1833–1843. https://doi.org/10.1038/s41380-018-0083-8

Wu, J., & Xie, X. (2006). Comparative sequence analysis reveals an intricate network among REST, CREB and miRNA in mediating neuronal gene expression. *Genome Biology*, *7*(9). https://doi.org/10.1186/gb-2006-7-9-r85

Xue, Q., Yu, C., Wang, Y., Liu, L., Zhang, K., Fang, C., Liu, F., Bian, G., Song, B., Yang, A., Ju, G., & Wang, J. (2016). MiR-9 and miR-124 synergistically affect regulation of dendritic branching via the AKT/GSK3β pathway by targeting Rap2a. *Scientific Reports*, *6*(May), 1–11. https://doi.org/10.1038/srep26781

Yao, Y., Robinson, A. M., Zucchi, F. C., Robbins, J. C., Babenko, O., Kovalchuk, O., Kovalchuk, I., Olson, D. M., & Metz, G. A. (2014). Ancestral exposure to stress epigenetically programs preterm birth risk and adverse maternal and newborn outcomes. *BMC Medicine*, *12*(1), 121. https://doi.org/10.1186/s12916-014-0121-6

Yi, R., Qin, Y., Macara, I., & Cullen, B. (2003). Exportin-5 mediates the nuclear export of pre-microRNAs and short hairpin RNAs. *Genes & Development*, *17*(24), 3011–3016. https://doi.org/10.1101/gad.1158803

Yu, J.-Y., Chung, K.-H., Deo, M., Thompson, R. C., & Turner, D. L. (2008). MicroRNA miR-124 regulates neurite outgrowth during neuronal differentiation. *Experimental Cell Research*, *314*(14), 2618–2633. https://doi.org/10.1016/j.yexcr.2008.06.002

Yuen, E. Y., Wei, J., Liu, W., Zhong, P., Li, X., & Yan, Z. (2012). Repeated Stress Causes Cognitive Impairment by Suppressing Glutamate Receptor Expression and Function in Prefrontal Cortex. *Neuron*, *73*(5), 962–977. https://doi.org/10.1016/j.neuron.2011.12.033

Yuen, Liu, W., Karatsoreos, I. N., Feng, J., McEwen, B. S., & Yan, Z. (2009). Acute stress enhances glutamatergic transmission in prefrontal cortex and facilitates working memory. *Proceedings of the National Academy of Sciences*, *106*(33), 14075–14079. https://doi.org/10.1073/pnas.0906791106

Yuen, Liu, W., Karatsoreos, I. N., Ren, Y., Feng, J., McEwen, B. S., & Yan, Z. (2011). Mechanisms for acute stress-induced enhancement of glutamatergic transmission and working memory. *Molecular Psychiatry*, *16*(2), 156–170. https://doi.org/10.1038/mp.2010.50

Zanos, P., Moaddel, R., Morris, P. J., Georgiou, P., Fischell, J., Elmer, G. I., Alkondon, M., Yuan, P., Pribut, H. J., Singh, N. S., Dossou, K. S. S., Fang, Y., Huang, X.-P., Mayo, C. L., Wainer, I. W., Albuquerque, E. X., Thompson, S. M., Thomas, C. J., Zarate, C. A., & Gould, T. D. (2016). NMDAR inhibition-independent antidepressant actions of ketamine metabolites. *Nature*, *533*(7604), 481–486. https://doi.org/10.1038/nature17998

Zanos, P., Moaddel, R., Morris, P. J., Riggs, L. M., Highland, J. N., Georgiou, P., Pereira, E. F. R., Albuquerque, E. X., Thomas, C. J., Zarate, C. A., & Gould, T. D. (2018). Ketamine and ketamine metabolite pharmacology: Insights into therapeutic mechanisms. *Pharmacological Reviews*, *70*(3), 621–660. https://doi.org/10.1124/pr.117.015198

Zarate, C. A., & Machado-Vieira, R. (2016). GSK-3: A key regulatory target for ketamine's rapid antidepressant effects mediated by enhanced AMPA to NMDA throughput. *Bipolar Disorders*, *18*(8), 702–705. https://doi.org/10.1111/bdi.12452

Zarate, C. A., Singh, J. B., Carlson, P. J., Brutsche, N. E., Ameli, R., Luckenbaugh, D. A., Charney, D. S., & Manji, H. K. (2006). A randomized trial of an N-methyl-D-aspartate antagonist in treatment-resistant major depression. *Archives of General Psychiatry*, *63*(8), 856–864. https://doi.org/10.1001/archpsyc.63.8.856

Zeng, Y., Wagner, E. J., & Cullen, B. R. (2002). Both Natural and Designed Micro RNAs Can Inhibit the Expression of Cognate mRNAs When Expressed in Human Cells. *Molecular Cell*, *9*(6), 1327–1333. https://doi.org/10.1016/S1097-2765(02)00541-5

Zeng, Y., Yi, R., & Cullen, B. R. (2003). MicroRNAs and small interfering RNAs can inhibit mRNA expression by similar mechanisms. *Proceedings of the National Academy of Sciences*, *100*(17), 9779–9784. https://doi.org/10.1073/pnas.1630797100

Zhang, Y., Wang, Y., Wang, L., Bai, M., Zhang, X., & Zhu, X. (2015). Dopamine Receptor D2 and

Associated microRNAs Are Involved in Stress Susceptibility and Resistance to Escitalopram Treatment. *International Journal of Neuropsychopharmacology*, *18*(8), pyv025–pyv025. https://doi.org/10.1093/ijnp/pyv025

Zhao, C., Sun, G., Li, S., Lang, M.-F., Yang, S., Li, W., & Shi, Y. (2010). MicroRNA let-7b regulates neural stem cell proliferation and differentiation by targeting nuclear receptor TLX signaling. *Proceedings of the National Academy of Sciences of the United States of America*, *107*(5), 1876–1881. https://doi.org/10.1073/pnas.0908750107

Zhao, C., Sun, G., Li, S., & Shi, Y. (2009). A feedback regulatory loop involving microRNA-9 and nuclear receptor TLX in neural stem cell fate determination. *Nature Structural and Molecular Biology*, *16*(4), 365–371. https://doi.org/10.1038/nsmb.1576

Zhou, L., Xiong, J., Lim, Y., Ruan, Y., Huang, C., Zhu, Y., Zhong, J., Xiao, Z., & Zhou, X.-F. (2013). Upregulation of blood proBDNF and its receptors in major depression. *Journal of Affective Disorders*, *150*(3), 776–784. https://doi.org/10.1016/j.jad.2013.03.002

Zuccato, C., Belyaev, N., Conforti, P., Ooi, L., Tartari, M., Papadimou, E., MacDonald, M., Fossale, E., Zeitlin, S., Buckley, N., & Cattaneo, E. (2007). Widespread Disruption of Repressor Element-1 Silencing Transcription Factor/Neuron-Restrictive Silencer Factor Occupancy at Its Target Genes in Huntington's Disease. *Journal of Neuroscience*, *27*(26), 6972–6983. https://doi.org/10.1523/JNEUROSCI.4278-06.2007

Zucchi, F. C. R., Yao, Y., Ward, I. D., Ilnytskyy, Y., Olson, D. M., Benzies, K., Kovalchuk, I., Kovalchuk, O., & Metz, G. A. S. (2013). Maternal Stress Induces Epigenetic Signatures of Psychiatric and Neurological Diseases in the Offspring. *PLoS ONE*, *8*(2), e56967. https://doi.org/10.1371/journal.pone.0056967

Żurawek, D., Faron-Górecka, A., Kuśmider, M., Kolasa, M., Gruca, P., Papp, M., & Dziedzicka-Wasylewska, M. (2013). Mesolimbic dopamine D2 receptor plasticity contributes to stress resilience in rats subjected to chronic mild stress. *Psychopharmacology*, *227*(4), 583–593. https://doi.org/10.1007/s00213-013-2990-3

8. LIST OF PUBLICATIONS ACHIEVED DURING THE PH.D.

Publications in scientific journals

I. Bono, F., Mutti, V., Piovani, G., Minelli, A., **Mingardi, J.**, Guglielmi, A., Missale, C., Gennarelli, M., Fiorentini, C., & Barbon, A. (2021). Establishment and characterization of induced pluripotent stem cell (iPSCs) line UNIBSi014-A from a healthy female donor. Stem cell research, 51, 102216. Advance online publication. https://doi.org/10.1016/j.scr.2021.102216

II. Bono, F., Mutti, V., Piovani, G., Minelli, A., **Mingardi, J.**, Guglielmi, A., Fiorentini, C., Barbon, A., Missale, C., & Gennarelli, M. (2020). Generation of two human induced pluripotent stem cell lines, UNIBSi012-A and UNIBSi013-A, from two patients with treatment-resistant depression. Stem cell research, 49, 102104. https://doi.org/10.1016/j.scr.2020.102104

III. Elhussiny, M., Carini, G., **Mingardi, J.**, Tornese, P., Sala, N., Bono, F., Fiorentini, C., La Via, L., Popoli, M., Musazzi, L., & Barbon, A. (2021). Modulation by chronic stress and ketamine of ionotropic AMPA/NMDA and metabotropic glutamate receptors in the rat hippocampus. Progress in neuro-psychopharmacology & biological psychiatry, 104, 110033. https://doi.org/10.1016/j.pnpbp.2020.110033

IV. Caffino, L., Mottarlini, F., **Mingardi, J.**, Zita, G., Barbon, A., & Fumagalli, F. (2020). Anhedonic-like behavior and BDNF dysregulation following a single injection of cocaine during adolescence. Neuropharmacology, 175, 108161. https://doi.org/10.1016/j.neuropharm.2020.10816

V. Tornese, P., Sala, N., Bonini, D., Bonifacino, T., La Via, L., Milanese, M., Treccani, G., Seguini, M., Ieraci, A., **Mingardi, J.**, Nyengaard, J. R., Calza, S., Bonanno, G., Wegener, G., Barbon, A., Popoli, M., & Musazzi, L. (2019). Chronic mild stress induces anhedonic behavior and changes in glutamate release, BDNF trafficking and dendrite morphology only in stress vulnerable rats. The rapid restorative action of ketamine. Neurobiology of stress, 10, 100160. https://doi.org/10.1016/j.ynstr.2019.100160

VI. Giacopuzzi, E., Gennarelli, M., Sacco, C., Filippini, A., **Mingardi, J.**, Magri, C., & Barbon, A. (2018). Genome-wide analysis of consistently RNA edited sites in human blood reveals interactions with mRNA processing genes and suggests correlations with cell types and biological variables. BMC genomics, 19(1), 963. https://doi.org/10.1186/s12864-018-5364-8

VII. **Mingardi, J.**, Musazzi, L., De Petro, G., & Barbon, A. (2018). miRNA Editing: New Insights into the Fast Control of Gene Expression in Health and Disease. Molecular neurobiology, 55(10), 7717–7727. https://doi.org/10.1007/s12035-018-0951-x

Abstract in scientific journals

I. Laura Musazzi, **Jessica Mingardi**, Kalevi Trontti, Paolo Tornese, Maurizio Popoli, Alessandro Barbon, and Iiris Hovatta. "A Putative Role for miR-9 in the Remodeling of Hippocampal Pyramidal Neurons Dendritic Arbor Induced by Chronic Stress and Ketamine" Biological Psychiatry 2020. Volume 87, Issue 9, Supplement, 1 May 2020, Pages S73-S74

Oral presentations at congress

I. **Jessica Mingardi**, Luca La Via, Giulia Carini, Maurizio Popoli, Iiris Hovatta, Laura Musazzi, Alessandro Barbon
"Putative role of miR-9 in the remodelling of hippocampal dendritic arborisation induced by chronic stress and ketamine"
National Meeting of PhD Students in Neuroscience (virtual meeting, 28-29 September 2020)

II. **Jessica Mingardi**, Daniela Bonini, Paolo Tornese, Nathalie Sala, Maurizio Popoli, Alessandro Barbon, Laura Musazzi
"Acute ketamine rescues the morphological changes induced by chronic mild stress in the CA3 of vulnerable animals: a putative role for miR-9"
GEPB – Lake Como School of Advanced Studies (Como, 9-13 April 2018)

Abstract at congress

I. Adrien Gigliotta, **Jessica Mingardi**, Sarah Cummings, Rashmi Kothary and Iiris Hovatta
"An in vitro stress model of primary oligodendrocytes from anxious and non-anxious mouse strains"
Brain & Mind Symposium (virtual meeting, 15-16 October 2020)

II. **Jessica Mingardi**, Luca La Via, Giulia Carini, Maurizio Popoli, Iiris Hovatta, Laura Musazzi, Alessandro Barbon
"Putative role of miR-9 in the remodelling of hippocampal dendritic arborisation induced by chronic stress and ketamine"
National Meeting of PhD Students in Neuroscience (virtual meeting, 28-29 September 2020)

III. **Jessica Mingardi**, Luca La Via, Giulia Carini, Maurizio Popoli, Iiris Hovatta, Laura Musazzi, Alessandro Barbon
"miR-9-5p as a putative target of chronic stress and ketamine action: its role in dendritic remodelling"
12th FENS Forum of Neuroscience (virtual meeting, 10-15 July 2020)

IV. Adrien Gigliotta, **Jessica Mingardi**, Sarah Cummings, Rashmi Kothary and Iiris Hovatta
"An in vitro stress model of primary oligodendrocytes from anxious and non-anxious mouse strains"
12th FENS Forum of Neuroscience (virtual meeting, 10-15 July 2020)

V. Adrien Gigliotta, **Jessica Mingardi** and Iiris Hovatta
"An in vitro stress model of primary oligodendrocytes from anxious and non-anxious mouse strains"
5th Finnish Biological Psychiatry Symposium (Helsinki, 16 December 2019)

VI. **Jessica Mingardi**, Paolo Tornese, Nathalie Sala, Luca La Via, Maurizio Popoli, Alessandro Barbon, Laura Musazzi
"Putative role of miR-9 in remodelling hippocampal dendritic arborisation induced by chronic stress and ketamine"
18th National Congress of the Italian Society of Neuroscience (Perugia, 26-29 September 2019)

VII. **Jessica Mingardi**, Paolo Tornese, Nathalie Sala, Maurizio Popoli, Alessandro Barbon, Laura Musazzi
"Remodeling of hippocampal dendritic arborization induced by chronic stress and ketamine: a role for miR-9?"
3rd Nordic Neuroscience Meeting (Helsinki, 12-14 June 2019)

VIII. **Jessica Mingardi**, Paolo Tornese, Nathalie Sala, Maurizio Popoli, Alessandro Barbon, Laura Musazzi
"A putative role for miR-9 in hippocampal morphological changes induced by chronic stress and ketamine"
National Meeting of PhD Students in Neuroscience (Napoli, 1 March 2019)

IX. Daniela Bonini, Paolo Tornese, **Jessica Mingardi**, Mara Seguini, Nathalie Sala, Maurizio Popoli, Laura Musazzi, Alessandro Barbon
"Changes in BDNF RNA dendritic trafficking associated with functional and morphological alterations induced by chronic stress and ketamine"
XVIII National Congress AIBG (Ferrara, 21-22 September 2018)

X. **Jessica Mingardi**, Daniela Bonini, Paolo Tornese, Nathalie Sala, Maurizio Popoli, Alessandro Barbon, Laura Musazzi
"Acute ketamine rescues the morphological changes induced by chronic mild stress in the CA3 of vulnerable animals: a putative role for miR-9"
11th FENS Forum of Neuroscience (Berlino, 7-11 July 2018)

XI. **Jessica Mingardi**, Daniela Bonini, Paolo Tornese, Nathalie Sala, Maurizio Popoli, Alessandro Barbon, Laura Musazzi
"Acute ketamine rescues the morphological changes induced by chronic mild stress in the CA3 of vulnerable animals: a putative role for miR-9"
GEPB – Lake Como School of Advanced Studies (Como, 9-13 April 2018)

9. ACKNOWLEDGEMENTS

I would like to thank Prof. Giuseppina De Petro and Prof. Eugenio Monti, coordinators of the PhD program.

An immense thank goes to Prof. Alessandro Barbon who, beyond being my tutor during the PhD program, gave me the opportunity to enter in the world of the scientific research and continues to teach me every day.

I am grateful to all the present and past members of the Lab without whom I could not have imagined arriving here: Daniela, Giulia, Luca, Alice and Isabella. Thank you for your support and also for the beautiful moments outside the Lab. A special thank to Luca who contributed to this project with patience and many hours at the microscope!

Thanks to Prof. Laura Musazzi for the inspiring collaboration and the precious help, to Dr. Paolo Tornese and Prof. Maurizio Popoli.

I would like to show my gratitude to Prof. Iiris Hovatta and the members of her Lab at the University of Helsinki for giving me the opportunity of working with them and having such an incredible experience in Finland.

Last but not least, I want to share this moment with my family and friends as they did with me in these years always supporting me.

Thanks to Stefano for his curiosity and attitude that inspire me every day.